uOttawa

L'Université canadienne
Canada's university

FACULTÉ DES ÉTUDES SUPÉRIEURES ET POSTOCTORALES

uOttawa

L'Université canadienne
Canada's university

FACULTY OF GRADUATE AND POSDOCTORAL STUDIES

Dino P. Petrin
AUTEUR DE LA THÈSE / AUTHOR OF THESIS

Ph.D. (Microbiology)
GRADE / DEGREE

Department of Biochemistry, Microbiology and Immunology
FACULTÉ, ÉCOLE, DÉPARTEMENT / FACULTY, SCHOOL, DEPARTMENT

Using the X-Linked Inhibitor of Apoptosis (XIAP) as a Therapeutic Agent in Rodent Models of Retinal Degeneration

TITRE DE LA THÈSE / TITLE OF THESIS

R. Korneluk
DIRECTEUR (DIRECTRICE) DE LA THÈSE / THESIS SUPERVISOR

C. Tsifildis
CO-DIRECTEUR (CO-DIRECTRICE) DE LA THÈSE / THESIS CO-SUPERVISOR

EXAMINATEURS (EXAMINATRICES) DE LA THÈSE / THESIS EXAMINERS

S. Bennett

R. Bremner

D. Bulman

M Griffith

Gary W. Slater
LE DOYEN DE LA FACULTÉ DES ÉTUDES SUPÉRIEURES ET POSTDOCTORALES /
DEAN OF THE FACULTY OF GRADUATE AND POSTDOCORAL STUDIES

USING THE X-LINKED INHIBITOR OF APOPTOSIS (XIAP) AS A THERAPEUTIC AGENT IN RODENT MODELS OF RETINAL DEGENERATION

A Thesis Submitted to the

School of Graduate Studies

University of Ottawa

In Partial Fulfillment of the Requirements for the Degree of

Doctor of Philosophy of Science

Department of Biochemistry, Microbiology and Immunology

Faculty of Medicine

By

Dino P. Petrin

Your file Votre référence
ISBN: 0-494-11009-0
Our file Notre référence
ISBN: 0-494-11009-0

ABSTRACT

Retinitis Pigmentosa (RP) is the leading cause of hereditary blindness. The clinical manifestations of RP are night blindness, loss of peripheral vision leading to tunnel vision and a decreased electroretinogram (ERG) amplitude. There are numerous genes that when mutated cause RP. Regardless of the causative mutation, the end point is the same, photoreceptor cell death by apoptosis or programmed cell death (PCD). Interestingly, though all photoreceptors in an affected individual would have a mutation, disease progresses at a relatively slow rate indicating the affected cells can function. It is unclear as to why completely unrelated mutations would cause photoreceptors to die via the same mechanism. Somatic gene replacement studies using viral vectors in animal models have been successful in slowing down disease. However, attempting to cure all retinal degeneration mutations by this approach would be costly and difficult for two reasons. First, there are some mutations that comprise a small percentage of all RP cases and the cost/benefit ratio to develop a therapeutic agent for a few people would be enormous. Secondly, a number of genes that cause retinal degenerations have not been cloned. A more practical approach involves preventing apoptosis of the photoreceptor cell. The advantage of this approach is that the causative mutation does not need to be known. Developing a single therapeutic agent to target RP would also be economically more favourable than developing multiple therapeutic agents.

The X-linked Inhibitor of Apoptosis (XIAP) can inhibit cell death from numerous triggers both *in vitro* and *in vivo*. XIAP prevents apoptosis by binding to and inhibiting caspase-3, -7 and –9. Work presented here shows that adeno-associated virus (AAV) encoding XIAP is neuroprotective when injected sub-retinally in an acute retinal

degeneration model in Sprague Dawley rats. In addition, transgenic mice overexpressing XIAP throughout the neural retina have normal retinal morphology and their ERGs appear normal. These findings suggest that XIAP holds promise as a therapeutic agent in the treatment of hereditary retinal diseases such as retinitis pigmentosa.

ACKNOWLEDGEMENTS

I would like to thank my supervisors Dr. Robert G. Korneluk and Dr. Catherine Tsilfidis for allowing me the opportunity to work on a project that I always dreamed of working on. I would like to acknowledge Dr. Peter Liston for the serendipitous encounter in the hallway that commenced the journey on the road to finding a cure for retinitis pigmentosa. A thank you for my committee member Dr. Ken Dimock for his support all these years. For Dr. Stuart Coupland, who without his input and expertise, this project would still be ongoing.

A special thanks to Adam Baker for his technical expertise on this project from day one. To Jennifer Brousseau for managing our rat and mouse colony. To the lab gang at ARC and at the Eye Institute, it has been great coming to work everyday to work with you all.

I would like to thank my family for all their help and support. To my mother Maria for her kindness and endless love. For my father Vittorio who inspired me to work on trying to find a cure for RP. My brother Paul who dishes out the best medicine, laughter, when I need it most. My brother Peter who watches over me always.

A very special thanks goes to my wife Heather, who has always been at my side from the very beginning of this thesis. I cannot thank her enough for everything that she has helped me through, and put up with. And to my son, Justin Pietro Champion Petrin, who is truly one of the best things that has ever happened to me. I am glad that I have finished my thesis before you started school.

TABLE OF CONTENTS

LIST OF FIGURES

LIST OF ABBREVIATIONS

β-PDE	beta-phosphodiesterase
4-VO	4-vessel occlusion
6-OHDA	6-hydroxydopamine
Aβ	amyloid beta
AAV	adeno-associated virus
Ac-DEVD-CHO	Ac-Asp-Glu-Val-aspartic acid aldehyde
AD	Alzheimer's disease
Ad#	adenovirus serotype #
ADA	adenine deanimase
ANOVA	analysis of variance
AP-1	activating protein-1
APP	amyloid beta precursor protein
ARVO	Association for Research in Vision and Ophthalmology
Bcl-2	b-cell lymphoma/leukemia-2
BDNF	brain derived neurotrophic factor
BIR	baculovirus inhibitory repeat
CBA	chicken beta actin
cDNA	complementary deoxyribonucleic acid
cGMP	guanosine 3', 5'-cyclic monophosphate
CMV	cytomegalovirus
CNS	central nervous system
CNTF	ciliary neurotrophic factor

CpGV	Cydia pomonella granulosis virus
CRX	cone-rod-otx like
DAPI	4', -6-diamidino-2-phenylindole
DMTU	dimethylthiourea
DNA	deoxyribonucleic acid
DOX	doxycycline
EAM	encapsidated adenovirus minichromosomes
ERG	electroretinogram
FGF#	fibroblast growth factor #
FIV	feline immunodeficiency virus
GAPDH	glyceraldehyde-3-phosphate dehydrogenase
GDNF	glial cell-derived neurotrophic factor
GDP	guanosine diphosphate
GFAP	glial fibrillary acidic protein
GFP	green fluorescent protein
GTP	guanosine triphosphate
H&E	haematoxylin and eosin
HA	hemaglutinin
hdAd	helper-dependent adenovirus
HIAP	human inhibitor of apoptosis
hILPIP	human ILP-interacting protein
HIV	human immunodeficiency virus
IAP	inhibitor of apoptosis

IgH	immunoglobulin heavy chain
IKKβ	inhibitory κB kinase-β
IL-1β	interleukin-1 beta
IOP	intraocular pressure
IP	intraperitoneal
IRBP	interphotoreceptor retinoid-binding protein
IRES	internal ribosome entry site
ISCEV	International Society for Clinical Electrophysiology of Vision
JNK1	c-jun N-terminal protein kinase
LCA	Leber's congenital amaurosis
LED	light emitting diode
LEDGF	lens epithelium-derived growth factor
MAPK	mitogen activated protein kinase
mERG	multifocal electroretinogram
MNU	N-methyl-N-nitrosourea
MPTP	1-methyl-4-phenyl-1,2,3,6-tetrahydropyridine
mRNA	messenger ribonucleic acid
NGF	nerve growth factor
NR	Naka-Rushton
NSE	neuronal specific enolase
O^6-meGua	O^6-methyl guanosine
OCT	optimal cutting temperature
OD	right eye (occhio destra)

ON	optic nerve
ONL	outer nuclear layer
OP	oscillatory potential
ORF	open reading frame
OS	left eye (occhio sinistra)
PBS	phosphate buffered saline
PCR	polymerase chain reaction
PEDF	pigment epithelium-derived factor
PFA	paraformaldehyde
PMSF	phenylmethylsulfonyl fluoride
PN	post natal
PVDF	polyvinylidene difluoride
rAAV	recombinant adeno-associated virus
rd	retinal degeneration
RGC	retinal ganglion cells
RING	really interesting new gene
RNA	ribonucleic acid
RP	retinitis pigmentosa
RPE	retinal pigment epithelieum
SD	Sprague-Dawley
SDS	sodium dodecyl sulphate
SIV	simian immunodeficiency virus
Smac/DIABLO	second mitochondria derived activator of caspases/direct IAP binding with low P1

SNpc	substantia nigra pars compacta
TAB1	TAK1 binding protein-1
TAK1	transforming growth factor-beta-activated kinase
TGα	alpha-subunit of transducin
TNF-α	tumour necrosis factor-alpha
TR	terminal repeats
TRE	tetracycline response element
TUNEL	terminal deoxynucleotidyl transferase-mediated deoxyuridine triphosphate-digoxigenin nick-end labelling
Ub	ubiquitin
XIAP	X-linked inhibitor of apoptosis
Z-VAD.FMK	benzyloxycarbonyl-Val-Ala-DL-Asp-[Ome] fluoromethyl-ketone

1 INTRODUCTION

1.1 The Retina

The retina is a complex neuronal tissue that is 500 μm thick and lines the back of the eye (Fig. 1). Over most of its area, the vertebrate retina is comprised of six layers. Starting at the back of the retina and moving toward the front of the eye are the outer nuclear layer (ONL), the outer plexiform layer (OPL), the inner nuclear layer (INL), the inner plexiform layer (IPL) the ganglion cell layer (GCL) and the optic fiber layer (OFL) (Ross et al., 1995). The nuclear layers contain the cell bodies of the neurons and the plexiform layers include axon to dendrite connections from the different cell types. The ONL consists of two types of photoreceptors called rods and cones. In humans there are approximately 120 million rods and 6 million cones. Rods are predominantly found in the periphery of the retina whereas the cones are concentrated in central portion of the retina called the macula. The retina is in contact with a layer of cells called the retinal pigment epithelium (RPE). The RPE rests on the choroid which provides nutritive support for the retina. The photoreceptors outer segments are in contact with the RPE. Rods make up approximately 97% of the cells in the ONL of the mouse and mediate vision in dim light (van Soest et al., 1999). Cones are responsible for detailed visual acuity and colour vision and are found primarily in the center of the retina called the macula. In the rods and cones, light is absorbed by visual pigments causing a biochemical change within the cells leading to an electrical signal which stimulates the bipolar and horizontal cells in the INL. The amacrine and bipolar cells of the INL synapse with the ganglion cells which

FIGURE 1. A schematic diagram of the retina illustrating the different layers and the five different neuronal cell types. The Müller cells are of glial origin (Ross et al., 1995).

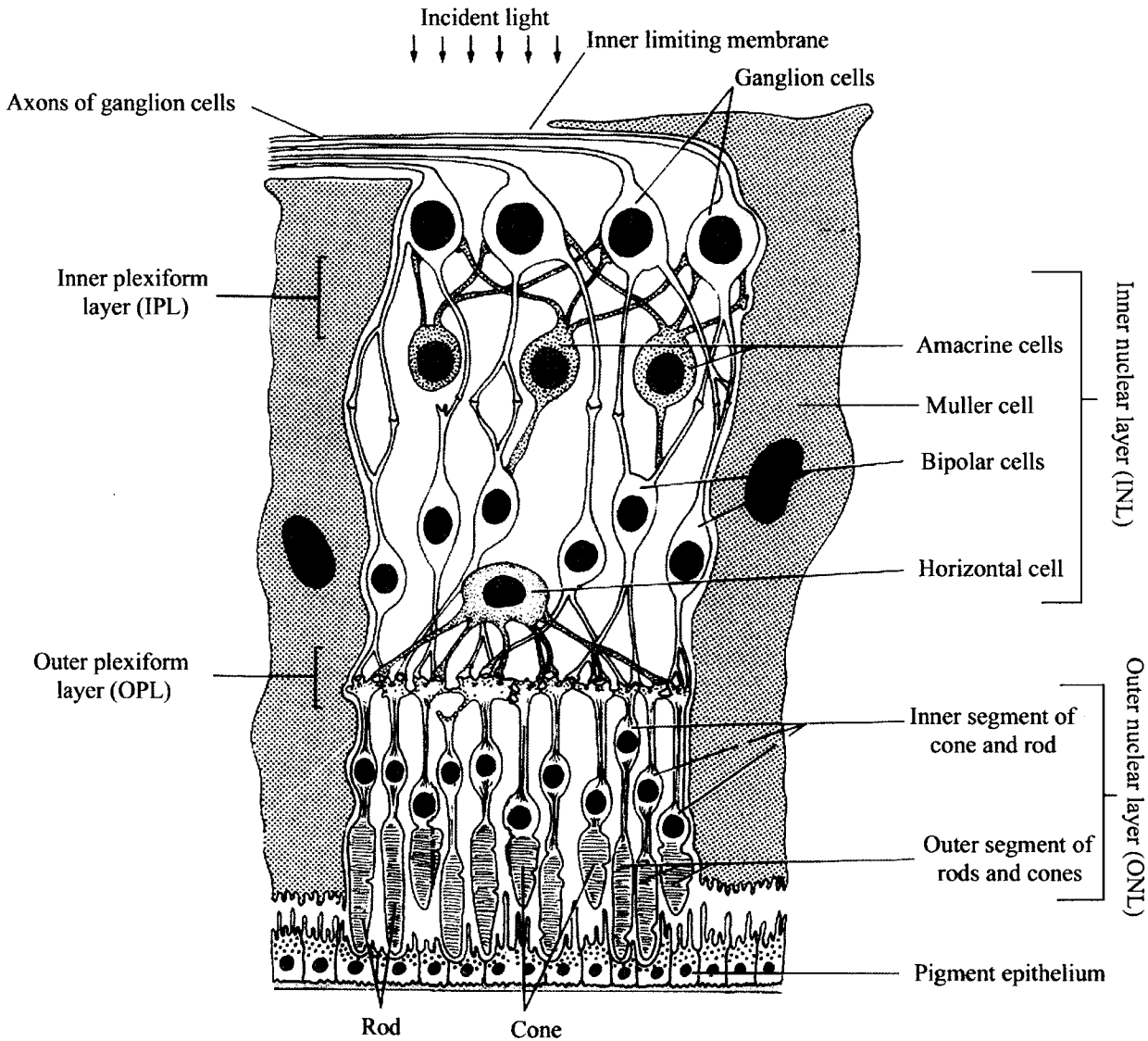
Incident light
Inner limiting membrane
Ganglion cells
Axons of ganglion cells
Inner plexiform layer (IPL)
Amacrine cells
Muller cell
Bipolar cells
Horizontal cell
Inner nuclear layer (INL)
Outer plexiform layer (OPL)
Inner segment of cone and rod
Outer segment of rods and cones
Outer nuclear layer (ONL)
Pigment epithelium
Rod
Cone

then transmit the signal through the optic nerve fiber, to the optic nerve and then to the visual cortex where the resulting image is processed.

1.2 The Electroretinogram- an Objective Measure of Electroretinal Function

The full-field flash electroretinogram (ERG) is a widely used electrophysiological measure (Marmor et al., 2003). It is a non-invasive measure that represents the electrical activity of different cell types within the retina and is an invaluable tool in assessing retinal function in humans (Robson and Frishman, 1998), primates (Khan et al., 2001), and other animals (Peachey and Ball, 2003; Rangaswamy et al., 2003). The International Society for Clinical Electrophysiology of Vision (ISCEV) was established in 1958 to standardize certain electrophysiological responses in humans so that they could be recorded comparably throughout the world (Marmor and Fishman, 1989). The first ERG standards were established in 1989. After being updated in 1999 (Marmor and Zrenner, 1998), another update of the ISCEV standards took place in 2003 (Marmor et al., 2003). Presently, no such standards are in place for non-primate mammals. This makes it difficult to compare results in animals between experimental studies. Every lab may have a different way of preparing and running the test. In addition, different ERG systems may evoke different responses that can lead to different results using the same protocol.

In 1908, Einthoven and Jolly reported three components of the ERG waveform, designating them as "a-", "b-" and "c-waves" (Einthoven and Jolly, 1908). In 1933, Granit suggested that the ERG consisted of three processes called PI, PII and PIII. PI, PII and PIII correspond to the c-, b- and a-waves, respectively. Increasing ether narcosis in the cat serially removed each process, PI followed by PII and then PIII (Granit, 1933). It is now known that the c-wave of the ERG originates from the pigmented epithelium

(Noell, 1954; Steinberg et al., 1970). Most studies in humans and animals have focused on the a- and b-wave components of the ERG (Fig. 2) (Bartz-Schmidt et al., 1996; Hood and Birch, 1990; Nozaki et al., 1983). Each waveform has two parameters, the implicit time or latency and the amplitude. The implicit time is the time from the stimulus to the peak of activity and the amplitude is the voltage magnitude at the peak of activity. The identification of the cellular origin of the ERG components has resulted from studying either cone or rod predominant retinae of various species, using chemotoxic insult to destroy specific retinal cell types (Vaegan and Millar, 1994; Xu et al., 1991), microelectrode studies of various retinal layers (Green and Kapousta-Bruneau, 1999; Grumet et al., 2000) and by observing the difference in ERG components by altering the stimulus intensity, duration and wavelength (Gottvall and Textorius, 1997; Sieving and Nino, 1988; Ueno et al., 2004).

For all the studies presented here, a scotopic-photopic intensity series was used to generate ERG amplitudes over a range of stimulus intensities, ranging from 0.001 cd·s/m^2 to 25 cd·s/m^2.

1.2.1 The Phototransduction Cascade Contributes to a- and b-wave Components of the ERG

How one sees an image is a complicated, stepwise process that involves photons of light and cross talk between various cell types in the retina, prior to sending the final image to the visual cortex in the brain. Opsin is a single polypeptide with seven transmembrane α-helical domains that are embedded in the lipid bilayer of a specialized photoreceptor organelle called a disc which is located in the outer segment of the photoreceptor (Steinberg et al., 1980). Within a hydrophobic pocket of each opsin

FIGURE 2. The ERG waveform. The a-wave occurs as a result of the hyperpolarization of photoreceptors and is indicated as a negative value. The implicit time (it) of the a-wave is measured from the onset of the stimulus to the trough of the a-wave. The b-wave commences at the trough of the a-wave and the amplitude is measured from the trough of the a-wave. The implicit time of the b-wave is measured from the onset of the stimulus to the maximal amplitude achieved in the b-wave. The b-wave occurs as a result of the polarization of the bipolar cells in the inner retina.

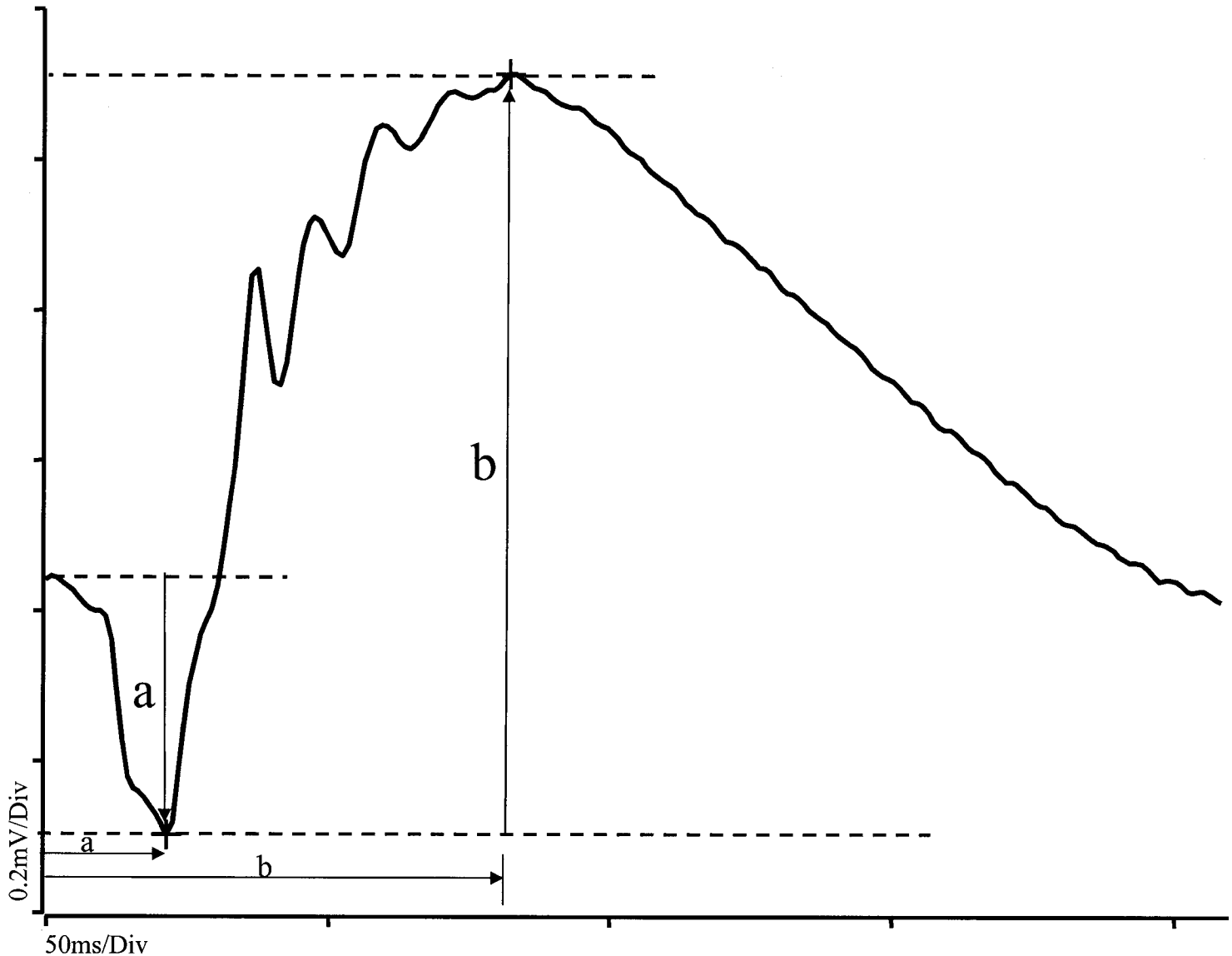
a
b
a
b
0.2mV/Div
50ms/Div

molecule, there is a chromophore derived from vitamin A called 11-*cis* retinal (Pepe et al., 1987). This chromophore is covalently attached to a lysine residue in the seventh α-helix (Schertler et al., 1993). Opsin and 11-*cis* retinal together make up rhodopsin (Palczewski et al., 2000). It is estimated that each rod photoreceptor contains 1000 discs and each disc contains approximately 1 million rhodopsin elements. This translates to 1 billion rhodopsin elements per photoreceptor (Pepe, 1999).

In the dark, there is a current that is carried by Na^+ and Ca^{2+} ions entering the outer segment of a photoreceptor through guanosine 3', 5'-cyclic monophosphate (cGMP)-gated channels (Schwarzer et al., 2000). This constant flow of ions, known as dark current, keeps the cytoplasmic membrane of the photoreceptors polarized (Ohyama et al., 2000). When a photon of light is absorbed by rhodopsin, it becomes activated to metarhodopsin, 11-*cis* retinal is isomerized to all-*trans* retinal and all-*trans* retinal detaches from opsin. Metarhodopsin catalyzes the exchange of guanosine diphosphate (GDP) for guanosine triphosphate (GTP) on many transducin G-proteins and the GTP bound α-subunit of transducin (TGα) dissociates from the β and γ subunits. One TGα binds and activates one phosphodiesterase (PDE) complex that subsequently hydrolyzes about 1000 cGMP complexes to 5'-GMP leading to the closure of the ionic channels. This closing of the ion channels in the photoreceptor causes a hyperpolarization of the cell and this negative electrical change can be measured as the a-wave of the ERG (Olshevskaya et al., 2002).

As opposed to the a-wave, the b-wave of the ERG is initiated by membrane depolarization (Tomita, 1963). Studies by Miller and Dowling (1970) showed that Müller cell responses were the only slow potentials observed that appeared similar to the ERG b-

wave form recordings in the mudpuppy retina. However, work in other species showed that the bipolar cells are the major contributors to the b-wave (Hood and Birch, 1996; Wurziger et al., 2001). It is possible that there are slight differences in origins of the b-wave among species.

1.2.2 The Naka-Rushton Equation

The Naka-Rushton (NR) equation was first reported in 1966 (Naka and Rushton, 1966). Since then, it has been used extensively in humans to identify the responsiveness, R_{max}, of the retina in a number of conditions (Balacco Gabrieli et al., 2003; Holopigian et al., 2004; Roecker et al., 1992). The non-linear relationship between the intensity of light and the amplitude of the ERG constitutes the luminance-response function that increases with increasing stimulus intensity. This relationship can be described empirically by fitting the b-wave amplitudes into the NR equation to generate a regression curve (Fig. 3). The equation, $f = (R_{max}*(L^n))/((L^n)+(K^n))$, generates 3 values, where R_{max} is saturated amplitude of the response, K is the stimulus intensity at ½ R_{max} and n proportional to the slope of the curve fit at K. L is the luminance of the stimulus (Wali and Leguire, 1992).

Up until now, investigators have primarily used ONL thickness and maximal amplitude as tools for mapping the disease course of genetic models of retinal degeneration over time (Machida et al., 2000). Though informative, ONL thickness measurements requires sacrificing the animal so that no further functional analysis can be obtained. Reporting only the maximal amplitude may allow investigator bias to influence outcomes. Fitting the ERG data with the NR equation from a large number of animals with the retinal degeneration will allow investigators the ability to assess whether there is functional protection of the retina over the course of disease without sacrificing the

FIGURE 3. The NR curve fit with the three parameters, R_{max}, K and n indicated. R_{max} is the maximal response of the retina, K is the saturation intensity at ½ R_{max} and n is the slope of the line at K. This curve fit was generated from an experimental animal used in the lab.

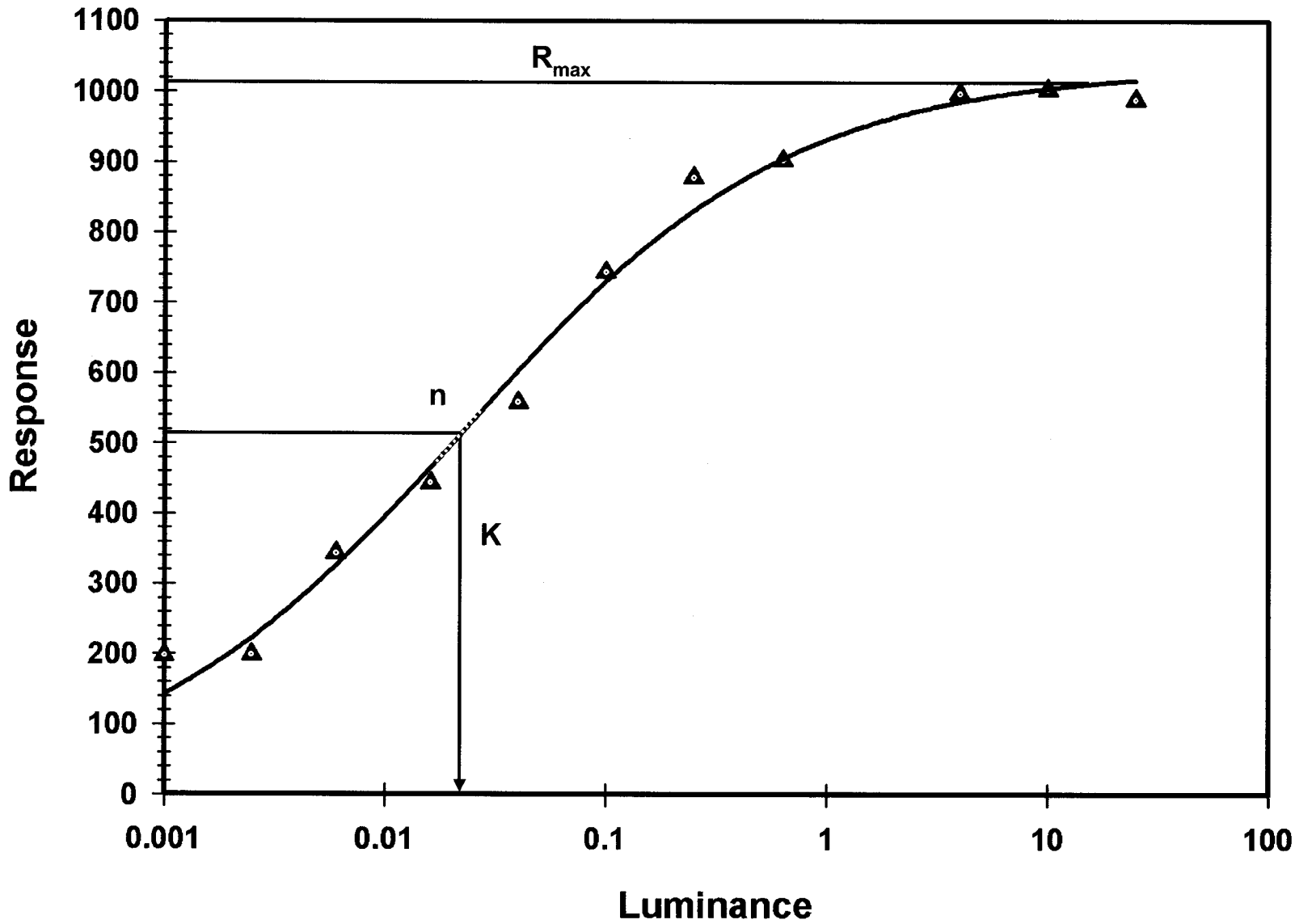
1100
1000
900
800
700
600
500
400
300
200
100
0
Response
R_{max}
n
K
0.001
0.01
0.1
1
10
100
Luminance

animal. Since all the degeneration models presented here have photoreceptor apoptosis as their underlying pathology and R_{max} is related to the number of active photoreceptors, it was decided to concentrate on analyzing changes in R_{max}.

1.3 Retinitis Pigmentosa

Retinitis Pigmentosa (RP) is the leading cause of hereditary blindness, estimated to affect between 1 in 3000 and 1 in 5000 people (Pagon, 1988). It is a disease that encompasses a group of genetic disorders, which result in the degeneration of the photoreceptor cells within the retina. RP is a heterogeneous disorder that can be inherited in an autosomal dominant, recessive or X-linked manner, and mitochondrial transmission has also been linked to RP (Allard, 1983; Boughman et al., 1980; De Vivo, 1993; Inglehearn, 1998; Wibrand et al., 2001). There are over 30 genes that when mutated, give rise to the classic symptoms of RP (Daiger et al., 2002). The mutated proteins can be structural proteins, transcription factors or proteins involved in the visual cascade. The symptoms that are associated with RP include decreased ERG amplitudes, night blindness and loss of the peripheral visual field. A fundus exam of an RP eye would reveal small specks of melanin released by the RPE, giving the retina the classic "bone spicule" appearance (Berson, 1973; Carr, 1969; Krill, 1972; Marmor, 1979; Merin and Auerbach, 1976).

The cell type predominantly associated with the classic presentation of RP is the rod photoreceptor cell. It is interesting to note that this cell has more mutations that cause disease coupled with it than any other mammalian cell type (Travis, 1998). However, mutations in other cell types are known to cause RP and other forms of retinal dystrophy. For example, one form of Leber's congenital amaurosis (LCA) is caused by a mutation in

the RPE cells, specifically the RPE65 gene (Gu et al., 1997). Another point of interest is that some genes have multiple mutations associated with them and depending on the mutation, can give rise to different forms of retinal dystrophy. Cone-rod-otx-like (CRX) is a photoreceptor homeobox transcription factor that is associated with dominant cone-rod dystrophy, recessive, dominant and *de novo* LCA and dominant RP (Freund et al., 1997; Sohocki et al., 1998; Swaroop et al., 1999). These examples illustrate the complex genetic heterogeneity of RP.

Though the term "retinitis pigmentosa" was first introduced over 140 years ago, an effective treatment for this complex disease has yet to be found. Gene replacement studies in a number of animal models have shown great promise in overcoming diseases in which the causative mutation is known (Acland et al., 2001; Ali et al., 2000; Sarra et al., 2001). However, this strategy is unlikely to become widely used for the treatment of RP since there is a diverse array of mutations to contend with, many of which are still unknown (Daiger et al., 2002). It has been well documented that irrespective of the causative mutation that gives rise to RP, the end result is the same: photoreceptor cell death by apoptosis (Adler, 1996; Luthert and Chong, 1998; Portera-Cailliau et al., 1994; Wong, 1995).

Apoptosis, or programmed cell death, is the body's normal method of disposing of damaged, unwanted or unneeded cells. A family of intracellular cysteine endopeptidases called caspases mediates this cellular programme. These caspases are divided into initiator and effector caspases. Initiator caspases cleave other caspases and effector caspases cleave numerous cellular substrates. This cascade of events leads to DNA fragmentation, cell membrane blebbing and eventually cell death.

In neurodegenerative diseases such as RP, mutations in photoreceptors lead to cell loss via the apoptotic cascade. Recently, investigators have tried to exploit this finding in an attempt to slow or prevent disease progression altogether. Several studies have examined nutritional supplementation as a means to slow the progression of the disease (Aonuma et al., 1997; el-Hifnawi el et al., 1995; Kiuchi et al., 2002; Li et al., 1998; Pasantes-Morales et al., 2002; Thomson et al., 2002a). Other investigators have attempted using caspase inhibitors (Bode and Wolfrum, 2003; Yoshizawa et al., 2002; Yoshizawa et al., 2000) or other pharmacological agents (Carmody and Cotter, 2000; Fox et al., 2003; Ranchon et al., 1999; Rotstein et al., 2003; Smith et al., 1988) to prevent the photoreceptor cell loss due to RP. Two current areas of research that hold the greatest promise for treating the numerous retinal dystrophies involve the use of survival promoting factors, such as growth factors and cytokines (Cayouette et al., 1998; Frasson et al., 1999; Green et al., 2001; LaVail et al., 1992; Okoye et al., 2003) which promote photoreceptor survival, or anti-apoptotic proteins (Petrin et al., 2003; Tsang et al., 1997) which inhibit key caspase enzymes to prevent photoreceptor cell death. These treatments can be administered directly to the retina through viral gene therapy vectors.

1.4 Viral Vectors in the Treatment of Retinal Degenerations

The words "gene therapy" have evolved from being a term born in the minds of science fiction writers to a clinically applicable tool in treating not only hereditary diseases (Nguyen et al., 2002; Onodera et al., 1998; Zern et al., 1999), but also infectious diseases (Haijema et al., 2004; Kamili et al., 2004; Li et al., 2003a), cancer (Hahn et al., 2004; Stanziale et al., 2004; Wang et al., 2004) heart disease, (Bartlett et al., 2004) and Fabry disease (Ziegler et al., 2004). The field of gene therapy has grown from the first

clinical trial in 1989 (ADA protocol, 1990) to over 330 clinical trials using different viral vectors and 113 nonviral approaches by 2001 (Marshall, 2001).

Since the advent of successful gene therapy clinical trials, researchers started to apply gene therapy to retinal diseases (Ali et al., 1996; Jones et al., 1994; Sargan et al., 1994). The retina is an ideal tissue for this technique for a number of reasons. First, transfer of exogenous genes to the retina is simple using common surgical techniques as opposed to deeply located organs such as the heart or liver. Secondly, the retina is separated from systemic circulation such that if complications do occur, they would likely remain within the eye. In addition, the blood-retinal barrier makes the eye an immune privileged organ allowing the use of viral vectors to transfer genes to retinal cells with little, if any, immune response (Sakamoto et al., 2001).

1.4.1 Retroviral Vectors

The first gene therapy trial used a retroviral vector to treat an adenosine deanimase deficiency (ADA) patient in 1989 (1990). Exogenous genes that are encoded in retroviruses achieve long-lasting gene expression since the gene integrates into the host chromosome (Hauswirth and McInnes, 1998). Another attractive property of this virus is the large cloning capacity allowing large promoters and regulating elements to be included with the targeted gene (Murata et al., 1997). The relative safety in using this vector made it attractive to treat retinal diseases, however, there has been little success with this virus. The reason for this is that retroviruses only infect actively dividing cells whereas the adult retina is post-mitotic (Sakamoto et al., 2001).

However, targeting the gene to the retina is possible using retinal-specific promoters in early post-natal individuals. Investigators showed that by using an internal

opsin promoter in a Moloney murine leukemia virus, gene expression of lacZ or β-phosphodiesterase (β-PDE) in photoreceptors can be achieved in explants from neonatal mice (Kido et al., 1996). In the future, this avenue of treatment may be applied to early-onset retinal degenerations in neonates where the mutation is known, prior to the onset of terminal differentiation in the retina.

One problem that retroviruses can have is random insertion into the host genome leading to insertional mutagenesis (Afanasieva et al., 2001; Hacein-Bey-Abina et al., 2003). This event, in theory, can disrupt a critical gene necessary for a particular retinal cell type to function properly, or by altering the expression of cell cycle regulators, can cause undesired proliferation in the retina.

1.4.2 Lentiviral Vectors

Lentiviruses belong to a subfamily of retroviruses, examples of which are the human immunodeficiency virus (HIV), simian immunodeficiency virus (SIV) and feline immunodeficiency virus (FIV) (Browning et al., 2001). These viral vectors encode a coat protein of another virus which alters the CD4+ T-cell tropism (Hauswirth and McInnes, 1998). This is known as pseudotype packaging. Pseudotyped lentiviruses have been generated to encode viral coats from Vesicular Stomatitis virus, Mokola virus, Murine leukemia virus and others (Duisit et al., 2002; Schnell et al., 2000). This has broadened the tropism of the lentivirus allowing cells in rodent retinae to be targeted successfully (Auricchio et al., 2001). Unlike their retroviral cousins, these viruses can infect both dividing and post-mitotic cells. Their integration into the host genome also allows for stable, long-term expression of target genes (Takahashi et al., 1999).

Problems associated with retroviruses also apply to the lentiviral vectors. Furthermore, the immune response of lentivirus has not been fully characterized and there is a small potential for the recombinant vector to revert back to wild-type HIV (Dejneka and Bennett, 2001).

1.4.3 Adenoviral Vectors

Adenovirus infection is common in humans and is responsible for the majority of common cold cases. By removing non-essential DNA, adenoviral vectors can package approximately 7.5kb of exogenous DNA and the deletion of early viral genes creates a replication-defective virus (Bennett et al., 1996). These viruses can be grown to very high titres with relative ease in the lab. The early onset of gene expression (within 24 hours) (Thorne et al., 1999) makes studying the effect of transgene expression in animals desirable. Unlike the retro- and lentiviral vectors, however, the duration of gene expression from adenoviral transduction is short-lived (Kreppel et al., 2002; Liang et al., 2002). Though able to infect some retinal cells with ease, adenoviral vectors, which are primarily serotype 5, (Ad5) do not transduce healthy photoreceptors efficiently (Sakamoto et al., 2001). Interestingly, these vectors can infect developing as well as degenerating photoreceptors making them potential candidates for retinal gene therapy (Dejneka and Bennett, 2001). Recently, however, strategies have been developed to retarget adenoviral vectors to healthy photoreceptors. By pseudotyping an Ad5 vector with the fibre protein of Ad37, photoreceptors were transduced *in vivo* by intravitreal injection in approximately one-third of eyes along with the RPE (Von Seggern et al., 2003). This surgical approach has advantages in that there is minimal disruption of the

retina, however it may not transduce as many photoreceptors as a sub retinal injection procedure.

One critical problem of adenoviral vectors is the immune response that it elicits due to the virion and the production of numerous viral proteins needed for infection (Martin-Martinez et al., 2004; Raper et al., 2003). However, the subretinal space is an immune privileged site and adenoviral delivery of transgenes elicits minimal inflammation indicating that adenoviruses could be used as gene therapy vectors (Anand et al., 2002).

1.4.4 Encapsidated Adenovirus Minichromosomes (EAMs).

The inherent immunogenic problem associated with adenoviral vectors has lead to the development of adenovirus minichromosomes (EAMs) (Kumar-Singh and Farber, 1998) or helper-dependent adenoviral vectors (hdAd) (Bramson et al., 2004). EAMs are adenoviral vectors packaged into adenoviral virions, which lack all protein encoding viral genes. The EAMs retain the beneficial properties of the parent adenovirus but reduce the immunogenicity (Brown et al., 2004; Ehrhardt et al., 2003; Li et al., 2003b). In some cases however, toxicity does occur after systemic administration of EAMs (Brunetti-Pierri et al., 2004) The EAMs have an increased cloning capacity of 36kb which can accommodate all known retinal genes including elaborate regulatory elements (Sargent et al., 2004). One of the first reports used an EAM in a gene replacement strategy in the *rd1* mouse (Kumar-Singh and Farber, 1998). The EAM vector containing β-PDE was subretinally injected at postnatal day (PN) 5 or 6. Expression of the β-PDE mRNA persisted for 18 weeks and expression of the exogenous protein was detected up to PN

90. Since that study, reports have demonstrated stable long-term transgene expression from improved EAMs in other animal models (Gilbert et al., 2003; Toietta et al., 2003).

However, in order to prepare EAMs, replication competent helper virus is required and earlier attempts at removing all the helper viruses from the EAM preparation proved difficult (Mitani et al., 1995). Recently, this problem has been addressed by flanking the packaging signal of the helper virus with loxP sites. Upon infecting 293 cells expressing Cre recombinase, this packaging signal is excised preventing the helper virus genome from being packed into virions (Parks et al., 1996). The helper virus retains the ability to provide all the necessary functions to grow and package EAMs (Fisher et al., 1996). This methodology has greatly reduced the contaminating helper virus to 0.1% of the EAM titre. This threshold still poses an immunogenic problem in treating humans. Nevertheless, the EAMs are promising candidates for treating retinal disease.

1.4.5 Adeno-associated Virus

Adeno-associated viruses (AAVs) are non-pathogenic human parvoviruses that require a helper virus (adenovirus) to propagate (Laughlin et al., 1982). In the absence of helper virus, AAV becomes replication defective and integrates at a preferred site called AAVS1on chromosome 19q-13qter (Kotin et al., 1992; Kotin et al., 1991). It is able to infect both dividing and non-dividing cells. It is unknown if recombinant AAV (rAAV) integrates into the genome in a site specific fashion or remains episomal (Kearns et al., 1996; Ponnazhagan et al., 1997). The optimal cloning capacity of this vector is the smallest of all the viral vectors presented, up to 4.9kb (Dong et al., 1996). Despite the limited cloning capacity, this vector infects photoreceptors efficiently and results in high

levels of transgene expression (Ali et al., 1996; Flannery et al., 1997). Depending on the serotype that is used to package a gene of interest, optimal expression of the protein product can begin as early as one day or as late as six weeks in neuronal cells (Green et al., 2001; Wu et al., 2002). Transgene expression is long-lived lasting at least a year following subretinal injection (Bennett et al., 1999; Guy et al., 1999; Nathwani et al., 2002). All these features make AAV an ideal vector in the treatment of retinal degenerations.

1.5 Models of Retinal Degeneration

1.5.1 Retinal Degeneration Induced by N-methyl-N-nitrosourea

N-methyl-N-nitrosourea (MNU) is an alkylating agent which has been used to study mammary carcinogenesis in rats (Sukumar et al., 1983). In addition, MNU has been used extensively to study acute photoreceptor cell death in various animal models including mouse, rat, rabbit and hamster (Nambu et al., 1997; Ogino et al., 1993; Taomoto et al., 1998; Yoshizawa et al., 1999). In rats, a dose of 75 mg/kg of MNU initiates a cascade of events that begin with the formation of 7-methyldeoxyguanosine DNA adduct formation which can be detected 12 hours post injection. Cell death in photoreceptors peaks at 24 hours post injection and continues until seven days after MNU treatment. Caspase activity peaks at 72 hours indicating that photoreceptor cell death occurs via the apoptotic cascade (Yoshizawa et al., 1999).

1.5.2 P23H-3 Transgenic Rats

There are three lines of transgenic rats that carry the P23H mutation in rhodopsin (LaVail, 2002) Line 3 (P23H-3) has an intermediate rate of loss of photoreceptors. Using

a computer morphometric system, it has been documented that the ONL thickness drops from approximately 45 μm to 8 μm over the course of one year (LaVail, 2002; Machida et al., 2000). This correlates with a drop in a- and b-wave amplitude (Machida et al., 2000).

1.5.3 P23H-1 and S334ter-4 Transgenic Rats

These two transgenic lines have similar rates of photoreceptor degeneration as observed by the thinning of the ONL thickness. Over the course of six months, the ONL thickness thins to approximately 4 μm in both lines (LaVail, unpublished). This more rapid onset of retinal degeneration is advantageous since it is slow enough for rAAV to express XIAP, but fast enough to see results in a shorter time period than in the P23H-3 model, which takes approximately one year.

1.6 Mechanisms Linking Retinitis Pigmentosa to Apoptosis

Work in *Drosophila* has focused on determining the molecular mechanisms that lead to photoreceptor cell loss via apoptosis. Investigators have demonstrated in a variety of retinal degeneration mutants in *Drosophila* the formation of stable and persistent complexes between rhodopsin and its regulatory protein arrestin (Alloway et al., 2000). Arrestin is involved in the conversion of activated rhodopsin to its inactive state. Furthermore, the accumulation of these complexes and their subsequent endocytosis via a clathrin-mediated process, triggers photoreceptor apoptotic cell death (Kiselev et al., 2000).

Work by Acharya et al. (2003) has shed further light into other molecules that may be involved in photoreceptor degeneration in *Drosophila*. This group looked

specifically at modulating the sphingolipid biosynthetic pathway *in vivo* and examined the effects on flies with defects in clathrin-mediated endocytosis. Ceramidase was cloned into an upstream activating sequence vector and expressed in the *Drosophila* eye. Expression of ceramidase in an arrestin mutant rescued the degeneration phenotype and ERG recordings showed functional preservation of the photoreceptors. Ceramide accumulation in the control mutants correlated with photoreceptor cell death whereas in the mutants expressing ceramidase, ceramide levels were reduced by 50%. The investigators also looked at flies that had defects in clathrin-mediated endocytosis. One specific mutation lies in the *shibere* gene which encodes dynamin guanosine triphosphatase which is essential for clathrin-mediated endocytosis (van der Bliek and Meyerowitz, 1991). This mutant undergoes retinal degeneration and photoreceptor cell loss was suppressed when photoreceptors expressed ceramidase. These findings demonstrated that clathrin-mediated endocytosis of rhodopsin is essential for photoreceptor cell survival and that ceramide production is required for the internalization process.

Another group has looked at the molecular mechanisms involved during light induced photoreceptor apoptosis using mice that had mutations in rhodopsin or proteins involved in the visual transduction cascade. It seems that depending on the intensity of light, apoptosis can occur by different mechanisms. As stated earlier, there are a number of proteins that are involved in the visual transduction cascade. Rhodopsin has been shown to be involved in retinal phototoxicity (Noell and Albrecht, 1971). Photoreceptors in rhodopsin-less mice, are completed protected from light-induced apoptosis (Grimm et al., 2000). Another protein that is involved in the regeneration of 11-*cis* retinal is Rpe65

(Grimm et al., 2000), a protein found in the RPE cells. Mice lacking Rpe65 are also protected from light-induced photoreceptor apoptosis. However, unlike the previous two proteins, c-fos, a proto-oncoprotein has been implicated in retinal degeneration. The loss of c-fos and therefore the AP-1 transcription factor that it is a component of, eliminated photoreceptor cell death under bright light conditions. Exactly how AP-1 induction leads to photoreceptor cell death need to be determined (Hafezi et al., 1997).

Hao et al. (2002) looked at whether rhodopsin activation alone was sufficient to cause light-induced photoreceptor cell loss or if there were other components further downstream the visual cascade that could contribute to photoreceptor cell death. Mutant mice were generated with mutations in rhodopsin kinase (*Rhok*-/-) and arrestin (*Sag*-/-). These two proteins function to terminate the light-activated state of rhodopsin even in low light conditions. Thus it can be deduced that these animals are in a state of constitutive phototransduction signalling. In mice that do not have α transducin as well as lacking rhodopsin kinase or arrestin, low levels of light failed in to induce photoreceptor apoptosis which would occur in Rhok-/- and Sag-/- mutants. Therefore the second pathway is induced by abnormal levels of activated rhodopsin in the Rhok-/- and Sag-/- mutants leading to a transducin dependent degeneration that is independent of AP-1 activity.

1.7 Treatment of Retinitis Pigmentosa

1.7.1 Nutritional Supplementation

From the 1960s through to today, many clinical trials have been undertaken in the hope that nutritional supplementation would be able to successfully retard disease progression in RP patients. Several of the early studies used vitamins A and E, (Bergsma

and Wolf, 1977; Berson et al., 1993a; Berson et al., 1993b; Chatzinoff et al., 1968; Hanna, 1965; Li et al., 1998; Massof and Finkelstein, 1993) based on the fact that vitamin A is a component of the abundant chromophores found in the disks of the photoreceptors, and vitamin E is an antioxidant. The results of all these trials have remained controversial, and it seems that these vitamins do not slow down the progression of RP. However, recent studies have been published using animal models of retinal degeneration that propose other nutritional supplements can protect photoreceptors from cell death. These supplements include nicotinamide in an acute chemical model of retinal degeneration (Kiuchi et al., 2003; Kiuchi et al., 2002), and xanthophylls and alpha-tocopherols in light damage models in the Japanese quail and albino rat, respectively (Aonuma et al., 1997; Thomson et al., 2002a; Thomson et al., 2002b). Lutein supplementation has been implicated as a possible factor in improving vision but this was based on patients that were self-tested over the internet (Dagnelie et al., 2000). Lutein supplementation can increase macular pigment in some patients, however, this may not translate to slowing disease progression (Aleman et al., 2001a).

1.7.2 Pharmacological Agents

To date, there has been no single therapeutic agent found to efficiently treat RP. This is in part due to the inherent complexity of the disease. Much of the data concerning pharmacological agents has come from light-damage models. In a rat light-damage model, the use of naftidofuryl, when delivered intraperitoneally, partially protected photoreceptors when compared with control animals (Safars et al., 1997). In other light-damage models, activation of the glucocorticoid receptor suppresses activating protein (AP-1) activity in albino BALB/c mice, which in turn prevented photoreceptor cell loss

and preserved retinal function (Wenzel et al., 2001). Interestingly, c-fos deficient mice [c-fos(-/-)] are protected against light damage since AP-1 activity remains low in comparison to c-fos(+/+) mice. These results indicate that AP-1 plays a key role in photoreceptor cell loss during prolonged exposure to light. In another study, rats that received an intravitreal injection of luzindole, a melatonin antagonist, had stronger ERGs and greater number of photoreceptors (Sugawara et al., 1998). Another group have shown that dimethylthiourea (DMTU) and Ginkgo bilboa extract, a synthetic and naturally occurring antioxidant respectively, both conferred structural and functional protection of photoreceptors against light-induced retinal damage (Ranchon et al., 1999). In a retinal explant model, the dopamine antagonists, 6-hydroxydopamine (6-OHDA) and pargyline prevented photoreceptor cell loss in *rd1* mouse explants (Ogilvie and Speck, 2002). The use of desmethyldeprenyl has also been proposed as a possible agent for slowing down the progression of RP. Desmethyldeprenyl is a metabolite of the anti-Parkinson's drug deprenyl and exerts an anti-apoptotic response in neuronal cells by increasing the expression of Bcl-2 and lowering the expression of Bax (Baumgartner, 2000). Though first hypothesized several years ago, no data has since been published to support this therapeutic approach.

1.7.3 Survival factors

Based on the fact that apoptosis of photoreceptors is a common theme among most if not all forms of retinal degeneration, several investigators have attempted to use cell survival factors to slow down disease progression in inherited dystrophies such as RP. In addition to the phototoxic models described previously, much of the work on growth factors used mice that have retinal dystrophies within certain strains or transgenic

rats that are engineered to express a mutant photoreceptor protein that causes progressive disease. These chronic genetic models are more relevant to the disease conditions that are seen in the human population.

1.7.3a Ciliary Neurotrophic Factor

One of the first attempts to use survival factors to slow down retinal degeneration was reported in 1997. This group used adenovirus encoding ciliary neurotrophic factor (CNTF) injected intravitreally into the *rd1* mouse (Cayouette and Gravel, 1997). In this report, the ONL in the treated eye contained more rows of photoreceptor nuclei than in the untreated eye up to 18 days after treatment. If CNTF protein was administered alone a smaller but significant protective effect was observed up to 9 days post injection. Since then, more reports on CNTF and analogues of CNTF in other animal models have shown protective effects in the retina not only at the structural level, but at a functional level as well (Cayouette et al., 1998; Chong et al., 1999; LaVail et al., 1998). LaVail and colleagues determined the efficacy of a single intravitreal injection of CNTF on a light damage model involving the Royal College of Surgeons (RCS) rat (LaVail et al., 1992). CNTF was found to be neuroprotective of photoreceptors using this model. Another study examined the use of rAAV-CNTF-GFP in the *rd2* mouse and the P23H and S334ter rhodopsin transgenic rat lines. Viral delivery of CNTF resulted in structural protection of the photoreceptors. However, the ERGs in the *rd2* mice were not altered and in the rat models, the eyes that received rAAV-GFP had higher ERG amplitudes than the ones that received CNTF (Liang et al., 2001). These results are puzzling and there is an obvious need to look at CNTF more closely in other animal models to see if the protective effects can be extended to humans.

1.7.3b Brain Derived Neurotrophic Factor

Another growth factor that has been used to treat photoreceptor apoptosis is brain derived neurotrophic factor (BDNF). LaVail and colleagues undertook a comprehensive study examining a series of neurotrophic factors including CNTF, Axokine (a mutein of CNTF), neurotrophin-3, neurotrophin-4, leukemia inhibitory factor, basic fibroblast growth factor, nerve growth factor, insulin-like growth factor II, as well as BDNF on several rodent models of retinal degeneration (LaVail et al., 1998). LaVail and colleagues also examined the effects of BDNF in the RCS rat (LaVail et al., 1992). Animals received a single injection of each factor intravitreally two days prior to being exposed to constant light for one week. BDNF was found to be protective in this phototoxic model and they reported that 1 μL of BDNF (1 mg/mL) also slowed down degeneration in 10% of nervous (*nr*) mice by four weeks post-injection but not in the other retinal degeneration rodent models. In a retinal explant model, Caffe and colleagues (Caffe et al., 2001) found that BDNF was able to maintain 3-4 rows of nuclei in the ONL by PN 28 as compared with 2-3 rows in the rd/rd untreated control explant. However, when BDNF was used in combination with CNTF, the number of rows of nuclei increased to 7-8. Interestingly, when the retinal explant was cultured with its RPE the combination of CNTF + BDNF prevented photoreceptor degeneration but opsin and arrestin expression were suppressed as well (Caffe et al., 2001). This resulted in suppressed rod differentiation. It is unknown whether this adverse effect would have any bearing on a mature retina that has completed the differentiation process.

Another group used transplanted syngeneic Schwann cells in an attempt to rescue photoreceptors. Schwann cells were isolated from PN 5-7 mouse pups and the cells were

grafted into the subretinal space of PN 35 rho(-/-) mice. At PN 70 the eyes were taken for analysis of various growth factors. They found that message for CNTF, BDNF and glial cell-derived neurotrophic factor (GDNF) was expressed and that there was a localized area of rescue where the cells were transplanted (Keegan et al., 2003). It is not known if this transplant procedure yielded functional rescue since no ERGs were performed on these animals. The same lab recently attempted using Schwann cells that secrete BDNF in the RCS rat (Lawrence et al., 2004). A Schwann cell line (SCTM41) was transfected with BDNF and these cells were injected into the subretinal space of three-week-old RCS rats. To test for visual function, the investigators used a head tracking methodology and found that the rats that received the BDNF transfected Schwann cells performed better than sham-operated controls. As with the previous study, no ERG data was presented to illustrate quantitatively the degree of functional protection in these animals. Histological sections indicated that the rats that received the BDNF Schwann cells had a greater number of photoreceptors and preservation of retinal structure than controls.

Another group has generated double transgenic mice with inducible expression of BDNF in photoreceptors. The transgenic mouse was generated by crossing a mouse that carried the reverse tetracycline transactivator under the control of the interphotoreceptor retinoid-binding protein [IRBP (photoreceptor specific)] promoter with a mouse that had the tetracycline response element (TRE) coupled to full-length rat BDNF cDNA. This homozygous mouse was then crossed with a mouse with a rhodopsin mutation (Q344ter) to yield triple hemizygous litters (IRBP/rtTA-TRE/BDNF-Q344ter), which were then randomly put into doxycycline-treated or untreated (DOX+, DOX-) litters respectively. In the DOX+ mice, there was expression of the BDNF gene at the mRNA level and ERGs

showed preservation of retinal function and several rows of nuclei were preserved. On the other hand, in the DOX- mice, there was an almost complete loss of photoreceptors with only one row of nuclei remaining by day 21 (Okoye et al., 2003). These results contradict the results presented by LaVail et al. (LaVail et al., 1998), which showed that BDNF did not protect photoreceptors in the Q344ter rhodopsin mouse. The reason for this is that in the LaVail study, animals were given a single bolus injection of the growth factors that were used, possibly limiting the protective effect to a short period of time. The advantage of the inducible transgenic model is that the expression of the gene of interest can be controlled over a longer period, and if undesired effects are seen, gene expression can be shut off.

1.7.3c Nerve Growth Factor

There have not been a lot of results published examining nerve growth factor (NGF) as an agent to prevent photoreceptor cell loss. One study applied NGF via either a single intraocular injection or multiple retro-ocular injections to determine if NGF prevented photoreceptor loss in the C3H mouse (Lambiase and Aloe, 1996). A significant increase in the ONL thickness was observed in treated animals in comparison to untreated controls. Other groups have not found that NGF works as well as the other growth factors (Caffe et al., 2001; LaVail et al., 1998). It may be too soon to rule out the use of NGF without testing it further in other models using alternative delivery systems.

1.7.3d Glial Cell-Derived Neurotrophic Factor

GDNF has also been studied as a photoreceptor survival agent in various degeneration models. One of the first reports to illustrate the protective effects of GDNF

came from a study using the *rd1* mouse (Frasson et al., 1999). GDNF was subretinally injected into the *rd1* mouse at 13 and 17 days of age. The mice were then subjected to ERG analysis, and the retinae were processed for whole mount immunohistochemistry using an anti-rod opsin antibody to count rod photoreceptors. No ERG traces were observed in the sham treated or untreated controls. However, in the GDNF treated mice, 4 out of 10 animals had detectable traces. Cell counts also showed a greater number of rods in the treated animals in comparison to the untreated or sham injected controls. Work in another lab used recombinant adeno-associated virus encoding GDNF under the control of the chicken beta actin promoter/immediate early cytomegalovirus enhancer (rAAV-CBA-GDNF) in the S334ter transgenic rat model of RP. Immunohistochemistry revealed that expression of the GDNF protein localized to the cell bodies, inner and outer segments of the photoreceptor cells as well as the RPE. The retinal structure was preserved as demonstrated by histology and there was functional improvement of the ERG in the treated eye as compared to the untreated contralateral eye (McGee Sanftner et al., 2001).

1.7.3e Fibroblast Growth Factor 2

Studies have also focused on using human basic fibroblast growth factor (hFGF2) in preventing photoreceptor cell loss in animal models (Cao et al., 2001; Faktorovich et al., 1990; LaVail et al., 1991). One group implanted encapsulated NIH 3T3 fibroblasts that secrete human FGF2 in the vitreous of the RCS rat (Uteza et al., 1999). The microcapsules were made from the biocompatible polymer AN69 and the fibroblasts were able to survive in the capsules *in vitro* and *in vivo* for up to 90 days as a result of being transfected with hFGF2. The microencapsulated cells were implanted at PN 21 and

were found to delay photoreceptor degeneration at 45 and 90 days post implantation. The protective effect was limited to approximately 2 mm^2 and 0.95 mm^2 of the retinal surface at 45 and 90 days, respectively. The area of protection was significantly smaller in animals that received hFGF2-deficient fibroblasts. Encapsulated cells secreting growth factors may be one way to promote cell survival in the short term, but delivery systems that allow for constitutive expression of transgenes are clearly more favourable, especially in dealing with the slow disease progression characteristic of RP. Lau et al., (2000) investigated using bovine FGF2 encoded in an AAV vector under the control of the constitutive cytomegalovirus (CMV) promoter (Lau et al., 2000). This vector (rAAV-CMV-bFGF2) was injected into the subretinal space of transgenic rats (S334ter-4 rhodopsin) at PN 15. Eyes that received the vector encoding FGF2 displayed a reduced rate of degeneration in comparison to the contralateral control or rAAV-LacZ injected eye as demonstrated by morphometric analysis. In addition to this finding, ERG recordings showed functional protection in the eyes that received FGF2 in comparison to the uninjected eyes. However, the ERG amplitudes from the FGF2 injected eyes were not significantly larger than the eyes that received rAAV-LacZ. One possible explanation for this observation is that endogenous growth factors are secreted due to the surgical procedure performed on the retina. This study has emphasized the importance of demonstrating functional protection in experiments where photoreceptor survival is being sought and that counting of photoreceptor nuclei may not directly translate to photoreceptor function.

However, there are also side effects that occurred after FGF2 administration reported from different laboratories. Investigators observed in one study that all animals

developed cataracts and an increase in neovascularization of the retina (Perry et al., 1995). In another study a single intravitreal injection of 1 μg of FGF2 caused an increase in Müller cells, microglia, RPE cells, and astrocytes (Lewis et al., 1992). Moreover, two different labs reported an infiltration of macrophages in the retina after intravitreal injection of FGF2 (Faktorovich et al., 1990; Lewis et al., 1992). Despite the protective effects reported using FGF2 in different animal models, the side effects are of concern and FGF2 may not be a suitable candidate for gene therapy use.

1.7.3f Fibroblast Growth Factor 5 and 18

Two other fibroblast growth factors have also been tested for preventing photoreceptor cell loss in rat models of RP (P23H and S334ter rhodopsin) (Green et al., 2001). Here, rAAV-CMV-FGF-5 or –FGF-18 was subretinally injected into the animals. Histologically, there was significant photoreceptor cell rescue when either growth factor was used. However, this did not translate to preserved ERG responses (functional rescue) in the treated eye as compared with the contralateral control. This effect may be attributable to the injection procedure that causes retinal trauma, or it may be because the growth factors were able to preserve cell bodies but not function.

1.7.3g Lens Epithelium Derived Growth Factor

Another growth factor that has been used as a photoreceptor protective agent is lens epithelium-derived growth factor (LEDGF). This growth factor protects photoreceptors from light damage in both the Lewis and RCS rats (Machida et al., 2001). LEDGF was also used in a serum free *rd1* mouse retina organ culture system (Ahuja et al., 2001). At the end of 26 days the LEDGF treated *rd1* mouse retina had increased

photoreceptor survival and did not alter the expression and localization of opsin and arrestin in the rod cells when the RPE was present. This differs from the finding of Caffe et al., (2001) when CNTF was used in a similar experiment described above, emphasizing that different growth factors can exert dissimilar effects on photoreceptors depending on when they are expressed and also on how much of the growth factor is present in the retinal microenvironment.

1.7.3h Pigment Epithelium-Derived Factor

Pigment epithelium-derived factor (PEDF) is a neurotrophic factor and a potent inhibitor of angiogenesis (Simonovic et al., 2001). It is synthesized by RGC and RPE cells (Ogata et al., 2002). In one study, 1μg of PEDF protein was intravitreally injected at 14 days in *rd1* and *rds* mice. The eyes were collected three days later and there was a transient delay in the *rd1* mice. In the *rds* mice there was no difference between the PEDF treated eyes and the untreated eyes. This was attributed to the slower degeneration rate in this line of mice (Cayouette et al., 1999).

Miyazaki et al. (2003) performed a subretinal injection with a simian lentiviral vector encoding PEDF to treat the RCS rat and found histological protection corresponding to the site of injection. TUNEL analysis showed fewer apoptotic cells in the PEDF treated eyes than in the sham or untreated eyes. They also claimed that there was functional protection, however, the data presented indicated that the ERG b-wave amplitudes were essentially extinguished, calling into question whether PEDF is a potential therapeutic agent in the treatment of retinal degenerations.

1.7.3i Cytokines

Cytokines have also been studied as potential therapeutic agents for the treatment of RP. In a light damage model in the RCS rat, researchers found that injecting certain cytokines protected photoreceptors (LaVail et al., 1992). Interleukin-1 beta (IL-1β) protected photoreceptors from light-induced damage. Protection was found to a lesser extent with insulin-like growth factor II (IGF-II) and tumour necrosis factor alpha (TNF-α). Another study confirmed these results obtained by LaVail's group using IL-1β (Whiteley et al., 2001). In this study, IL-1β was able to rescue photoreceptors in a dose dependant manner using a much lower dose (the highest dose being 5 μg/mL) than was reported by LaVail et al., (1992). Retinal structure was preserved and retinal function was determined by an opto-kinetic response. Results were comparable to animals that were treated with FGF2 at a dose of 1000 ng/mL (Faktorovich et al., 1992).

1.8 Apoptotic Suppressive Strategies in Treating Retinal Degenerations

1.8.1 Synthetic Caspase Inhibitors

A number of investigators have examined using caspase inhibitors to slow down retinal degeneration. Apoptosis has been demonstrated to be prevalent in both natural and transgenic animal models of retinal degeneration (Bode and Wolfrum, 2003; Liu et al., 1999). In the S334ter rat, there is a C-terminal truncation in the rhodopsin transgene that results in a progressive disease that is very similar to human RP. Caspase-3 activity coincides with the rapid degeneration of photoreceptors. Using the tubby mouse, an Usher syndrome 1 model, a time course experiment was set up to map out the progression of the disease. Investigators found that during retinal differentiation no difference was

evident between the tubby mice and wild type controls. However, TUNEL staining, which is indicative of cells undergoing apoptosis, became prominent in the ONL of the tubby mice retinae peaking at post-natal day 19, whereas in the wild type mice, no TUNEL positive staining was detected. Administration of a caspase-1 inhibitor did not reduce the number of apoptotic cells, while the use of a caspase-3 inhibitor did significantly reduce the number of apoptotic photoreceptors (Bode and Wolfrum, 2003). Ac-Asp-Glu-Val-aspartic acid aldehyde (Ac-DEVD-CHO) is a caspase-3 inhibitor that has been used in both mouse and rat models of retinal degeneration (Chen et al., 2001; Yoshizawa et al., 2002). In an acute model of retinal degeneration, using MNU in Sprague Dawley rats, investigators found that treating the rats with Ac-DEVD-CHO (4000ng) intravitreally at the time of MNU injection and 10 days post-MNU treatment significantly reduced the number of apoptotic photoreceptors (Yoshizawa et al., 2000). In a more recent study Tsubura's lab used intraperitoneal injections of Ac-DEVD-CHO to treat C3H mice. These mice have a naturally occurring mutation in rod-specific phosphodiesterase. In the treated animals, the caspase inhibitor transiently delayed photoreceptor degeneration based on TUNEL analysis of the photoreceptors (Yoshizawa et al., 2002). Studies have also been done on a photoreceptor-derived cell line known as 661W using the synthetic caspase inhibitor benzyloxycarbonyl-Val-Ala-DL-Asp-[Ome] fluoromethyl-ketone (Z-VAD.FMK). This pan-caspase synthetic peptide inhibitor was shown to be protective after 661W cells were subjected to a cytotoxic insult (Tuohy et al., 2002). The evidence described above lends support to the notion that inhibiting caspase activity may be an effective way to prevent photoreceptor cell death *in vivo*.

1.8.2 Bcl-2

The B-cell lymphoma/leukemia 2 (Bcl-2) gene was the first member of the bcl-2 family of proteins discovered (Tsujimoto and Croce, 1986; Tsujimoto et al., 1984). At that time greater than 80% of human follicular lymphomas carried a t(14;18)(q32;q21) chromosome translocation that involved the bcl-2 gene and the immunoglobulin heavy chain (IgH) locus. This translocation placed the bcl-2 open reading frame close to the IgH enhancer, leading to increased expression of bcl-2 (Tsujimoto et al., 1987). Bcl-2 was the first identified regulator of programmed cell death. To date, several members of the bcl-2 family have been discovered, and these include both anti-apoptotic and pro-apoptotic members (Fig. 4) (Cory et al., 2003; Coultas and Strasser, 2003). Members of the family control cytochrome-c release from the mitochondria, which is the first step in the intrinsic apoptotic pathway (Susin et al., 1996).

The Bcl-2 family of apoptotic inhibitors have been studied extensively as cytoprotective agents in a wide array of animal models (Chierzi et al., 1998; Fink et al., 2003; Iwata et al., 2003; Jolicoeur et al., 2003; Levy et al., 2003). In the retina, anti-apoptotic bcl-2 family member effects on retinal degeneration have been studied extensively in transgenic mice (Chen et al., 1996; Eversole-Cire et al., 2000; Joseph and Li, 1996; Shinoda et al., 2001; Strettoi and Volpini, 2002; Tsang et al., 1997). Transgenic mouse lines over-expressing bcl-2 in the retina leads have retinal degeneration and the speed and severity of the degeneration is dependent on the level of bcl-2 over-expression (Joseph and Li, 1996; Quiambao et al., 2001). Nevertheless, these mice have been crossed with several different retinal degeneration mice and the effects on disease progression have been examined. Bcl-2 and related anti-apoptotic family member over-

FIGURE 4. Primary structure of known mammalian Bcl-2 family of proteins. Bcl-2 homology domains 1 through 4 (BH1-4) are indicated. TM is indicative of a transmembrane domain.

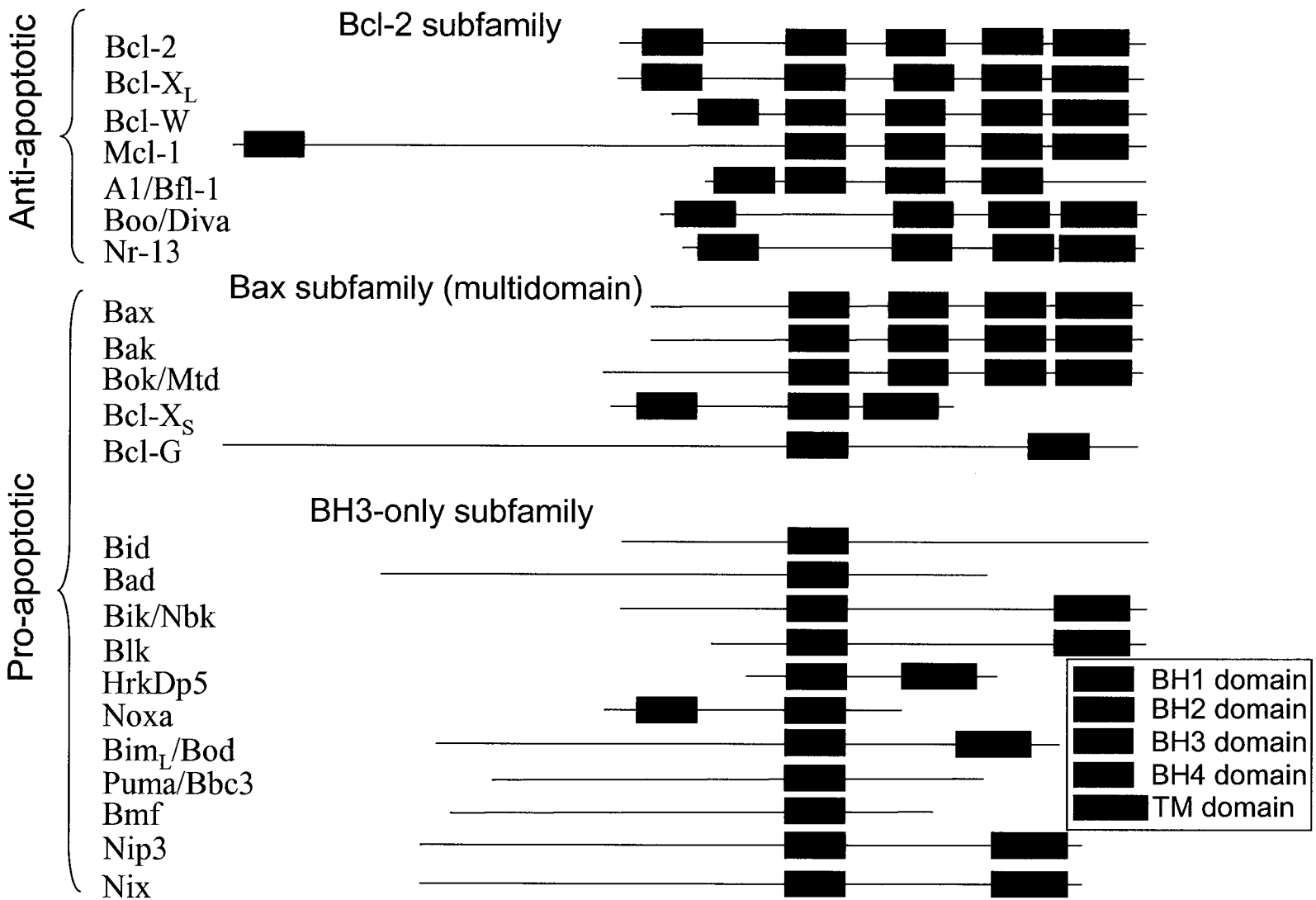
Anti-apoptotic
Pro-apoptotic
Bcl-2 subfamily
Bcl-2
Bcl-X$_L$
Bcl-W
Mcl-1
A1/Bfl-1
Boo/Diva
Nr-13
Bax subfamily (multidomain)
Bax
Bak
Bok/Mtd
Bcl-X$_S$
Bcl-G
BH3-only subfamily
Bid
Bad
Bik/Nbk
Blk
HrkDp5
Noxa
Bim$_L$/Bod
Puma/Bbc3
Bmf
Nip3
Nix
BH1 domain
BH2 domain
BH3 domain
BH4 domain
TM domain

expression has also been tested in light damage models of retinal degeneration (Chen et al., 1996; Joseph and Li, 1996; Shinoda et al., 2001). In general, the transgenic studies either show no protection (Joseph and Li, 1996) or limited transient protection that lasts little more than two weeks to under two months (Chen et al., 1996; Tsang et al., 1997).

In order to bypass potential developmental defects induced by transgenic bcl-2, an adenoviral gene therapy approach has been used to increase bcl-2 expression in the *rd1* mouse (Bennett et al., 1998). Photoreceptor rescue was documented in these studies but the experiment was terminated at the three-week time point, calling into question the long-term efficacy of bcl-2 in retinal degeneration.

1.8.3 Inhibitors of Apoptosis Proteins

In the mid nineties a novel anti-apoptotic protein that differed from the bcl-2 protein family was discovered in baculoviruses (Crook et al., 1993). The gene encoding this protein was isolated from Cydia pomonella granulosis virus (CpGV) and was designated an inhibitor of apoptosis (IAP) gene. The protein product of this gene was found to block cellular apoptosis during baculovirus infection. Since then, multiple IAP proteins have been found in fission and budding yeast, fruit fly, nematode and several mammalian species (Deveraux and Reed, 1999; LaCasse et al., 1998). These proteins can block cellular apoptosis from a wide array of triggers (Liston et al., 1996; Roy et al., 1997). Members of the IAP family share a novel domain of ~70 amino acids with conserved spacing of cysteine and histidine residues ($Cx_2Cx_6Wx_3Dx_5Hx_6C$) termed the baculoviral IAP repeat (BIR) (Verhagen et al., 2001). This BIR motif was first described by Miller and colleagues in two baculoviral genes, called Cp-IAP and Op-IAP, respectively (Birnbaum et al., 1994). All members of the IAP family have at least one

BIR domain although up to three BIRs within a protein have been reported. In addition to the BIR domains, three of the IAP family members (X-linked IAP (XIAP), Human IAP 1 and 2 (HIAP 1 and 2)) also have a RING (really interesting new gene) zinc-finger domain at their carboxy termini. This motif contains seven cysteines and one histidine residue (C_3HC_4) (Yang and Li, 2000) and confers E3 ubiquitin ligase activity (Lewis et al., 2004; Yang et al., 2000). This allows these IAPs to auto ubiquinate or to ubiquinate other proteins. Proteins ubiquinated by XIAP include the caspases and Smac/DIABLO (second mitochondria derived activator of caspases/direct IAP binding with low P1), which bind directly to the IAPs. These proteins are thereby targeted for proteosomal degradation (MacFarlane et al., 2002; Suzuki et al., 2001). In addition, HIAP1 and 2 also have a caspase recruitment domain (CARD) in between the last BIR and the RING domain (Fig. 5).

1.8.3a The X-linked Inhibitor if Apoptosis

XIAP has been studied extensively and has been referred to as the prototype IAP family member (Holcik et al., 2001). It inhibits cell death by binding and directly inhibiting specific initiator (caspase–9) and effector caspases (caspase-3 and -7). Distinct BIR domains or the linker region between two BIR domains interact with different caspases. Caspase-9 inhibition is modulated by XIAP's BIR3 domain (Srinivasula et al., 2001; Sun et al., 1999; Takahashi et al., 1998; Wu et al., 2000) whereas caspase-3 inhibition is mediated by the linker region between BIR1 and BIR2 and caspase-7 inhibition requires BIR2 and the linker region between BIR1 and BIR2 (Chai et al., 2001; Riedl et al., 2001; Roy et al., 1997; Takahashi et al., 1998). This mechanism is distinct from the bcl-2 family that acts within the mitochondria, which is further up the apoptotic

FIGURE 5. The IAP family of the known mammalian anti-apoptotic proteins. The BIR domains, which mediate caspase binding and inhibition, are present in all members. Four of the seven members contain a RING finger motif.

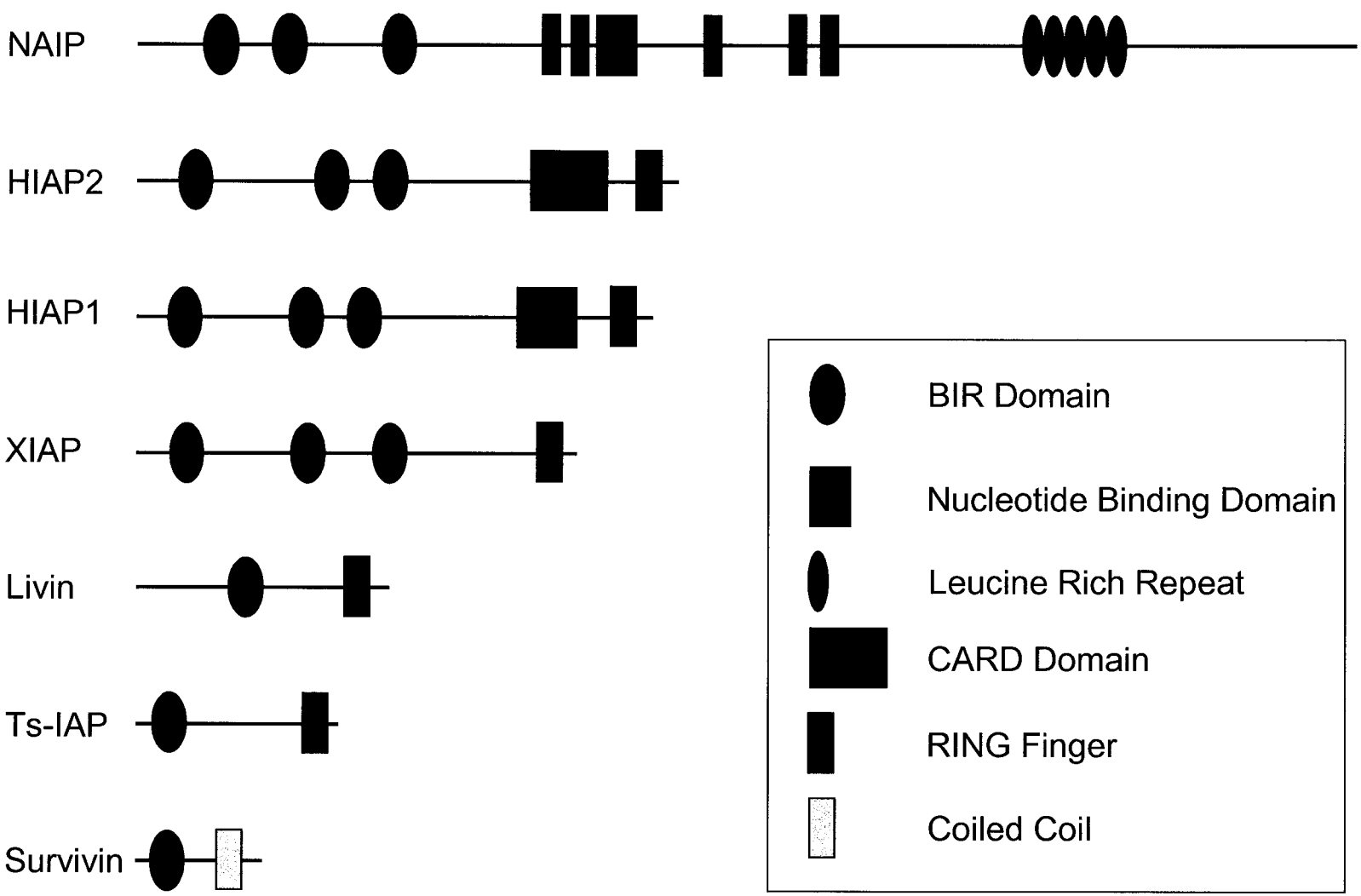
NAIP
HIAP2
HIAP1
XIAP
Livin
Ts-IAP
Survivin
BIR Domain
Nucleotide Binding Domain
Leucine Rich Repeat
CARD Domain
RING Finger
Coiled Coil

cascade. With bcl-2, other cell death triggers can be activated which bypass the cytochrome-c release from the mitochondria and continue the apoptotic programme leading to cell death.

However, XIAP's anti-apoptotic activity does not stop there. XIAP has been shown to indirectly inhibit the caspase cascade by acting as a cofactor in other signal transduction pathways in the cell, which in turn inhibit programmed cell death. Interestingly, these anti-apoptotic mechanisms do not involve the BIR domains (Lewis et al., 2004). In tumour necrosis factor-α (TNFα) and caspase-1-induced apoptosis, transforming growth factor-β-activated kinase (TAK1) and TAK1 binding protein (TAB1), link XIAP to mitogen activated protein kinase (MAPK) which activates c-jun N-terminal protein kinase (JNK1), ultimately preventing apoptosis (Sanna et al., 2002a). In addition, human ILP-interacting protein (hILPIP) enhances XIAP-mediated activation of JNK1 which in turn leads to cell survival (Sanna et al., 2002b).

XIAP's interaction with TAK1 is not limited to the JNK pathway. XIAP is also known to indirectly turn on NFκB gene transcription to promote cell survival via TAK1 (Hofer-Warbinek et al., 2000; Kucharczak et al., 2003). The BIR domains of XIAP bind to TAB1 and this complex recruits TAK1. Using a dominant negative form of TAK1 it has been shown that XIAP down regulates NFκB transcription. TAK1 activates IκB kinase-β (IKKβ) and phosphorylation of IκBα by IKK-β, dissociates the NFκB-IκBα complex, allowing the NFκB p65 subunit to translocate to the nucleus and transcribe a variety of target genes (Hofer-Warbinek et al., 2000) including XIAP. Thus, a positive feed back loop promotes cell survival until the crisis has passed.

1.8.3b Neuroprotection Using the Inhibitors of Apoptosis

The IAP family can prevent cell death at various stages of the apoptotic cascade, including the "point of no return" by blocking caspase-3 activation from a wide array of insults. Knowing this, the therapeutic potential of the IAP family and in particular XIAP, is enormous for the treatment of neurodegenerative diseases such as RP. Using XIAP for the treatment of retinal dystrophies in animal models is still in its infancy, but the following neurodegenerative models have demonstrated the great promise of XIAP in protecting post-mitotic neurons from apoptosis.

The first report of the neuroprotective effects that the IAPs demonstrated was delayed apoptosis in cerebellar granule neurons in culture when the potassium content in the medium was dropped from 25mM to 5 mM (Simons et al., 1999). This protection was short-lived lasting only 24h, suggesting that *in vitro*, apoptosis of cerebellar granule neurons is delayed but not blocked completely by over-expression of XIAP.

1.8.3c XIAP Neuroprotection in a Four Vessel Occlusion Model of Ischemia

An *in vivo* model for studying stroke involves permanent occlusion of the vertebral arteries by electrocauterization, one day prior to ischemia. On the day of ischemia the carotid arteries are tied off for 12 min. This method is known as four-vessel occlusion (4-VO) (Pulsinelli and Buchan, 1988). In the rat, this procedure results in transient forebrain ischemia causing delayed death of CA1 neurons in the hippocampus. Active caspase-3 is elevated in CA1 neurons after 4-VO, indicating that these cells die via apoptosis. Adenovirally encoded XIAP under the control of the chicken beta-actin (CBA) promoter delivered to the hippocampus was shown to prevent caspase-3 activation and protect CA1 neurons in this model. More importantly, these protected CA1 neurons

were proven to function normally, as demonstrated by spatial learning performance in the Morris water maze two weeks after the ischemia (Xu et al., 1999).

1.8.3d XIAP Neuroprotection in MPTP Parkinson's Models

Eberhardt et al., (2000) used ectopically expressed XIAP and GDNF in a 1-methyl-4-phenyl-1,2,3,6-tetrahydropyridine (MPTP) mouse model of Parkinson's disease. Parkinson's disease occurs as a result of the loss of dopaminergic neurons in the substantia nigra pars compacta (SNpc) and apoptosis has been implicated as the mechanism of cell loss in this disease (Waldmeier and Tatton, 2004). In the MPTP mouse model, adenovirally encoded XIAP and GDNF, under the control of the CMV promoter, were injected into the striatum either alone or in combination in 10-12 week old mice. Mice were subsequently injected with MPTP hydrochloride five times at 24-hour intervals one-week after adenoviral gene transfer and sacrificed seven days after the last MPTP injection. The investigators found that XIAP rescued dopaminergic cell bodies in the SNpc, but did not prevent the loss of dopaminergic terminal markers in the striatum. GDNF had the opposite effect in that the terminal markers were preserved, but GDNF did not prevent dopaminergic cell death. When used in combination, XIAP and GDNF acted synergistically in preventing the loss of dopaminergic neurons and preserving the dopaminergic terminals.

A transgenic mouse was generated with XIAP under the control of the neuronal specific enolase (NSE) promoter. This model has distinct advantages over the virally mediated expression of XIAP in that this tissue specific promoter would only express XIAP in neuronal cells or cells of neuronal lineage (Crocker et al., 2003). These transgenic mice developed normally and were found to express higher levels of XIAP in

brain and more specifically in the SNpc, compared to wild type littermates. The non-transgenic mice exposed to MPTP had a 40% reduction in dopaminergic neurons, while the NSE-XIAP mice did not show a measurable loss of neurons after treatment with MPTP. In the study by Eberhardt et al., (2000) the dopaminergic nerve terminals were not protected by XIAP administration alone and required GDNF in combination to rescue both the cells and the nerve terminals. In the transgenic study following MPTP treatment, the wild-type mice had a significant loss of nerve terminals (>60%), whereas the NSE-XIAP mice did not lose as many terminals following MPTP treatment (35% reduction) (Crocker et al., 2003).

Since XIAP was able to confer histological protection of neurons, (Crocker et al., 2003) the investigators wanted to determine if XIAP could also elicit functional protection after MPTP treatment. When wild-type rodents are placed in the centre of a field, they initially explore along the walls of the enclosure, which is known as thigmotactic behaviour, prior to venturing to the centre. MPTP causes an increase in thigmotaxis resulting in mice that rarely venture to the centre and stay in the corners of the arena. Unlesioned mice and transgenic NSE-XIAP mice subjected to MPTP treatment did not exhibit thigmotaxis suggesting that XIAP does provide functional protection at the behavioural level.

1.8.3e XIAP Neuroprotection in a 6-hydroxydopamine Model of Parkinson's

In another Parkinson's disease model, investigators used 6-OHDA to study cell death in cultured SH-SY5Y neuroblastoma cells (von Coelln et al., 2001). An adenovirus encoding XIAP (Ad-XIAP) was used to infect the cells to test whether they became resistant to 6-OHDA induced apoptosis. Cells given Ad-XIAP showed greatly suppressed

6-OHDA toxicity in comparison to Ad-LacZ infected control cells. These studies lend credence to using XIAP to prevent apoptotic cell loss in post-mitotic neurons. In addition, the use of neurotrophic co-factors in combination with XIAP may enhance the survival and allow for increased retention of function in some neurodegenerative disorders.

1.8.3f XIAP Neuroprotection in Alzheimer's Disease

Alzheimer's disease (AD) is the most common neurodegenerative disorder and affects >10% of the population over 65 and 50% of people over 85 years of age (Waldmeier and Tatton, 2004). Signs of AD include progressive memory loss and marked impairment in cognitive ability. The pathology of AD includes deposition of amyloid-β peptide (Aβ) plaques, accumulation of intracellular neurofibrillary tangles and pronounced hippocampal, septal and cortical neuronal cell loss due to apoptosis. Aβ peptide formation is the result of the Aβ precursor protein (APP) being cleaved predominantly by caspase-3 during apoptosis of hippocampal neurons (Gervais et al., 1999). This multifactorial disease has proven difficult to treat due to the complex neuropathophysiology. Though XIAP has not been used in AD animal models at this time, there is evidence that XIAP can play a role in preventing neuronal cell loss in this disease. Aβ plaque accumulation has been implicated as the hallmark of AD pathogenesis, though it remains unclear as to why this leads to senile dementia in AD patients. In an *in vitro* culture system, Aβ is toxic to cerebral endothelial cells (CECs) and these cells exhibit apoptotic characteristics when exposed to Aβ. Caspases-8 and –3 are activated in CECs upon exposure to Aβ, and treating the cells with broad-spectrum caspase inhibitors could inhibit cell death. Yin et al., (2002) found that Smac/DIABLO is

released by the mitochondria, thereby sequestering XIAP and allowing the apoptotic cascade to continue, leading to cell death. It is likely that over-expressing XIAP in Aβ treated CECs would prevent these cells from an apoptotic fate. *In vivo* transgenic mice (APP23) have been developed that over-express the amyloid precursor protein causing these mice to develop Alzheimer's-like disease later on in life. Recently, a transgenic mouse has been developed expressing XIAP under the control of the ubiquitin promoter (Ub-XIAP). These Ub-XIAP mice express XIAP in all tissues and appear to develop normally. Crossing these mice with the APP23 mice may lead to neuronal protection and lessening of disease severity.

1.8.3g XIAP Neuroprotection in a Glaucoma Model

Though XIAP treatment in the retina is still in its infancy, other neuroprotective models using XIAP in the eye have been reported. In a hypertensive rat model of glaucoma, an AAV vector encoding CBA-XIAP was injected into the intravitreal space of wild type rats. One month later, ocular hypertension was induced in the same eye by injecting hypertonic saline into the limbus. This causes sclerosis of aqueous humor outflow channels and a subsequent rise in intraocular pressure (IOP). This sustained elevation in IOP was maintained for 12 weeks. AAV-XIAP significantly promoted optic nerve axon survival compared to eyes treated with AAV-GFP or balanced salt solution. This evidence demonstrates that XIAP does protect neuronal cells over a period of time in a chronic disease model (McKinnon et al., 2001).

Axonal lesions in the CNS leads to apoptotic death of affected neurons. Optic nerve (ON) axotomy in the adult rat results in 85% of ganglion cells dying within 14 days (Garcia-Valenzuela et al., 1994). Adult rats were injected with an adenoviral vector

encoding XIAP under the control of the CMV promoter into the optic nerve within 5 minutes of axotomy. After 14 days the operated eyes were removed and processed for further analysis. Investigators showed that Ad.XIAP was as efficient as Ad.p35 in rescuing retinal ganglion cells (RGCs) in this model (Kugler et al., 2000). More recently, Straten et al., (2002) showed a synergistic effect when Ad.GDNF an Ad.XIAP were used in concert in the same ON axotomy model. In this case, Ad.GDNF was delivered to the vitreous and Ad. XIAP was delivered to the ON prior to the lesion.

Over the years, there have been many attempts at curing RP with no success. Targeted gene replacement strategies have shown that in animals, rescue of a disease phenotype is possible. However, this strategy is unlikely to become a mainstream treatment protocol, since there are many mutations that cause RP and the cost of developing each one for safety and efficacy would be enormous. The best candidates thus far have been certain growth factors and anti-apoptotic proteins such as Bcl-2 family members and the IAP gene family. Growth factors may be problematic over the long term because cells that express the secretable protein may continue to produce excess protein that may lead to unforeseen retinal changes. However, it may be possible to create an inducible system to switch on and off gene expression as required. The Bcl-2 family is of concern as well, since the transgenic mice that have been generated do undergo retinal degeneration. The IAPs, in particular XIAP, have an added advantage in that they inhibit the apoptotic cascade at multiple points in the apoptotic cascade. Ub-XIAP mice that have been generated appear to have normal functioning retinae as demonstrated by ERG. ERGs in mice are being recorded on an on going basis and at three months of age, appear to retain ERG amplitudes comparable to wild-type controls (unpublished data).

Another avenue of research in the treatment of RP that has not been explored lies in the combination of XIAP and certain growth factors like GDNF. A synergism was observed using this approach in an MPTP model of Parkinson's disease (Eberhardt et al., 2000) and a rat axotomy model (Straten et al., 2002). Coupled with an inducible system and long-term expression vectors such as AAV, this combinational approach may lead to prolonged vision in animal models of disease.

1.9 Overview of Thesis Research

Apoptotic suppressive strategies hold great promise for finding a cure or effective treatment to prevent blindness caused by RP. One of the first reports to suggest that visual function can be retained by blocking apoptosis was reported by Davidson and Steller (1998). They found that mutant flies expressing p35, a baculoviral survival protein, retained significant visual function over flies not expressing p35. This implies that preventing photoreceptor cell death alone may be sufficient to delay, if not prevent photoreceptor cell death in higher organisms. The X-linked inhibitor of apoptosis is a potent inhibitor of caspases. In various animal models of neurodegeneration, XIAP has demonstrated the ability to preserve neuronal cell structure and function alone or in concert with GDNF (Perrelet et al., 2002; Xu et al., 1999). XIAP has not been used in any animal models of retinal degeneration to date. The results presented here illustrate that XIAP can protect photoreceptor cells at a histological and functional level in an acute chemotoxic model of retinal degeneration. Moreover, given that MNU is such a potent apoptotic trigger in photoreceptors (Yoshizawa et al., 1999), an MNU dose titration experiment was carried out to determine a dose that would not completely extinguish the ERG response. This MNU dose could be used to screen potential therapeutic agents that

may slow down retinal degenerations. A similar MNU titration experiment was also carried out in mice. In an age-related experiment, rats injected with XIAP sub-retinally showed much larger b-wave amplitudes in the treated eye eight months post-injection. In addition, transgenic mice have been generated that over-express XIAP in their photoreceptors. The retinae in these mice develop normally and have normal ERG responses (unpublished data). Since many stains of mice have retinal degenerations (rd), the XIAP transgenic mice can be bred to the rd strains to observe whether the rd phenotype can be rescued in the offspring.

2 MATERIALS AND METHODS

2.1 METHODS FOR MNU PROTOCOL

2.1.1 Animals

Fifty-two 6-week-old, male Sprague-Dawley rats were purchased from Charles River Laboratories (Wilmington, MA). The rats were cared for in accordance with the ARVO Statement for the Use of Animals in Ophthalmic and Vision Research and the guidelines of the University of Ottawa Animal Care Committee. Rats were reared under standard laboratory conditions (22 ± 2°C, 60% ± 10% relative humidity, and a 12-hour light–dark cycle) and had free access to food and water throughout the experiment.

2.1.2 Construction of the rAAV Vectors Expressing XIAP or GFP

A cDNA expression construct encoding the full-length human XIAP open reading frame (ORF) including XIAP's upstream IRES (Internal Ribosome Entry Site) element was cloned into pCI vector (Promega). A hemaglutinin (HA) tag was engineered at the N-terminus of the protein resulting in the formation of pCI-IRES-HA-XIAP. The NheI site in the pCI vector was knocked out and replaced with a NotI site at the 5' end of the gene. Digesting the vector with XhoI and religating it made another construct without the IRES element (pCI-HA-XIAP). The NotI fragments (IRES-HA-XIAP and HA-XIAP) were then cloned into the pTRUF2 vector at the University of Florida (Gainesville, Florida). This vector contains the terminal repeats (TR) of AAV and the UF designation stands for user friendly. The pTRUF2 vector also contains the proximal murine rod opsin promoter (+86 to –385) (MOP500), which restricts expression to the photoreceptors. The resultant constructs, mOp-IRES-HA-XIAP-rAAV (rAAV-IRES-XIAP), mOp-HA-XIAP-rAAV (rAAV-XIAP) and mOp- green fluorescent protein -rAAV (rAAV-GFP) (Fig. 6),

FIGURE 6. Vectors and constructs used in the generation of rAAV and transgenic mice. Vectors **A**, **B** and **C** were used in the generation of recombinant adeno-associated virus. Vectors **D** and **E** were the constructs used to generate transgenic mice expressing XIAP under the control of the mouse opsin minimal promoter and ubiquitin promoter, respectively.

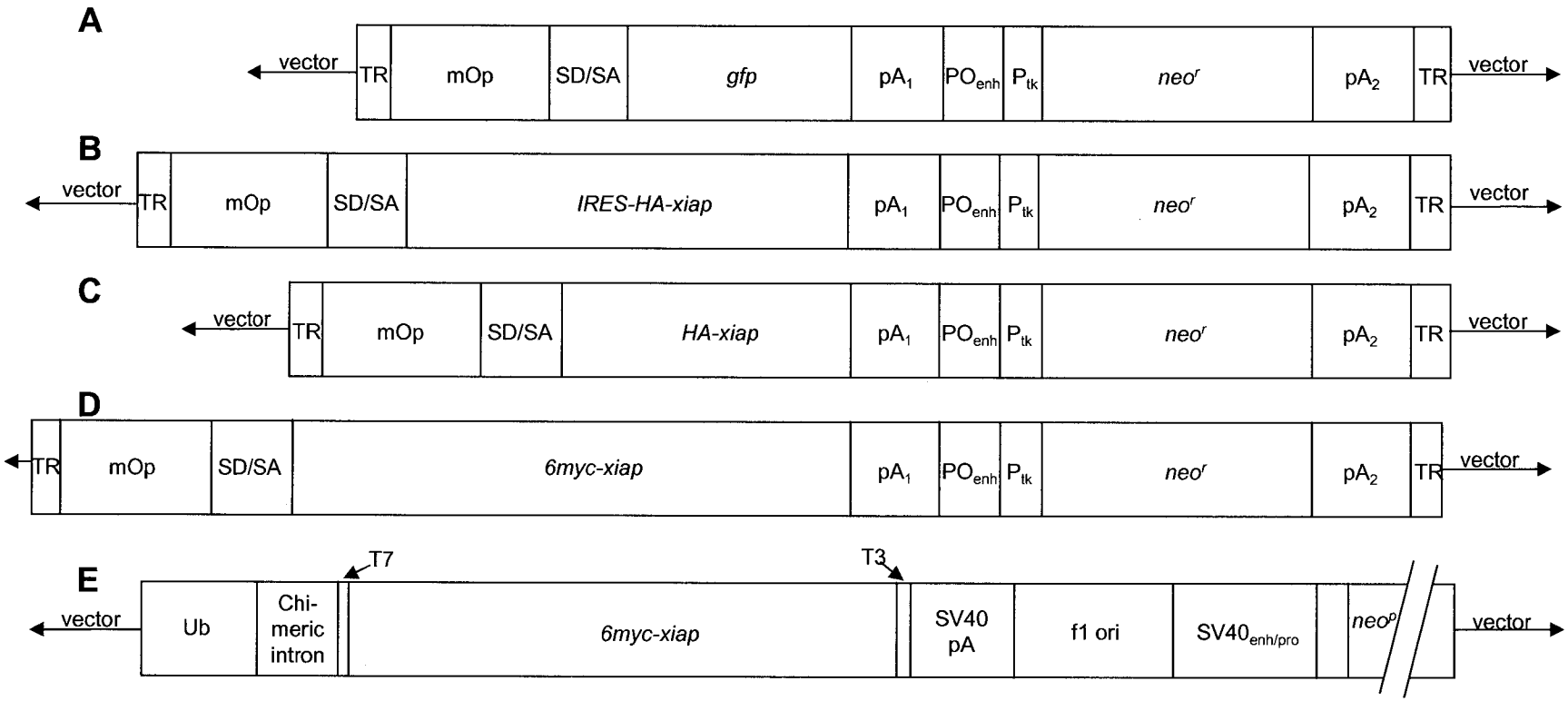

TR	AAV terminal repeats	Ub	ubiquitin promoter
mOp	mouse opsin minimal promoter	T7/T3	T7 and T3 promoters
SD/SA	SV40 splice donor and acceptor signal	SV40 pA	SV40 late polyadenylation signal
$pA_{1and\ 2}$	polyadenylation sites	f1 ori	phage f1 region
PO_{enh}	poyloma virus enhancer	$SV40_{enh/pro}$	SV40 enhancer and early promoter
P_{tk}	herpesvirus thymidine kinase promoter	$SV40_{ori}$	SV40 minimum origin of replication
neo^r	neomycin resistance gene, Tn5	neo^p	neomycin phosphotransferase

were used to package, purify, concentrate, and titre recombinant AAVs, as previously described (Hauswirth et al., 2000; Zolotukhin et al., 1996). The titres of rAAV serotype 2 vectors using the opsin promoter (rAAV-IRES-XIAP, rAAV-XIAP and rAAV-GFP) were adjusted to 4 X 10^{12} physical particles/mL. Ratios of physical-to-infectious particles were all less than 100. For production of these vectors, a mini-Ad helper plasmid pDG (Grimm et al., 1998) was co-transfected with the above vectors to produce rAAV vectors with no detectable adenovirus or wild-type AAV contamination. After a 60 hour incubation, rAAV was harvested by undergoing 3 freeze/thaw cycles and heat inactivating pDG Ad at 56°C for 30 min. Cellular debris was pelleted out by centrifugation and rAAV vectors were purified using iodixanol gradient/heparin-affinity chromatography. Virus stocks were more than 99% pure, as judged by polyacrylamide silver-stained gel electrophoresis at Dr. Hauswirth's lab. Contaminating helper adenovirus and wild-type AAV, assayed by serial dilution cytopathic effect or infectious centre assay respectively, were below detection levels.

2.1.3 Subretinal Injections

Rats were anaesthetized by halothane gas inhalation for the entire injection procedure. The subretinal injections were performed as previously described (Timmers et al., 2001). Briefly, the right eye of each rat was dilated fully with 1% tropicamide and 2.5% phenylephrine hydrochloride (Alcon Canada, Mississauga, Ontario, Canada). A drop of 0.5% proparacaine (Alcon Canada) was used as a topical anaesthetic. The vibrissae of the rats were matted down with a lubricant (KY Jelly™; Johnson & Johnson, New Brunswick, NJ) to obtain an unobstructed view of the eye. Hydroxypropyl methylcellulose (Gonak; Akorn, Buffalo, NY) was applied to the cornea to keep the eye

hydrated and to obtain a clear view of the retina. The cornea was punctured with a 28½-gauge needle approximately 1 mm from the dilated pupillary margin. A 33-gauge blunt needle (Hamilton, Reno, NV) was inserted through the corneal puncture, manoeuvred around the lens displacing it medially, and advanced through the retina. A 2 μL volume of virus with fluorescein tracer was injected into the subretinal matrix of the eye. The 33-gauge blunt needle was slowly withdrawn and an anti-infective agent (Maxitrol™, Alcon) was applied to the cornea to prevent infection. The subretinal injection induced a localized retinal detachment that was readily visualized, due to the presence of the fluorescein tracer. Sixteen rats were injected subretinally in the right eye with rAAV-IRES-XIAP, thirty-six rats were injected with rAAV-XIAP, and 10 rats received rAAV-GFP. Left eyes served as controls.

2.1.4 Experimental Procedure

MNU (Sigma, St. Louis, MO) was dissolved in physiological saline to a final concentration of 10 mg/mL immediately before use and kept on ice. Six weeks after unilateral subretinal injection of rAAV vectors, rats received a 60 mg/kg dose of MNU by intraperitoneal (IP) injection. ERGs were recorded, and animals were sampled at 0, 24, 48, and 72 hours and at 1 week after MNU injection. Each time point had two animals injected with rAAV-GFP, three animals with rAAV-IRES-XIAP, and six animals injected with rAAV-XIAP.

2.1.5 Electroretinography

All rats were weighed and dark-adapted overnight before ERG analysis. Under safelight conditions, rats were given an anesthetic cocktail consisting of 80 mg/kg

ketamine and 6.4 mg/kg xylazine. Pupils were dilated with 1% tropicamide and a topical anesthetic (0.5% proparacaine) was applied. DTL microconductive fibre electrodes were placed on each eye. A gold minidisc reference electrode was moistened in saline and placed on the tongue. A ground needle electrode was placed subcutaneously in the tail. Hydroxypropyl methylcellulose was applied to both eyes to maintain corneal hydration and to assist in the appropriate positioning of the DTL electrode. The rat was then positioned inside a Ganzfeld (model GS2000; Nicolet Instruments, Madison, WI) facing the rear of the globe. ERGs were amplified 50,000 times and recorded (Pathfinder II™; Nicolet Instruments) with a band-pass filter of 0.3 to 300 Hz. Twenty ERG traces were averaged over a luminance range of -3.0 to 1.4 log cd-s/m2. ERGs were recorded at pre-treatment baseline (time 0) and at 24, 48, and 72 hours and 1 week after MNU injection.

2.1.6 Tissue Fixation and Processing

At each of the five time points, eleven animals (two GFP-treated, three IRES-XIAP-treated and six XIAP-treated) were transcardially perfused with 4% paraformaldehyde (PFA) for tissue fixation. The eyes were scored with a white-hot 18-gauge needle before their removal for orientation purposes during embedding. After enucleation, a portion of the cornea was removed, and the eyes were placed in 4% PFA overnight. Eyes were washed three times in PBS, the lenses were removed, and the eyecups were placed in 30% sucrose and left at 4°C until saturated. The eyes were then placed in a 1:1 mixture of 30% sucrose-optimal cutting temperature (OCT) compound and allowed to equilibrate in the mixture for 1 to 2 hours at 4°C. The left and right eye cups from each rat were placed in plastic base molds, filled with 1:1 OCT-sucrose, cornea side up, and aligned by their score mark. The mold was lowered carefully onto a Petri

dish floating on liquid nitrogen. Once completely frozen, the moulds were transferred to a -80°C freezer where they were stored until sectioned. Cryosections (16 μm) were prepared using a Shandon cryostat, air dried for 3 hours, and stored at -20°C with desiccant. 4', -6-diamidino-2-phenylindole (DAPI) and haematoxylin and eosin staining was performed according to standard protocols.

2.1.7 TUNEL Staining

Cell death assays were performed on retinal sections, by using a peroxidase *in situ* detection kit according to the manufacturer's instructions (Apotag Plus™, Intergen, Purchase, NY). TUNEL sections were counterstained with eosin.

2.1.8 mRNA Expression Levels

Three rats were killed 12 weeks after undergoing a subretinal injection of rAAV-XIAP. The eyes were enucleated and the retinae dissected. The retinae were either frozen at –80°C or processed immediately. Retinae were suspended in an extraction reagent (Trizol™; Gibco, Grand Island, NY) and homogenized. RNA was isolated as per the manufacturers protocol and further purified (RNeasy™ column; Qiagen, Valencia, CA) according to the manufacturer's instructions. The purified RNA was quantitated using a Beckman DU-640 spectrophotometer and real-time RT-PCR analysis (Taqman™, Applied Biosystems, Foster City, CA) was performed on XIAP-injected eyes and uninjected contralateral control eyes with XIAP-specific primers. The primers and probe (5' GGTGATAAAGTAAAGTGCTTTCACTGT 3', 6FAM-CAACATGCTAAATGG-TATCCAGGGTGCAAATATC-TAMRA AND 5' TCAGTAGTTCTTACCAGACAC-TCCTCAA 3') span exon 3 and 4 of XIAP and overlap an intron-exon boundary to

ensure that no genomic DNA was amplified. The RNA was reverse-transcribed using the Taqman™ EZ TR-PCR kit in the ABI Prism 7700 Sequence Detection System™ (Applied Biosystems). Primers and probes were used at 600 nM and 200 nM concentrations, respectively. The conditions for amplification were 50°C for 2 min, 60°C for 30 min, and 95°C for 5 min followed by 45 cycles of PCR (94°C for 20 s, and 60°C for 1 min). Primers for rodent glyceraldehyde-3-phosphate dehydrogenase (GAPDH) served as an RNA integrity control. The total amount of RNA used in the reactions was 25 and 100 ng. A DNAse treatment of the experimental samples was also performed to ensure that the amplified product was not a result of contaminating DNA. To further ensure that the resulting amplification was from cDNA and not genomic DNA, an RNase treatment was performed on the samples.

2.1.9 Protein Expression Levels

Three rats were killed 6 weeks after receiving a subretinal injection of rAAV-XIAP. The eyes were enucleated, and the retinae dissected. Each retina was sonicated in 200 μL RIPA buffer (50 mM Tris-HCl (pH 7.4), 150 mM NaCl, 1 mM EDTA, 1% NP-40, 0.25% Na-deoxycholate, 1 mM NaF, 1 mM Na_3VO_4, 1 mM phenylmethylsulfonyl fluoride (PMSF), and 10 μg/mL each of leupeptin and aprotinin). Thirty micrograms of protein from XIAP-injected retinae and uninjected contralateral controls were electrophoresed on a denaturing 10% SDS polyacrylamide gel and transferred onto polyvinylidene difluoride (PVDF) membrane (Immobilon P™; Millipore, Bedford, MA). Blots were probed with antibodies to RIAP3 (rat XIAP) or to the HA epitope tag (Roche Molecular Biochemicals, Indianapolis, IN). The secondary antibodies used for anti-RIAP3 and anti-HA were anti-rabbit and anti-rat horseradish peroxidase, respectively.

2.2 METHODS FOR MNU DOSE RESPONSE

2.2.1 Animals

Twenty male Sprague-Dawley rats, age three weeks, were purchased from Charles River Laboratories (Wilmington, MA). They were housed at the University of Ottawa Health Sciences Centre and cared for under the guidelines outlined in the ARVO Statement for the Use of Animals in Ophthalmic and Vision Research and the University of Ottawa Animal Care Committee. Rats were reared on a diurnal cycle at 22°C ± 2°C with 60% ± 10% relative humidity and had free access to food and water throughout the duration of the experiment.

2.2.2 Experimental Procedure

Rats were placed into five groups (n=4) and weighed prior to being injected intraperitoneally. MNU (Pfaltz and Bauer) was dissolved in cold physiological saline to a concentration of 5 mg/mL and kept on ice immediately prior to use. Each group of four animals received a subsequently higher dose of MNU: 20, 30, 40, 50 and 60 mg/kg, respectively. After the one-week time point ERG, animals were euthanized by CO_2 overdose.

2.2.3 Electroretinography

All rats were weighed and dark-adapted overnight prior to ERG recordings. Under safelight conditions, rats were anaesthetized using an 80 mg/kg ketamine and 6.4 mg/kg xylazine cocktail. Both pupils were dilated with 1% tropicamide and anaesthetized using 0.5% proparacaine. Goniosoft™ (2.5% hydroxypropyl methylcellulose OcuSoft; Richmond TX) was placed on the eyes to keep them hydrated during ERG recordings.

Platinum wire loop electrodes were placed on the central cornea of each eye using an electrician's third hand. A gold reference mini-disc electrode was moistened with PBS and placed in the mouth. A subcutaneous needle electrode was placed in the tail as a ground. Inter-electrode impedances were balanced and maintained below 5 Kohms. The rat was placed on a table on a heated pad to prevent heat loss and the Ganzfeld (Espion™, Diagnosys LLC, Littleton, MA) was positioned over the animal's head using an articulated arm assembly. Binocular ERGs were recorded at 11 luminance levels, the electroretinal signals were amplified 10,000 x and bandpass filtered between 0.3-300 Hz. Six artifact-free ERG traces of 250 ms were averaged for every intensity over a luminance range of –3.0 to 1.4 log cd.s/m^2. For each averaged ERG tracing the a-wave and b-wave peak latency and amplitudes were determined through visual inspection. The a- and b-wave peak latency and amplitudes were determined at pre-treatment baseline (T0), 24 (T24), 72 (T72) hours and one-week (1 WK) at which point the animals were euthanized.

The electroretinography protocol presented above was also used for all transgenic rat lines as well as the wild type and transgenic mice.

2.3.4 Naka-Rushton Analysis

For each rat, the averaged ERG peak latencies and amplitude values of the a-waves and b-waves were exported to MS-Excel worksheets. The b-wave amplitude values for each eye were then imported into SigmaPlot 8.0 and a plot of luminance vs. b-wave amplitude was constructed for each intensity series. The data were fitted using the NR equation: $f = (R_{max}*(L^n))/((L^n)+(K^n))$ where Rmax is the maximum b-wave amplitude

attained, L is the luminance, n is the slope of the response function and logK is the luminance where the b-wave amplitude was ½ R_{max}.

The R_{max} data obtained from the 40 eyes were analyzed by repeated measures analysis of variance (ANOVA), and post-hoc analysis for specific dose effect on the responsiveness and sensitivity was determined.

2.3 METHODS FOR ELECTRORETINOGRAPHY ON MICE

Mice had their ERGs recorded on the Espion™ system using the same scotopic-photopic intensity series outlined above. The only difference from the rat protocol was that DTL fibre eye electrodes were used in place of the platinum wire electrodes.

2.4 METHODS FOR MNU DOSE RESPONSE IN MICE

Wild type C57Black/6 mice were injected with different doses of MNU. Five groups of four mice were injected with 20, 25, 30, 35 and 40 mg/kg of MNU IP, respectively. Baseline ERGs were taken prior to MNU treatment. Mice had their ERGs recorded one-week post-MNU treatment. The b-wave amplitudes of each group of mice were averaged and NR plots were generated. An ANOVA was performed to see if there was any significant difference between the five groups.

2.5 METHODS FOR AGE RELATED STUDY OF ANIMALS INJECTED WITH rAAV-XIAP

Four animals were injected at six weeks of age with rAAV-XIAP in the right eye. These animals had their ERGs recorded as outlined above on the Espion™ system on a periodic basis to compare treated versus untreated eyes. The amplitudes for treated and

untreated eyes at each intensity was averaged (n-=4) and a Student's t-test was performed to determine if there was a significant difference between eyes.

2.6 METHODS FOR GENE THERAPY USING rAAV-XIAP in GENETIC MODELS OF RP

2.6.1 P23H-3 Naka-Rushton Plots

P23H line 3 (P23H-3) transgenic rats were obtained from Matt LaVail (University of California, San Francisco). This line has a gradual retinal degeneration that progresses over the course of more than one year. Homozygous rats were bred with wild type Sprague-Dawley rats to produce heterozygous offspring. At approximately two weeks of age (when the eyes open) the rats were subretinally injected in the right eye with rAAV-XIAP (or rAAV-GFP as a control). Left eyes served as uninjected controls. The progression of disease was monitored by ERG over a period of more than a year (from 177 to 455 days). The ERG protocol used is outlined in section 2.2.3

2.6.2 P23H-1 and S334ter-4 Naka-Rushton Plots

P23H line 1 (P23H-1) and S334ter line 4 (S334ter-4) have a retinal degeneration that is much more rapid in its progression than P23H-3. This disease completes its course over a period of five to six months instead of over a year. Similarly, to P23H-3, P23H-1 and S334ter-4 were subretinally injected in the right eye with rAAV-XIAP (or rAAV-GFP) at two weeks of age. Disease progression was monitored over the next four months by ERG (see section 2.2.3 for protocol).

2.7 METHODS FOR DEVELOPING TRANSGENIC MICE

Animals were housed at the University of Ottawa's Health Science Animal Care Facility. Mice were reared on a diurnal cycle at 22°C ± 2°C with 60% ± 10% relative humidity and had free access to food and water throughout the duration of the experiment. The generation of the transgenic mice took place in the barrier facility at the University of Ottawa.

Transgenic mice were developed using the pTRUF2 vector containing the mop-GFP, mOp-IRES-HA-XIAP construct, the mOp-6myc-XIAP construct and the Ub (ubiquitin)-6myc-XIAP construct (Fig. 6). The DNA was microinjected into C3H/C57/Black 6 mouse zygotes. This service was provided by Dr. Kothary's lab at the University of Ottawa. Protein and mRNA levels were assessed as described previously. In addition, Western blot detection of the 6-myc epitope tag was carried out using anti-myc antibody from Sigma. ERG analysis was carried out on wild type and transgenic mice as previously stated (section 2.6). Genotyping for mice was carried out by Southern blot and/or PCR. Southern analysis was carried out by digesting the mouse-tail DNA with EcoR1 and BamH1 overnight. The DNA was electrophoresed on a 0.75% agarose gel at 4°C at low voltage. The gel was post-stained with ethidium bromide and photographed. The DNA was transferred to a nylon membrane using the capillary transfer technique. The open reading frame of the cDNA of human XIAP was radiolabled with αP^{32}-dCTP and used to probe the mouse Southern for the transgene. For PCR the following conditions were used. For the mice containing the HA tag the forward primer was 5' GAGACACCCTTTCCTTTCTTTA 3' and the reverse was 5' ATTTATCCTCCAAAC-CTGGACA 3'. The cycling conditions for this primer set was 95°C for 2 min, then 30

cycles of PCR (94°C for 1 min, 60°C for 1 min and 68°C for 1 min 30 s) followed by a hold at 4°C until the samples were retrieved. This resulted in the generation of a 600 bp product in the positive samples. For the mice containing the mouse opsin promoter and the 6-myc tag, the primer set was 5' CTAGATTAAAGTCCTTTCAGAACTG 3' and 5' TTTCTTGGAAGATTTGTTGAATTTG 3', resulting in an amplicon of 283 bp. The cycling parameters were: denaturation of DNA at 95°C for 2 min then PCR (94°C for 45 s, 66°C for 1 min, 68°C for 2 min) for 35 cycles followed by a hold at 16°C. In some samples a second primer set was used (5' GCCCAGAACATCATCCCTG 3' and 5' CAGTGAGCTTCCCGTTCAG 3') to amplify rodent GAPDH (an 82 bp amplicon) to ensure the integrity of the DNA. The cycling conditions used to amplify the XIAP and GAPDH amplicons in the same reaction were 95°C for 2 min followed by PCR (94°C for 45 s, 55°C for 1 min and 68°C for 1 min) for 35 cycles. For the ubiquitin promoter construct the primer set was 5' CAGGATCCATGTCTGATGCTGTGAGTTCTG 3' and 5' GACTCGAGCTAAGTAGTTCTTACCAGACAC 3'. The cycling parameters were one cycle at 94°C for 10 min followed by 35 cycles at 50°C for 2 min, 72°C for 1 min and 94°C for 2 min. The resulting 364 bp product is a portion of XIAP's BIR 3 domain. In all the PCRs, the primer concentrations were 200 nM. The probe for the Southern blot was the XIAP cDNA ORF.

2.7.1 Electroretinography of Transgenic Mice and Wild type Littermates

The scotopic-photopic ERG series used for mice in section 2.7 was also used in this experimental series.

2.7.2 Tissue Fixation and Processing of Mouse Retinal Sections

Procedures for collecting sections were the same for rats and mice with the following exceptions. Transgenic and wild type mice were transcardially perfused with 10 mL of PBS followed by 10 mL of 4% PFA. Eyes were not scored prior to removal. 10 μm thick retinal sections were collected. DAPI, H&E were carried out using standard procedures. Immunohistochemistry was performed using the following primary antibodies; anti-myc, -rhodopsin and -glial fibrillary acidic protein (GFAP)

2.8 STATISTICAL ANALYSIS

For the MNU dose response experiments and mapping the degeneration over time in the transgenic rat lines an ANOVA was used. Simple linear regression was also used in charting disease progression. For the age related study a Student's t-test was used.

3 RESULTS

3.1 The Electroretinogram

3.1.1 The Intensity Series

Figure 7 shows a typical scotopic-photopic ERG response from a wild type Sprague-Dawley rat (SD 19). Intensities of light presented are -3.0 to 1.4 log cd·s/m^2. As the intensity of light increases, the b-wave amplitude increases and the latency decreases. The a-wave amplitude becomes more prominent, showing an increase in hyperpolarization of photoreceptors at higher intensities while the a-wave latency decreases. Oscillatory potentials (OPs) become apparent around the third intensity (0.006 cd·s/m^2) and more pronounced as the flash intensity increases. The maximal b-wave amplitude typically occurs between the eighth and tenth intensity inclusive (Table 1). This extensive raw data can be analyzed using the NR equation $f = (R_{max}*(L^n))/((L^n)+(K^n))$ to yield comparisons between intraocular and interocular ERGs.

3.1.2 ERG Traces in Mice

Figure 8 is typical intensity series of a wild type mouse. Of note are the oscillatory potentials which are noticeable from the first intensity (0.001 cd·s/m^2) and the maximum b-wave amplitude in mice is typically on the second or third OP.

3.1.3 The Naka-Rushton Equation

The NR equation was developed by W.A.H. Rushton, an electrophysiologist and K.I. Naka, a mathematician in the mid-1960s (Naka and Rushton, 1966) and measures the responsiveness of the retina. This function condenses the b-wave

FIGURE 7. Scotopic-photopic intensity series of a wild type rat. This rat has been labelled Sprague-Dawley 19 (SD 19). Panel **A** is the series for the left eye (OS) and panel **B** is the right eye (OD). The plus signs identify the peaks of the a- and b-waves. Each trace is an average of at least 4 traces at the same intensity. For simplicity, in cases where the left and right eyes are being presented, the left eye will always be on the left side of the page in subsequent figures. The log values of the intensities are presented beside each trace on the right side of panel **B**. OPs are a subcomponent of the ERG seen on the ascending limb of the b-wave. The bipolar and amacrine cells are the probable generators of the OPs and are thought to reflect neuronal synaptic activity in inhibitory feedback circuits generated by the amacrine cells in the inner retina (Wachtmeister, 1998).

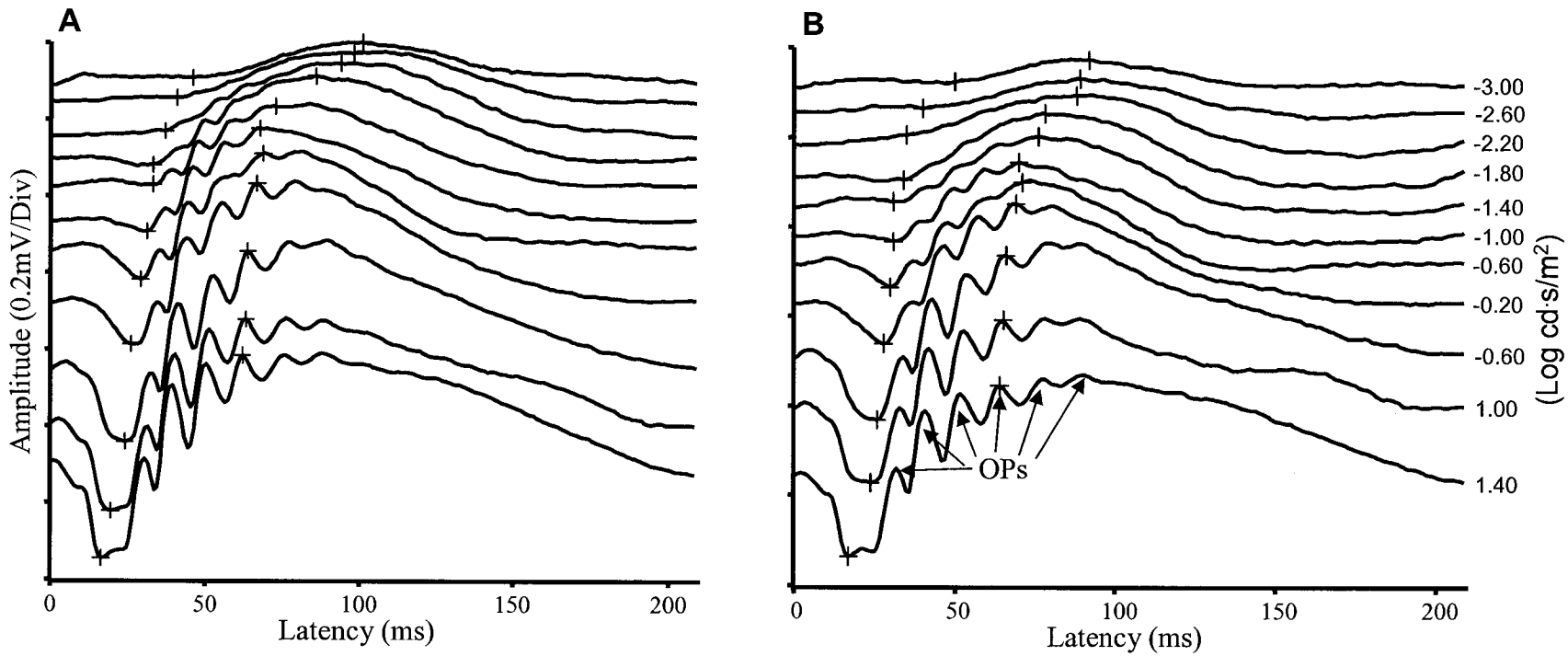
A
B
Amplitude (0.2mV/Div)
0
50
100
150
200
Latency (ms)
-3.00
-2.60
-2.20
-1.80
-1.40
-1.00
-0.60
-0.20
-0.60
1.00
1.40
OPs
(Log cd·s/m²)

TABLE 1. Raw data table of the scotopic-photopic intensity series for rat SD 19. Every intensity series presents the raw data in this format. For every flash, four data values are generated per eye. These are the a-wave and b-wave latency and amplitude values. The a-wave values are presented as a negative number due to the hyperpolarization of the photoreceptors. The b-wave amplitude is a positive value that begins at the trough of the a-wave.

wave form	eye	step	latency	amplitude	wave form	eye	step	latency	amplitude
a-wave	OD	1.1.5	40	2.963	b-wave	OD	1.1.5	82	48.25
a-wave	OS	1.2.5	36	-7.814	b-wave	OS	1.2.5	91	93.51
a-wave	OD	2.1.5	30	9.707	b-wave	OD	2.1.5	79	65.25
a-wave	OS	2.2.5	31	7.443	b-wave	OS	2.2.5	88	117
a-wave	OD	3.1.5	25	17.87	b-wave	OD	3.1.5	78	86.98
a-wave	OS	3.2.5	27	12.19	b-wave	OS	3.2.5	84	175.6
a-wave	OD	4.1.5	24	-13.38	b-wave	OD	4.1.5	68	148.5
a-wave	OS	4.2.5	23	-18.73	b-wave	OS	4.2.5	76	230.5
a-wave	OD	5.1.5	21	1.85	b-wave	OD	5.1.5	66	145
a-wave	OS	5.2.5	23	-4.243	b-wave	OS	5.2.5	63	204.7
a-wave	OD	6.1.5	21	-18.08	b-wave	OD	6.1.5	60	177.5
a-wave	OS	6.2.5	21	-32.98	b-wave	OS	6.2.5	58	271.1
a-wave	OD	7.1.5	20	-63.86	b-wave	OD	7.1.5	61	234.7
a-wave	OS	7.2.5	19	-93.81	b-wave	OS	7.2.5	59	330.5
a-wave	OD	8.1.5	18	-91.88	b-wave	OD	8.1.5	59	313.6
a-wave	OS	8.2.5	16	-113.7	b-wave	OS	8.2.5	57	421.4
a-wave	OD	9.1.5	16	-134	b-wave	OD	9.1.5	56	367.6
a-wave	OS	9.2.5	14	-178.5	b-wave	OS	9.2.5	54	498.3
a-wave	OD	10.1.5	14	-143.9	b-wave	OD	10.1.5	55	362
a-wave	OS	10.2.5	10	-183.1	b-wave	OS	10.2.5	54	504
a-wave	OD	11.1.5	7	-139.4	b-wave	OD	11.1.5	54	371.4
a-wave	OS	11.2.5	7	-182.6	b-wave	OS	11.2.5	53	531.8

FIGURE 8. Scotopic-photopic intensity series for a wild type C57Black/6 mouse.

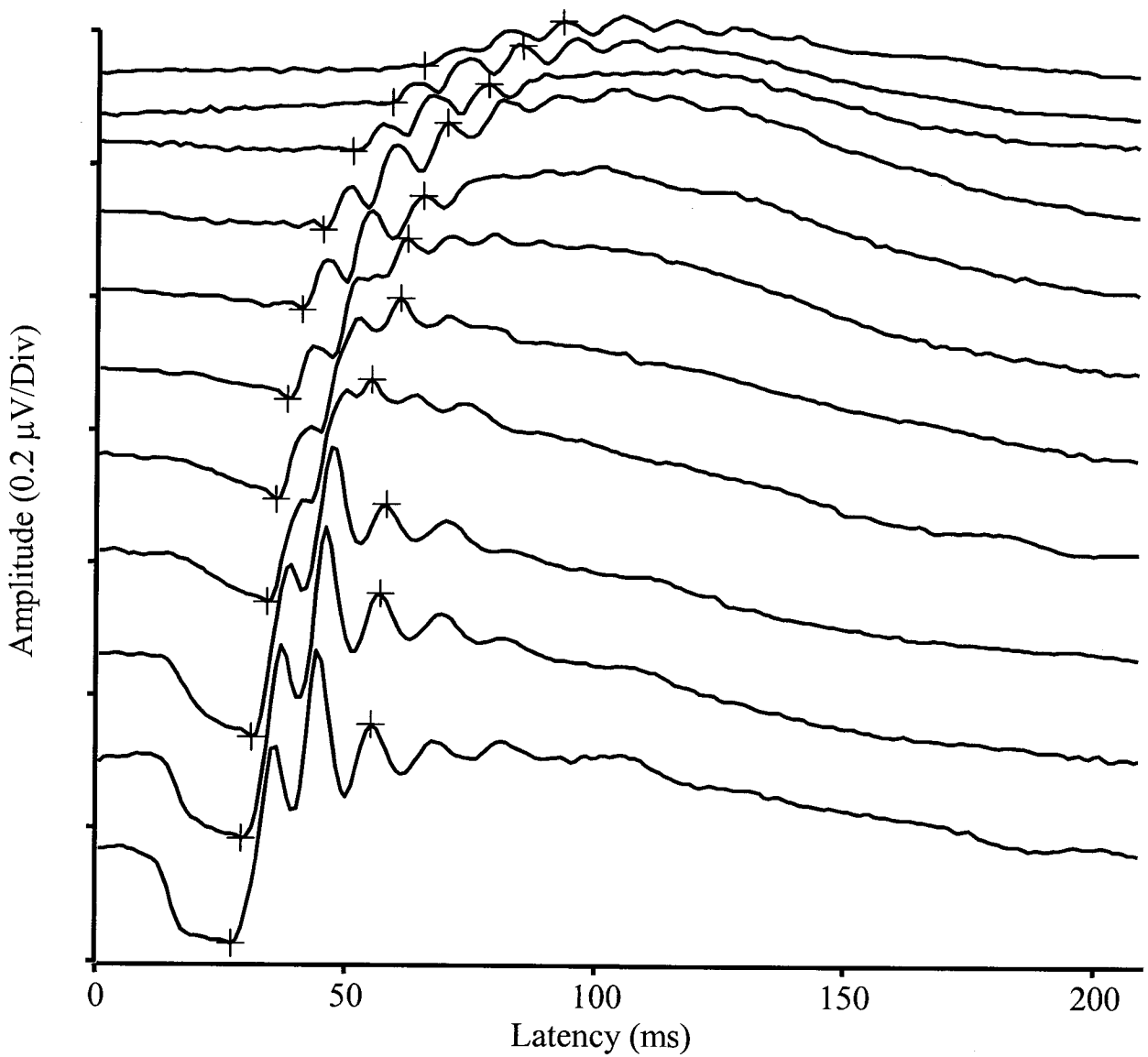
Amplitude (0.2 μV/Div)
0
50
100
150
200
Latency (ms)

amplitude data from each flash intensity step into a single curve fit. Figure 9 is an NR plot for the right and left eyes of 2 rats. The R_{max} values for the first rat (Fig. 9, panel A and B) are 946.34 and 870.16 for the left and right eyes, respectively. The calculated difference in R_{max} between the eyes is 9%. For the second rat (Fig. 9, panel C and D) the R_{max} values for the left and right eyes are 631.52 and 442.34, which corresponds to a 30% difference in retinal responsiveness between the eyes. Therefore, differences in baseline values between the left and right eye are considered before an animal is included in a study whenever possible.

3.2 Dilation Effects

Published ERG methods with albino rats have always used 1% tropicamide to dilate the pupils (Aleman et al., 2001b; Timmers et al., 2001). In order to see if this had an effect on R_{max}, rats were tested under different dilation conditions. NR plots were generated from animals that were tested on four consecutive days (Fig. 10). Table 2A summarizes the R_{max} values obtained from both animals. Overall, the NR analysis showed variability in ERG profiles from day-to-day. This appears to be independent of dilation status. However, interocular comparisons of R_{max} in both animals did not show significant differences ($\leq$ 17%) day-to-day whether the animals had their pupils dilated or not the only exception being in rat D1 on 26/09/01 where the R_{max} values differed by 24%.

In addition to looking at dilation effects, the NR plots shown in figure 10 also serve to show the test/re-test applicability of the Espion™ system. In dark-adapted humans, ERG amplitudes can vary up to 20% from one test series to the

FIGURE 9. NR plots of two wild type rats. The R_{max} values between the left (**A**) and right (**B**) eyes of this rat differ by 9% whereas in the second rat the left (**C**) and right (**D**) eyes are differ by 30%. When possible, rats that show significant differences between eyes at baseline are removed from the study.

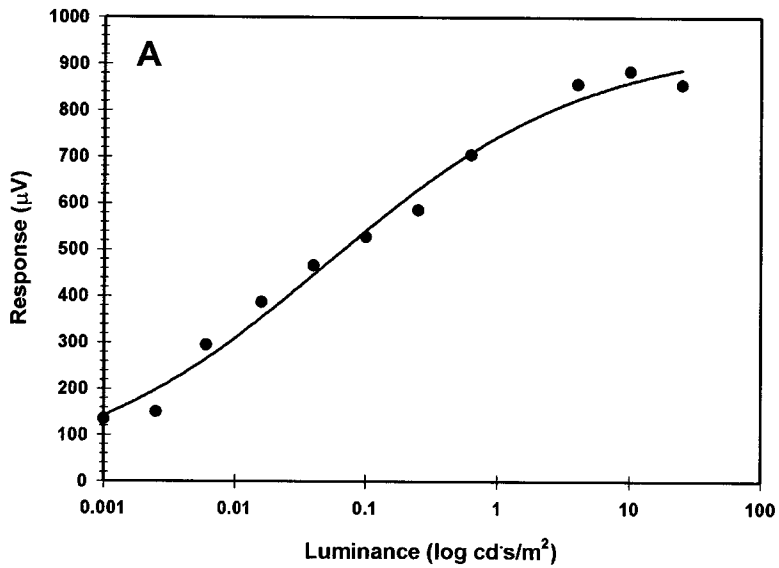
A
Response (μV)
1000
900
800
700
600
500
400
300
200
100
0
0.001
0.01
0.1
1
10
100
Luminance (log cd·s/m²)

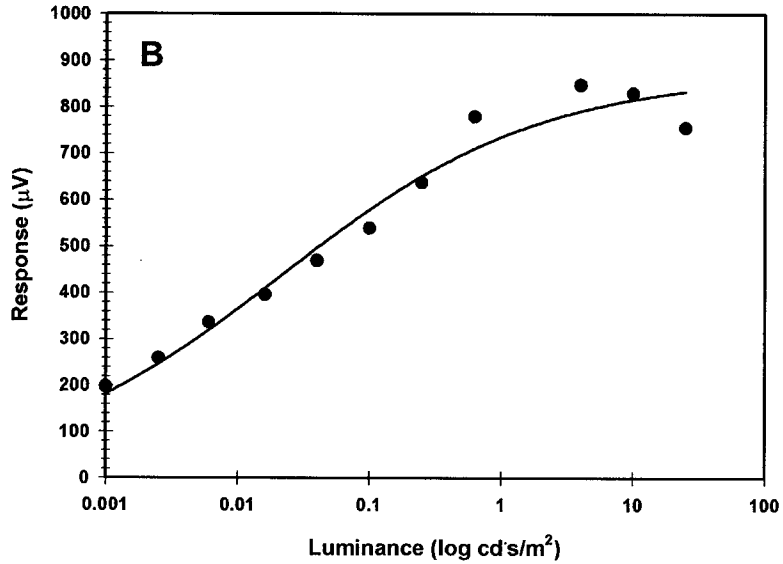
B
Response (μV)
1000
900
800
700
600
500
400
300
200
100
0
0.001
0.01
0.1
1
10
100
Luminance (log cd·s/m²)

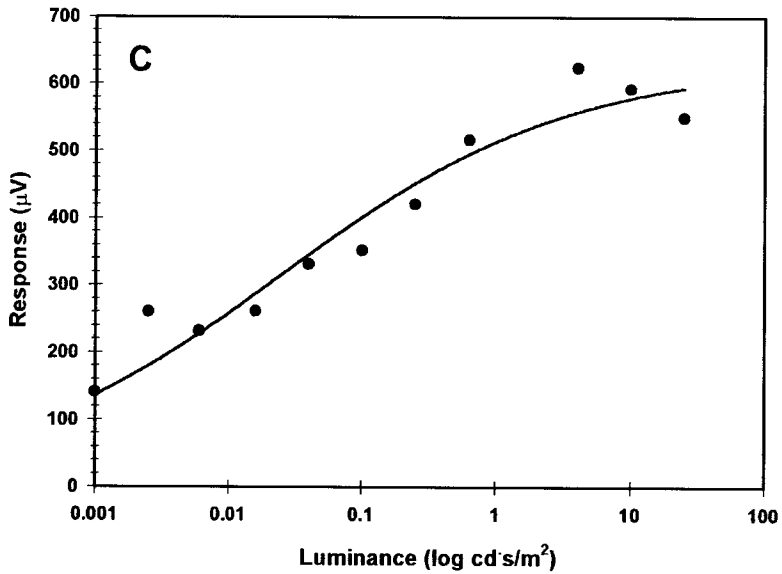
C
Response (μV)
700
600
500
400
300
200
100
0
0.001
0.01
0.1
1
10
100
Luminance (log cd·s/m²)

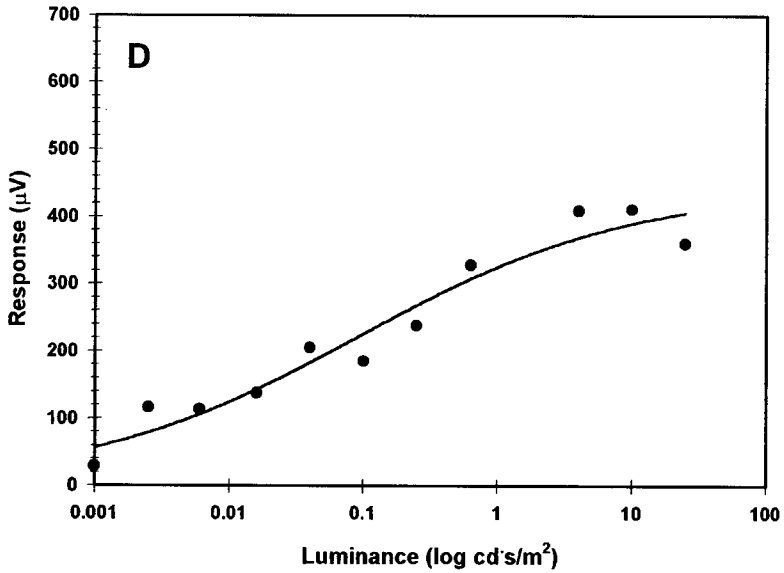
D
Response (μV)
700
600
500
400
300
200
100
0
0.001
0.01
0.1
1
10
100
Luminance (log cd·s/m²)

FIGURE 10. NR plots from four consecutive days of ERGs on two wild type rats after various dilation procedures were performed on each eye on different days. The left (**A**) and right (**B**) eyes are of rat D1. The left and right eyes of rat D2 are represented in panel **C** and **D**, respectively.

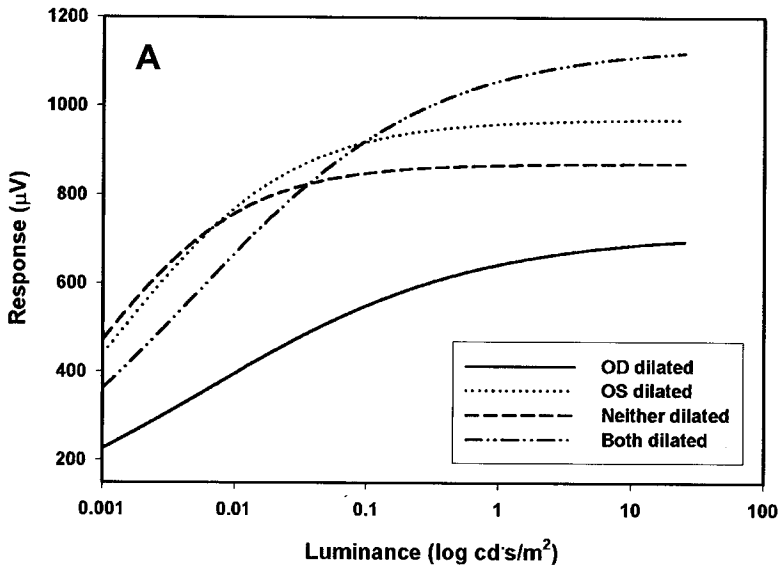
A
1200
1000
800
600
400
200
Response (μV)
0.001
0.01
0.1
1
10
100
Luminance (log cd·s/m²)
OD dilated
OS dilated
Neither dilated
Both dilated

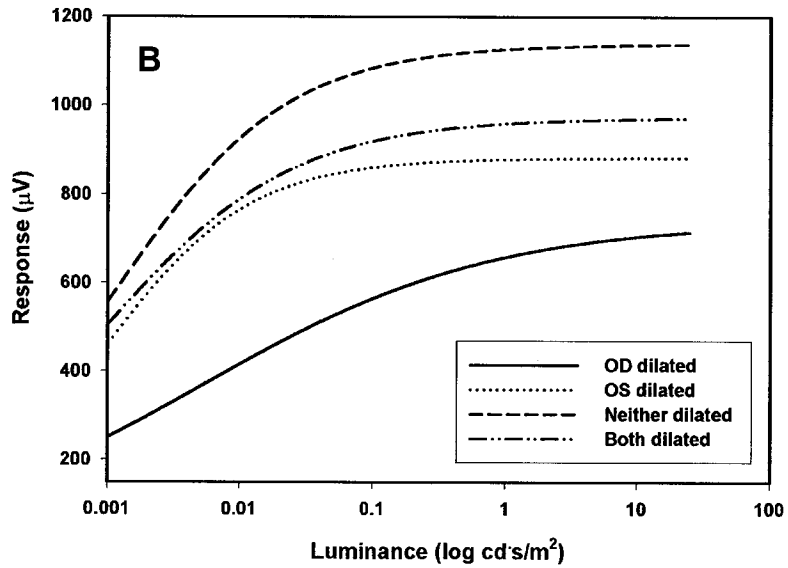
B
1200
1000
800
600
400
200
Response (μV)
0.001
0.01
0.1
1
10
100
Luminance (log cd·s/m²)
OD dilated
OS dilated
Neither dilated
Both dilated

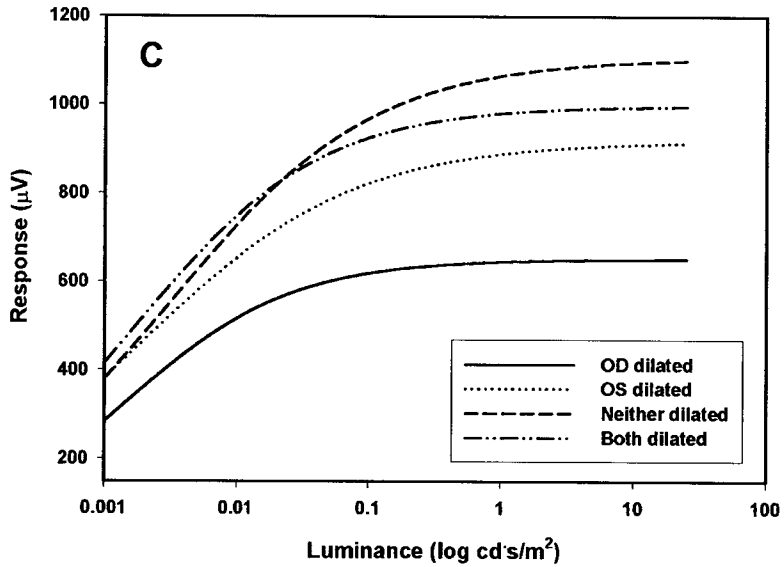
C
1200
1000
800
600
400
200
Response (μV)
0.001
0.01
0.1
1
10
100
Luminance (log cd·s/m²)
OD dilated
OS dilated
Neither dilated
Both dilated

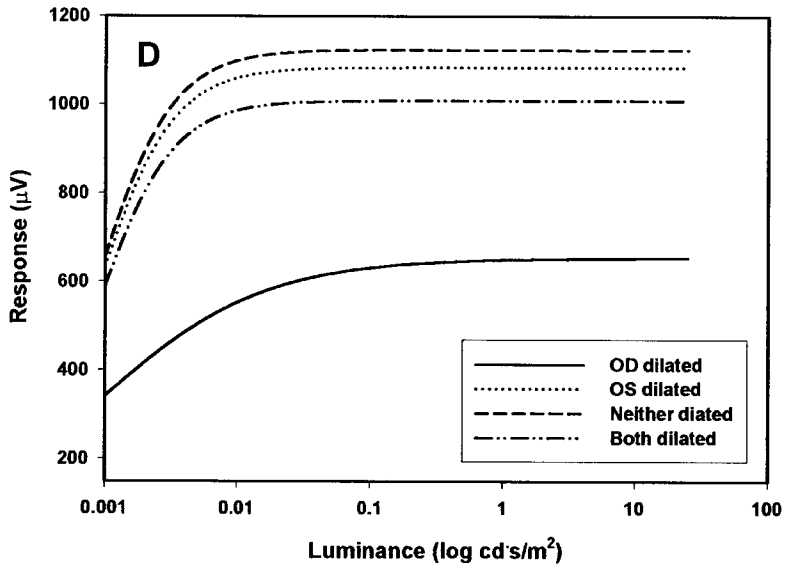
D
1200
1000
800
600
400
200
Response (μV)
0.001
0.01
0.1
1
10
100
Luminance (log cd·s/m²)
OD dilated
OS dilated
Neither diated
Both dilated

TABLE 2. (**A**) R_{max} values of rats D1 and D2 over four consecutive test days. (**B**) Calculated differences in R_{max} between individual eyes and the average R_{max} obtained over the course of four days.

A

	Rat D1		Rat D2	
	R_{max}		R_{max}	
Test Date	OS	OD	OS	OD
24/09/01 OD dilated	738.93	715.14	652.12	654.36
25/09/01 OS dilated	882.14	971.61	918.87	1084.21
26/09/01 neither dilated	1138.84	871.11	1107.03	1124.16
27/09/01 both dilated	973.14	1138.08	999.32	1009.27

B

Animal	Date	OD	Difference from average	Perent Difference
D1	24-Sep	738.93	194.33	>20%
	25-Sep	882.14	51.12	<20%
	26-Sep	1138.84	-205.58	>20%
	27-Sep	973.14	-39.88	<20%
	Average Rmax	933.26		
D2	24-Sep	654.36	313.64	>20%
	25-Sep	1084.21	-116.21	<20%
	26-Sep	1124.16	-156.16	<20%
	27-Sep	1009.27	-41.27	<20%
	Average Rmax	968.00		
Animal	Date	OS		
D1	24-Sep	715.14	208.85	>20%
	25-Sep	971.61	-47.62	<20%
	26-Sep	871.11	52.87	<20%
	27-Sep	1138.08	-214.10	>20%
	Average Rmax	923.99		
D2	24-Sep	652.12	267.21	>20%
	25-Sep	918.87	0.46	<20%
	26-Sep	1107.03	-187.69	>20%
	27-Sep	999.32	-79.98	<20%

next (Grover et al., 2003). No published data on rodents is available as to whether or not the same effect holds true. The average R_{max} values over the course of four days for the left and right eyes of rat D1 were 923.99 and 933.26, respectively. For rat D2 the values were 919.34 and 968.00 for the left and right eyes. On two out of the four days of testing, both the left and right eye of rat D1 had R_{max} values that differed less than 20% of the average. The left eye of rat D2 showed a similar trend as the eyes of rat D1. The right eye of rat D2 had R_{max} values that differed less than 20% of the average on three out of the four days of testing (Table 2B). It should be noted that the +/- differences from each eye are have a random distribution (see Table 2B).

The scotopic-photopic intensity series was also tested on a pigmented rat strain known as Long Evans. The intensity showed no gross differences in the ERG waveform compared to the Sprague-Dawley strain (data not shown).

3.3 MNU Dose Titration in Sprague Dawley Rats

3.3.1 Naka-Rushton analysis

Baseline NR plots were generated for OS and OD for all dosages (Fig. 11). An ANOVA test revealed that the R_{max} values between the left and right eye were not significantly different ($F(1,8)=0.529$; $p<0.49$ F crit=5.32). In addition, there was no significant difference in R_{max} between the different dose groups ($F(4,5)=3.83$; $p<0.09$ F crit=5.19).

Since there was no significant difference in the NR plots between OS and OD, only the NR plots from the right eye are presented here. However, all ANOVA analyses include data from both eyes. For animals at the 20 and 30mg/kg dose there were no significant decreases in R_{max} from T_0 to 1_{Wk} post MNU (Fig.12 and

FIGURE 11. OS and OD baseline NR plots. Panel **A** (OS) and panel **B** (OD) are the baseline NR plots of each eye for all the dose groups. Each curve was obtained by averaging the b-wave amplitudes of each group (n=4), and fitting the average to the NR equation.

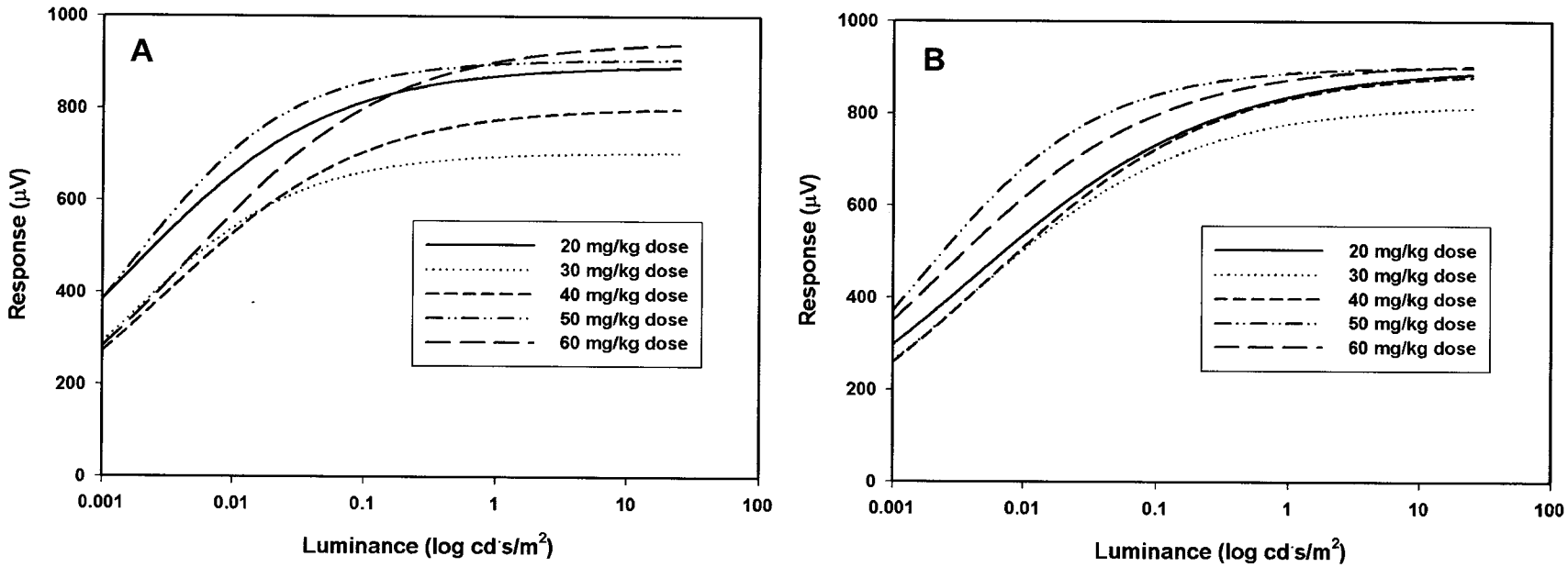
A
B
Response (μV)
Luminance (log cd·s/m²)
0
200
400
600
800
1000
0.001
0.01
0.1
1
10
100
20 mg/kg dose
30 mg/kg dose
40 mg/kg dose
50 mg/kg dose
60 mg/kg dose

FIGURE 12. NR plots for the right eye at various doses post-MNU. This figure illustrates the effect of MNU dosage over the course of one week. Panel **A** is the OD baseline plot. Panel **B** is 24 hours post MNU injection. Panel **C** is 72 hours post MNU injection and panel **D** is one-week post MNU. Each curve is the average b-wave amplitude for four animals.

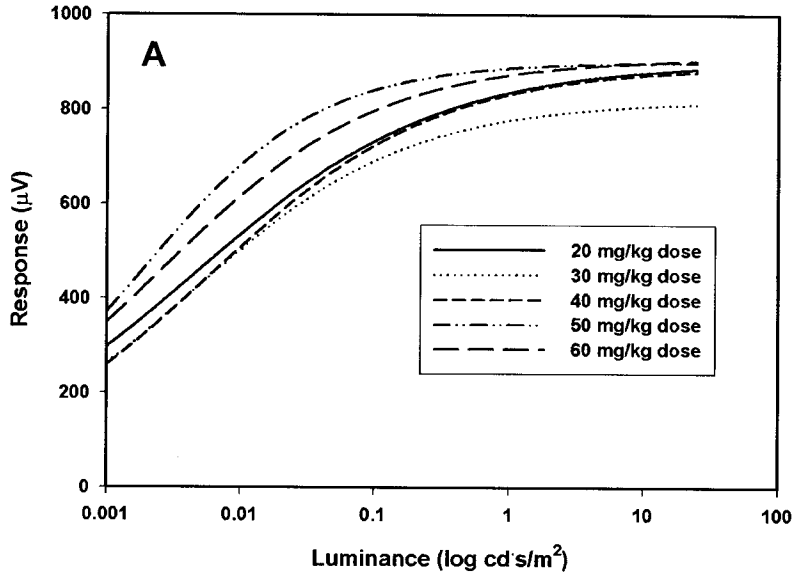
A
Response (μV)
1000
800
600
400
200
0
0.001
0.01
0.1
1
10
100
Luminance (log cd·s/m²)
20 mg/kg dose
30 mg/kg dose
40 mg/kg dose
50 mg/kg dose
60 mg/kg dose

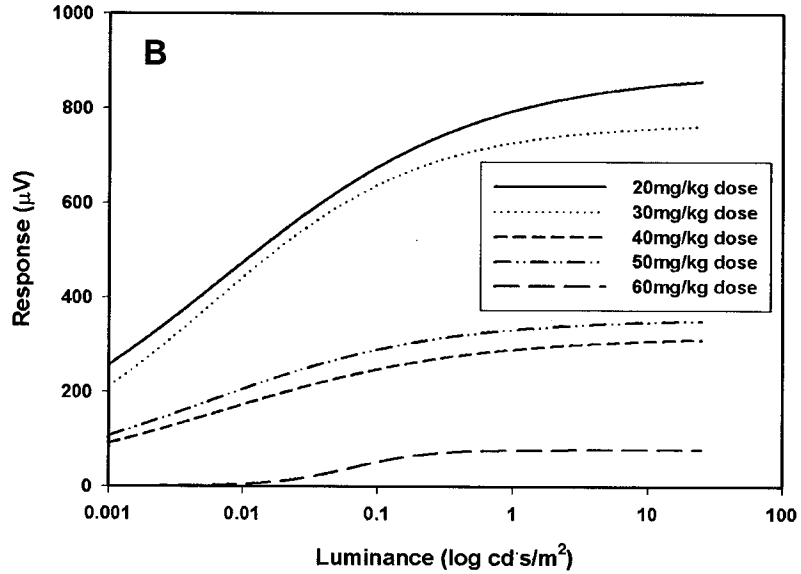
B
Response (μV)
1000
800
600
400
200
0
0.001
0.01
0.1
1
10
100
Luminance (log cd·s/m²)
20mg/kg dose
30mg/kg dose
40mg/kg dose
50mg/kg dose
60mg/kg dose

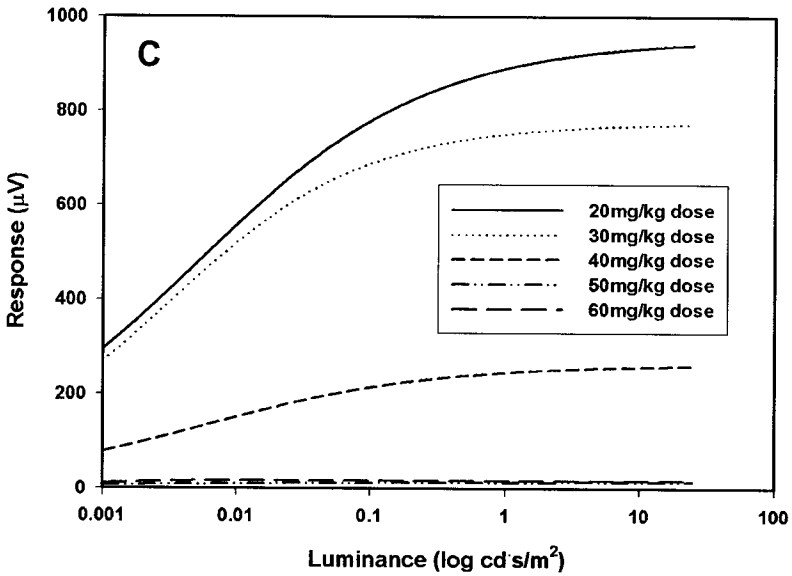
C
Response (μV)
1000
800
600
400
200
0
0.001
0.01
0.1
1
10
100
Luminance (log cd·s/m²)
20mg/kg dose
30mg/kg dose
40mg/kg dose
50mg/kg dose
60mg/kg dose

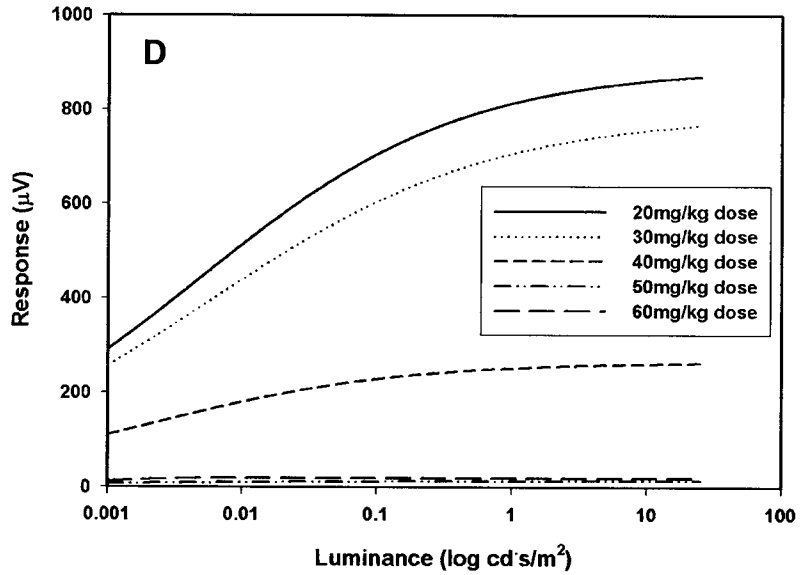
D
Response (μV)
1000
800
600
400
200
0
0.001
0.01
0.1
1
10
100
Luminance (log cd·s/m²)
20mg/kg dose
30mg/kg dose
40mg/kg dose
50mg/kg dose
60mg/kg dose

TABLE 3. Average R_{max} values of each dose group over time (**A**). There were four animals in each dose group. **B** is a summary table of the ANOVA of all the dose groups illustrating the change of R_{max} from T0 to T1Wk. The ns designates non significance ($p<0.05$). The F critical value in all the dose groups was 2.94668.

A

Dose Group mg/kg (n=4)	Baseline R_{max}	T24 R_{max}	T72 R_{max}	T1wk R_{max}
20	898.6155	797.3886	792.6312	874.3614
30	764.61	732.252	697.7906	711.8046
40	853.3405	316.5081	297.8526	269.474
50	938.3301	75.34991	17.44718	20.96709
60	910.8418	91.14451	19.74021	13.88169

B

MNU Dosage mg/kg	# of eyes	F-value	P value
20	8	0.707039	0.556505 (ns)
30	8	0.295492	0.828311 (ns)
40	8	27.67185	1.6E-08
50	8	191.7284	9.14E-19
60	8	255.4375	1.95E-20

Table 3). In striking contrast, there were highly significant decreases in R_{max} at 1_{Wk} for those animals receiving MNU in dosages ranging from 40-60 mg/kg. These dosage-dependent reductions in R_{max} were readily apparent within 24 hours following MNU administration (T24, F=35.1, p<0.00000019) and remained significantly decreased at one-week post MNU (Table 3 and Fig. 12). In figure 12 panels A through D illustrate the NR curve fitting for animals at all five doses.

At the 40 mg/kg dose there was a significant decrease in R_{max} at the 24h-time point (Fig. 12B) and this value did not change significantly at 72h and at one week (Fig. 12C, D). At 50 and 60 mg/kg, there was an initial significant decrease in the R_{max} value at 24 hours post-MNU treatment which decreased further by 72 hours. There were no significant differences in R_{max} at the one-week time point in comparison to the 72h time point (Fig. 12A-D).

3.4 MNU Dose Response in Mice

Figure 13 shows the baseline NR plots from the left (panel A) and the right eyes (panel B) of mice prior to MNU treatment. Each dose group had four mice. An ANOVA test indicated that there was no significant difference in R_{max} between the left and right eye ($F(1,8)=0.76$; $p<0.41$, F crit =5.32) and between the different dose groups ($F(4,5)=1.83$; $p<0.26$, F crit=5.19). Figure 14 shows the NR plots after one-week post MNU injection. ANOVA revealed that there was no significant difference between the two eyes at each dose after MNU treatment ($F(1,8)=0.05$; $p<0.833$, F crit=5.32). At this one-week time point, there was no significant difference in R_{max} at the 20, 25 and 30 mg/kg doses ($F(2,3)=3.00$; $p<0.19$, F crit=9.55). However, the 35 mg/kg dose is significantly different in R_{max} in comparisons to doses 20-30 mg/kg

FIGURE 13. Baseline NR plots in wild type mice prior to MNU dosing for the left (**A**) and right (**B**) eyes. Each plot is an average of four animals.

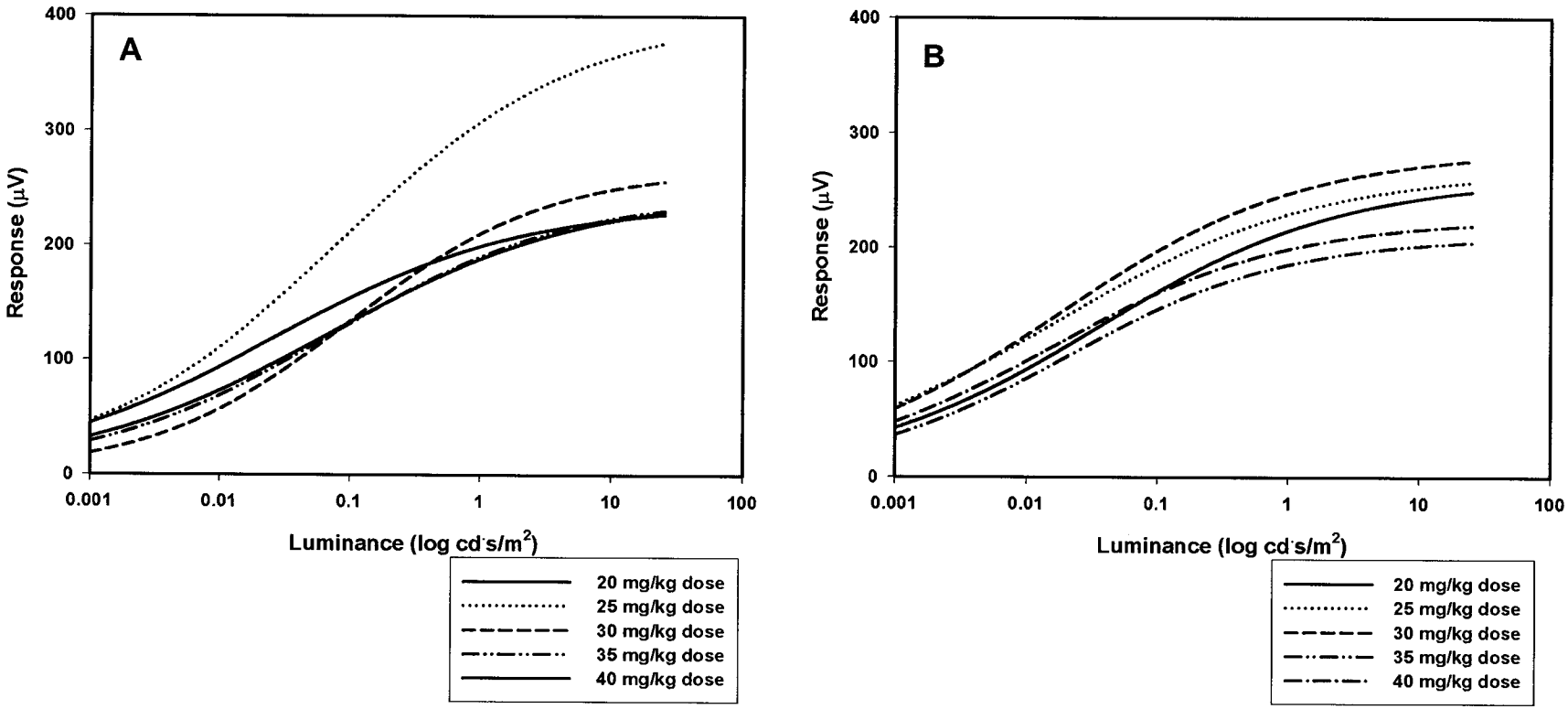
A
B
400
300
200
100
0
Response (μV)
0.001
0.01
0.1
1
10
100
Luminance (log cd·s/m²)
20 mg/kg dose
25 mg/kg dose
30 mg/kg dose
35 mg/kg dose
40 mg/kg dose

FIGURE 14. NR plots post MNU in C57/Black6 mice. Panel **A** and **B** are the plots of the left and right eyes, respectively at one-week post MNU. Each plot represents an average of four animals.

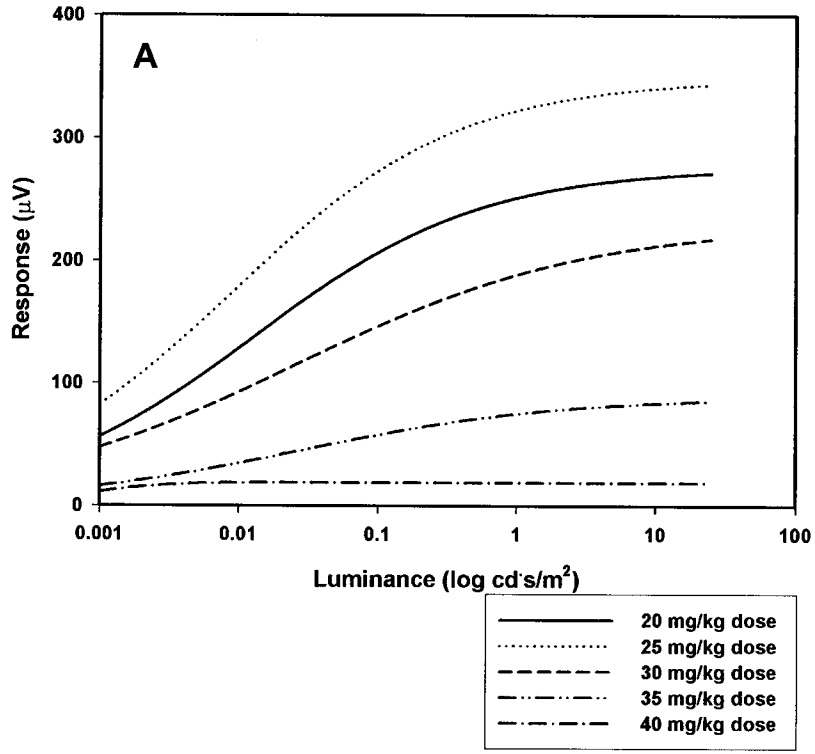
A
400
300
200
100
0
Response (μV)
0.001
0.01
0.1
1
10
100
Luminance (log cd·s/m²)
20 mg/kg dose
25 mg/kg dose
30 mg/kg dose
35 mg/kg dose
40 mg/kg dose

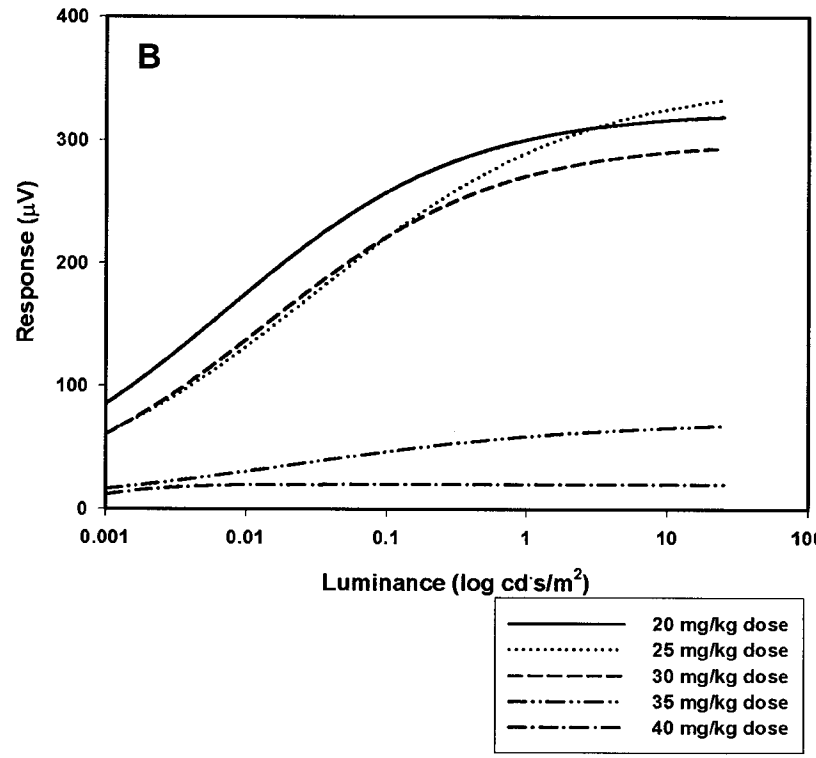
B
400
300
200
100
0
Response (μV)
0.001
0.01
0.1
1
10
100
Luminance (log cd·s/m²)
20 mg/kg dose
25 mg/kg dose
30 mg/kg dose
35 mg/kg dose
40 mg/kg dose

($F(3,4)=29.91$; $p<0.0034$, F crit=6.59) and this difference is much more pronounced when the 40 mg/kg dose is included in the analysis ($F(4,5)=56.51$; $p<0.0002$, F crit=5.19). The 40 mg/kg dose caused extinction of the b-wave in the mouse ERG (Fig. 14A, B).

3.5 XIAP Protects Photoreceptors from Chemotoxic Insult

The purpose of this experiment was to test the therapeutic effects of rAAV-XIAP in a MNU induced model of retinal degeneration.

3.5.1 XIAP Over-expression in the Retina

Real-time PCR analysis (*Taq*man™; Applied Biosystems) with primers specific to human XIAP (but which also cross-hybridize to endogenous rat IAP) verified XIAP over-expression in the rAAV-XIAP–injected eye in relation to endogenous IAP levels in the uninjected eye (Fig. 15). GAPDH was used as an internal control to confirm the integrity of the mRNA. Western blot analysis confirmed that over-expression of XIAP also occurred at the protein level (Fig. 16). The XIAP injected retina showed high levels of HA-tagged protein, which was absent in the contralateral control (Fig. 16A). Studies with the RIAP3 antibody (which binds with both the human XIAP transgene and the endogenous rat IAP) showed a clear over-expression in the XIAP-injected eye in comparison with the contralateral uninjected eye (Fig. 16B). Given that the protein extract was made from the whole retina, and only a fraction of the retina was covered by the subretinal injection, the level of XIAP over-expression at the site of the injection would be even greater than the Western blot indicates.

FIGURE 15. XIAP transgene mRNA is over-expressed in animals subretinally injected with rAAV-XIAP Taqman™ analysis of retinal samples at 12 weeks following injection shows that expression of XIAP mRNA is 13 fold greater in the eyes that received rAAV-XIAP than in the uninjected controls (GAPDH was used as a normalizing internal control). RNase treatment of samples abolished the amplification signal.

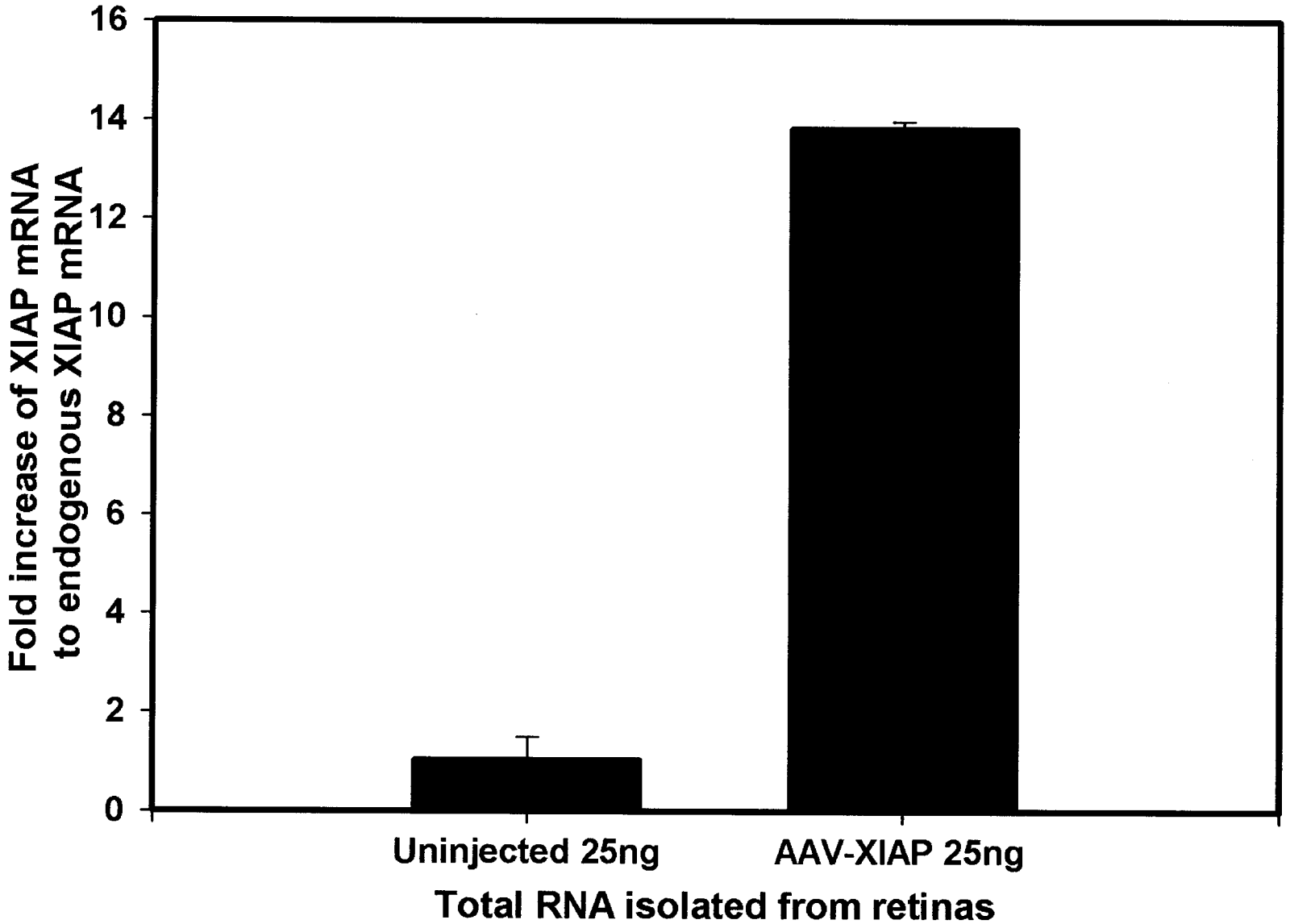
16
14
12
10
8
6
4
2
0
Fold increase of XIAP mRNA to endogenous XIAP mRNA
Uninjected 25ng
AAV-XIAP 25ng
Total RNA isolated from retinas

FIGURE 16. HA-XIAP protein is expressed in eyes treated with rAAV-XIAP. The Western blot confirms XIAP over-expression in the right eye of a rat given a subretinal injection of rAAV-XIAP. Retinae were harvested at 12 weeks post injection of AAV-XIAP. Evidence for the presence of the transgene is found in (**A**), which was probed with an antibody to the HA tagged protein. The level of over-expression is shown in (**B**), which was probed with an antibody to riap3. This antibody reacts with endogenous rat IAP as well as the XIAP transgene. *Arrows*: bands of interest.

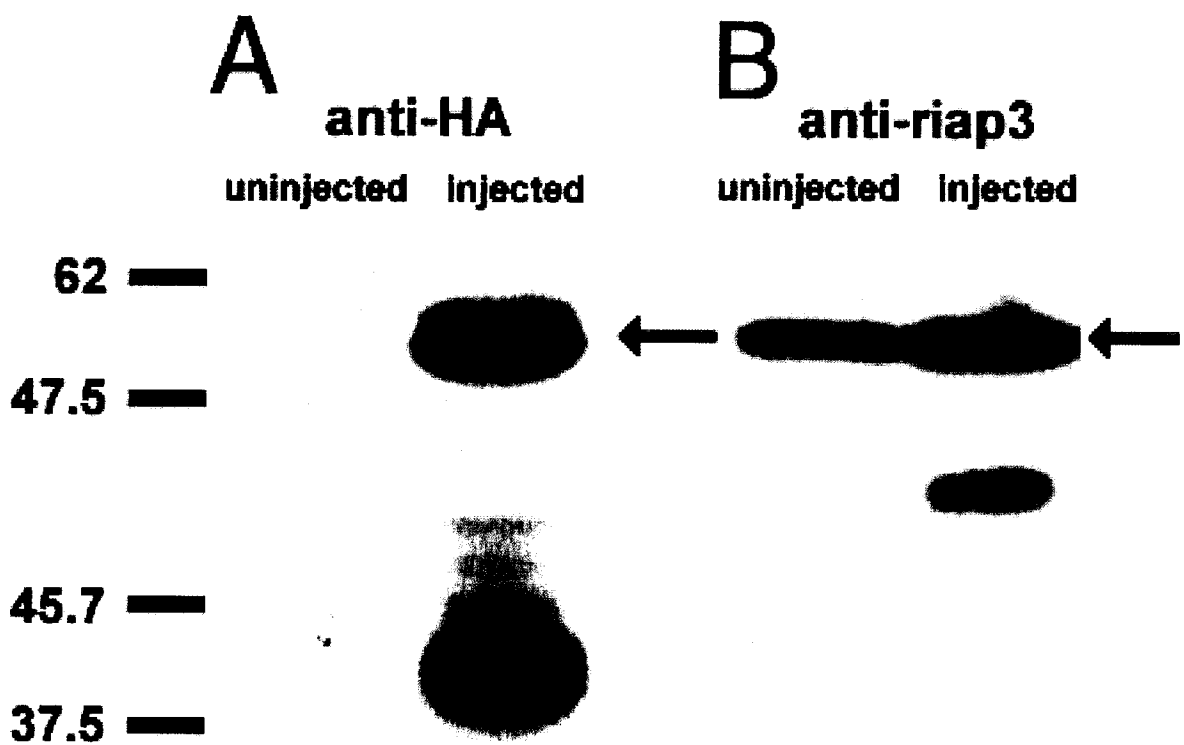
A
anti-HA
uninjected
injected
B
anti-riap3
uninjected
injected
62
47.5
45.7
37.5

3.5.2 TUNEL Staining

To assess whether XIAP protects the photoreceptor cells from acute chemotoxic insult with MNU, TUNEL staining was performed. At 24 hours after MNU treatment, the rAAV-XIAP–injected eye showed significantly fewer TUNEL-positive (apoptotic) cells than the uninjected eye of the same animal (Fig. 17). Eyes that received a rAAV-GFP subretinal injection had apoptotic profiles similar to those of uninjected controls.

3.5.3 Morphological Protection of Photoreceptors

Haematoxylin and eosin (H&E) and DAPI staining techniques were used to assess the degree of morphological protection by XIAP against MNU-induced photoreceptor apoptosis. Loss of photoreceptors was not evident at 24 hours after MNU, although the rAAV-XIAP injected eyes showed fewer TUNEL positive cells. With both H&E and DAPI staining, the retinal morphologies of the rAAV-GFP injected, rAAV-XIAP injected and uninjected eyes were indistinguishable (Figs. 18A–C, 19C, 19D). At 48 hours there was widespread destruction of the photoreceptors in the uninjected and GFP-injected eye, whereas the rAAV-XIAP–injected eye showed preservation of the ONL (Figs. 18D–F; Figs. 19E, 19F). The differences between AAV-XIAP–injected and control eyes were further accentuated at 72 hours post-MNU, when there was virtually complete destruction of the ONL in the uninjected and rAAV-GFP–injected eyes, but continued protection from apoptosis in the rAAV-XIAP–injected eye (Figs. 18G–I; Figs. 19G, 19H). At 1 week, the photoreceptors of the control eyes were essentially destroyed, whereas rAAV-XIAP–treated retinae still showed structural integrity of the photoreceptors at the injection site (Figs. 18J–L, Figs. 19I, 19J). Overall, XIAP-injected eyes showed histological protection of the ONL in 66% of the animals (four

FIGURE 17. XIAP protects photoreceptor cells from apoptosis. TUNEL staining at 24 hours post MNU treatment. Note the fewer TUNEL-positive cells in the ONL of the XIAP-injected right eye (**B**) in comparison with the uninjected left eye (**A**). 400x magnification

A

Uninjected

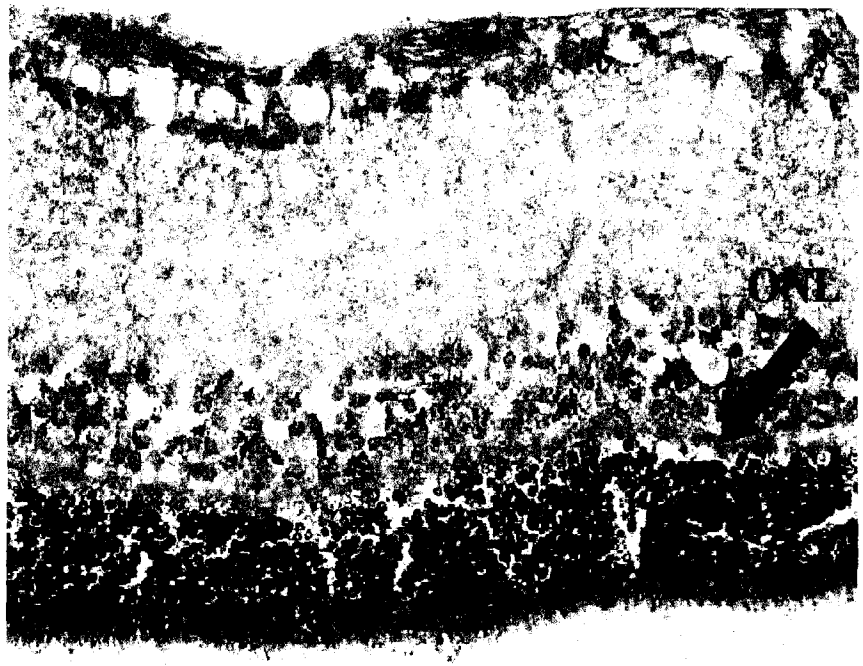

B

XIAP-injected

FIGURE 18. XIAP preserves photoreceptor structure post MNU injection. Retinal H & E sections at selected time points after MNU injection. No histological differences were apparent at 24 hours after MNU (**A**, **B**, **C**). By 48 hours after MNU, the XIAP injected ONL (**F**) had many more photoreceptor nuclei than in the GFP injected eye (**D**) or uninjected control (**E**). Differences were much more pronounced at 72 hours (compare **I** with **G**, **H**). At 1 week, XIAP injected eye showed preserved morphology of the ONL (**L**) however, this layer had completely degenerated in the GFP injected (**J**) and uninjected control (**K**). 400x magnification

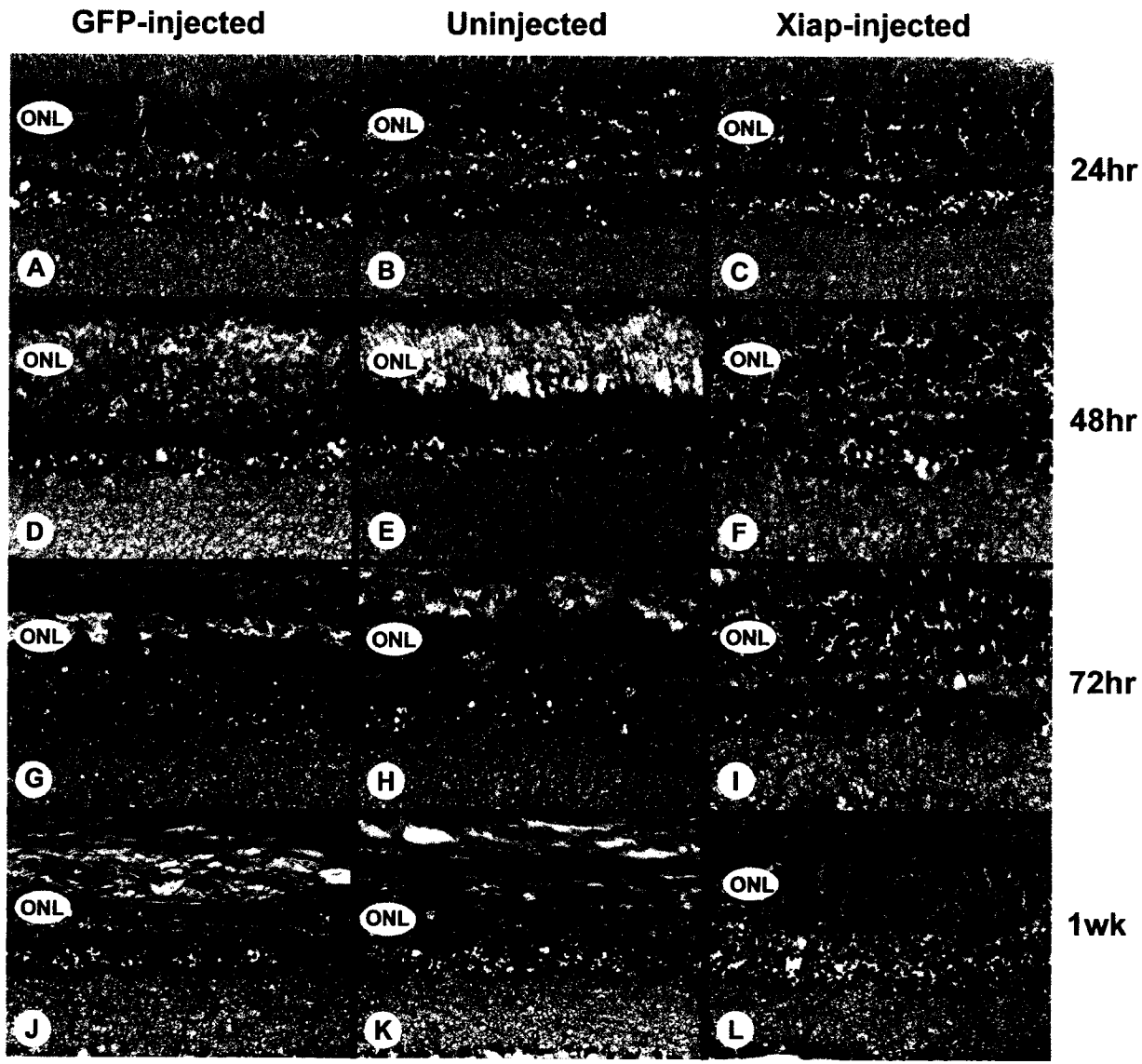
GFP-injected
Uninjected
Xiap-injected
24hr
48hr
72hr
1wk
ONL
A
B
C
D
E
F
G
H
I
J
K
L

FIGURE 19. XIAP prevents photoreceptor cell loss post MNU injection. DAPI staining of XIAP injected (**B**, **D**, **F**, **H**, **J**) and uninjected (**A**, **C**, **E**, **G**, **I**) retinae. Morphological integrity was preserved in the XIAP treated ONL up to 1 week after MNU treatment. The ONL had degenerated in uninjected retinae at 72 hours and 1 week (**G** and **I**, respectively). 400x magnification

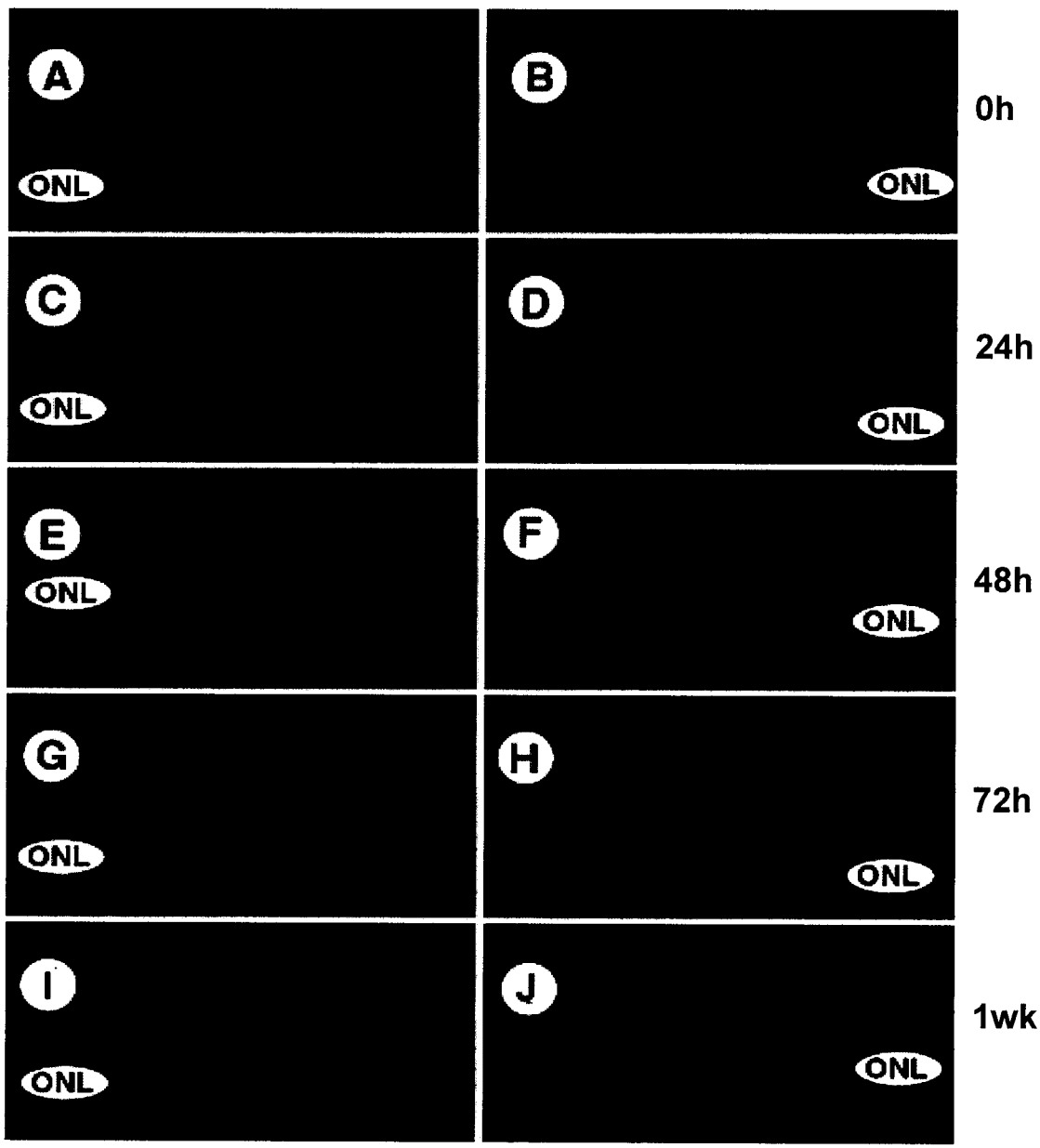
A
ONL
B
ONL
0h
C
ONL
D
ONL
24h
E
ONL
F
ONL
48h
G
ONL
H
ONL
72h
I
ONL
J
ONL
1wk

of six) at each of the time points tested. The greatest degree of protection was seen in the vicinity of the subretinal injection. Protection diminished and eventually disappeared, moving away from the injection site.

3.5.4 Functional Protection of Photoreceptors against MNU

ERG recordings were taken to ascertain whether functional protection correlated with histological rescue at designated times after MNU treatment. At 24 hours after MNU, both the XIAP-treated and the control eye showed reductions in both the a- and b-wave amplitudes indicating that functional changes preceded structural alterations. This trend continued at the 48- and 72-hour time points. However, at 1 week after MNU, the uninjected eye showed an extinguished ERG, whereas the rAAV-XIAP–treated eye showed a diminished but recordable ERG response in two of the four animals that showed morphological protection (Fig. 20). These animals had b-wave amplitudes of 10.2 and 26.0 μV at an intensity of 0.25 cd·s/m2. The average normal b-wave amplitude at this intensity is 206.4 ± 81.2 μV. Thus, the 1-week ERG in the rAAV-XIAP–treated eyes retained 5% to 15% of the b-wave amplitude in comparison with the pre-MNU baseline.

3.6 Age Related Study of rAAV-XIAP Treated Rats

The four rats that were chosen for this study were extra animals that were left over from the MNU protocol. These animals had their ERGs recorded seven months after being injected sub-retinally with rAAV-XIAP. Figure 21 shows the average b-wave amplitudes between the treated eye (OD) and the untreated eye (OS) of four animals.

FIGURE 20. XIAP preserves retinal function post MNU injection. Representative full-field flash ERGs from a control rat (*two upper traces*) before MNU injection. The lower two traces are ERGs from a XIAP-treated right eye (OD) and untreated left eye (OS) of an experimental subject at 7 days after MNU treatment. The intensity of the flash in all four traces was 0.25 cd·s/m^2. The XIAP-treated eye showed a recordable ERG with greatly reduced a- and b-wave amplitudes. The unprotected eye showed an extinguished and nonrecordable ERG trace.

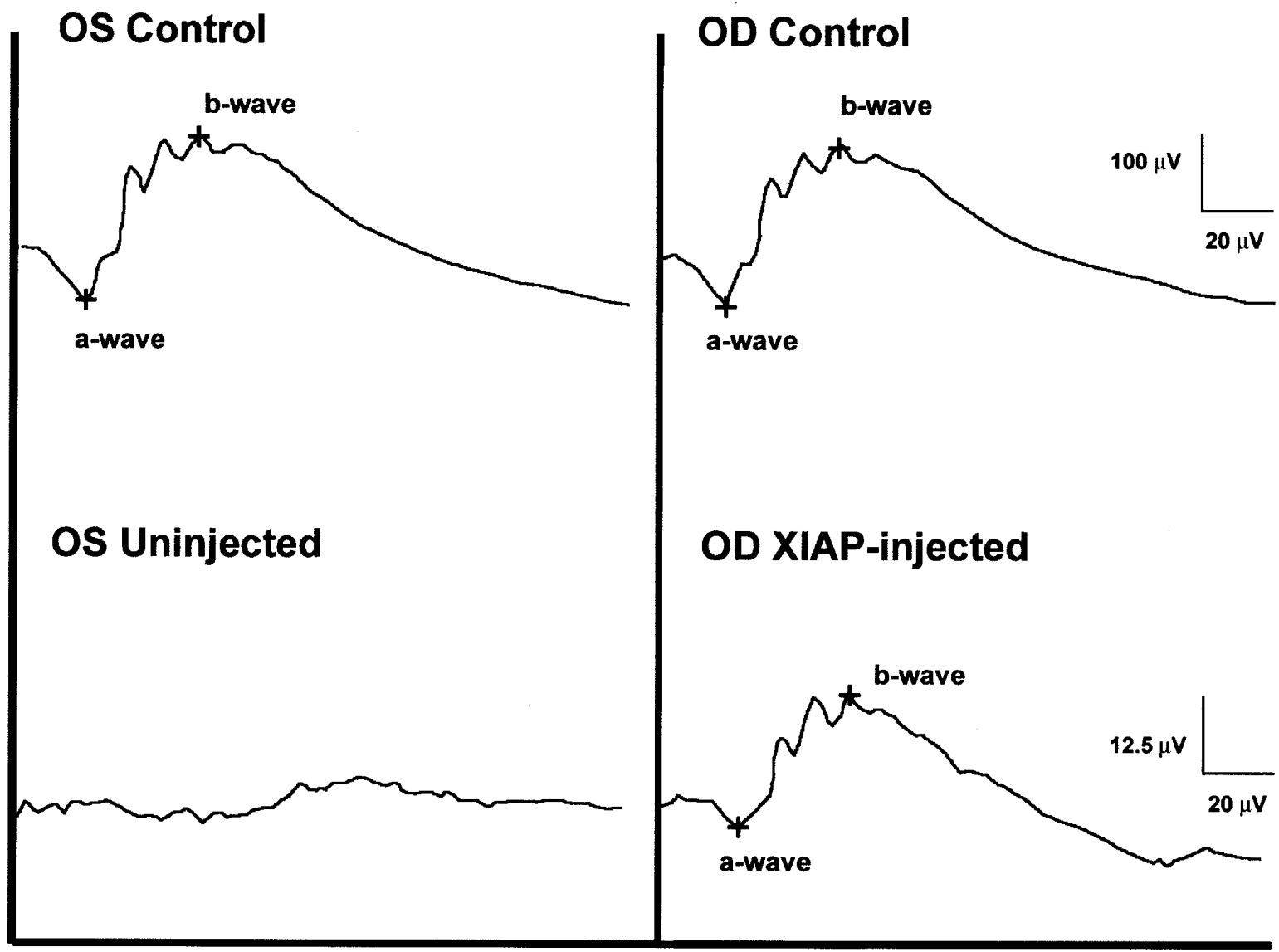
OS Control
b-wave
a-wave
OD Control
b-wave
100 µV
20 µV
a-wave
OS Uninjected
OD XIAP-injected
b-wave
12.5 µV
20 µV
a-wave

FIGURE 21. XIAP improves photoreceptor function in aging rats. Average of ERG amplitudes across the 11 stimulus intensities of four animals treated with XIAP in the right eye at seven months post injection. * indicates significant difference in amplitude between OD and OS as determined by Student's t-test ($p < 0.05$).

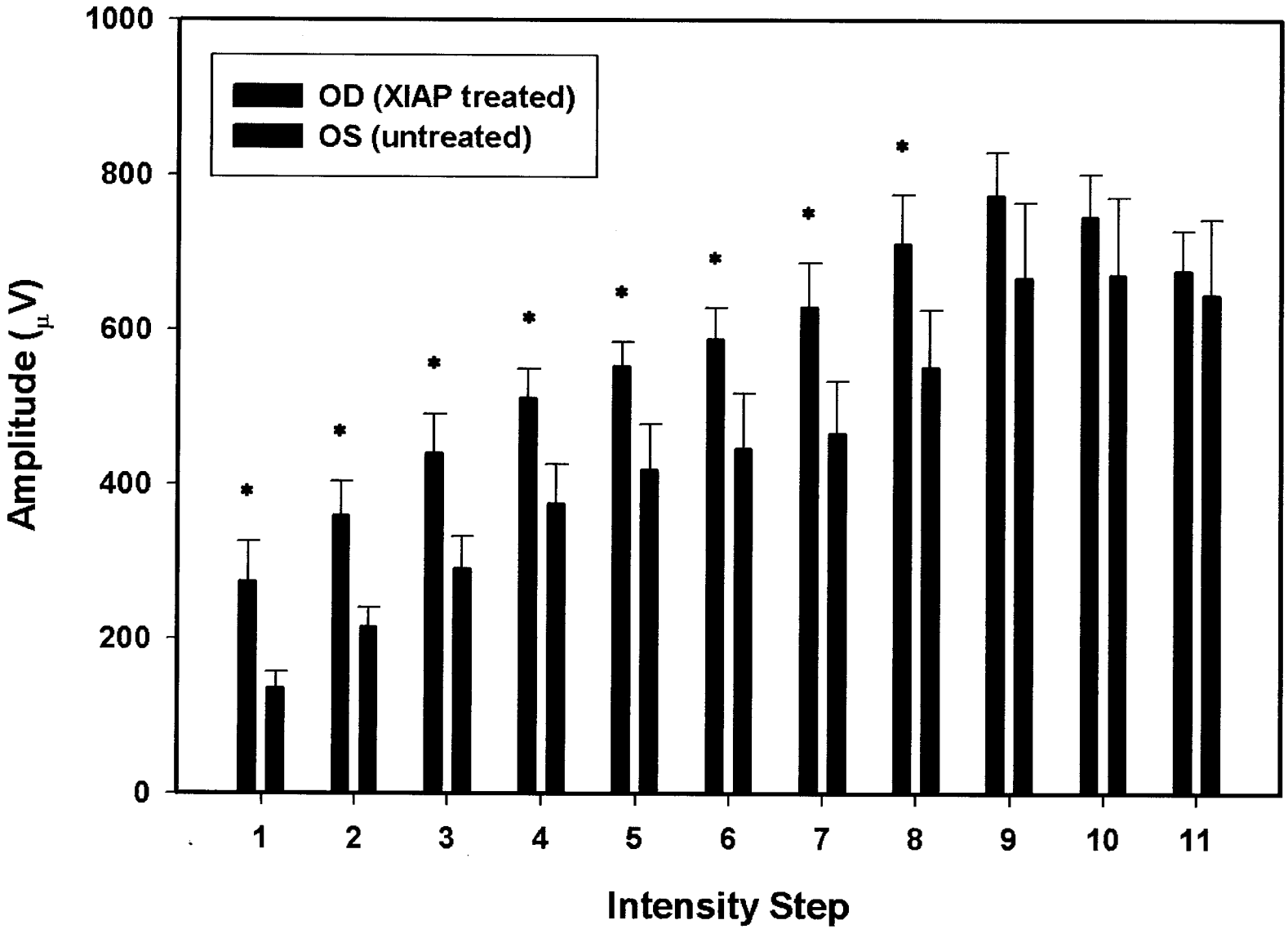
1000
800
600
400
200
0
Amplitude (μV)
OD (XIAP treated)
OS (untreated)
*
1
2
3
4
5
6
7
8
9
10
11
Intensity Step

There is a statistically significant difference in ERG amplitude through the first eight intensities as demonstrated by a Student's t-test ($p < 0.05$). All animals had a stronger b-wave response in the treated eye through the first three intensity steps. Two out of four had stronger b-wave amplitudes through the first eight steps and one animal had a stronger response in the treated eye at all eleven intensities.

3.7 XIAP Gene Therapy in Three Transgenic Rat Models of Retinal Degeneration

The P23H and S334ter-4 transgenic rats carry autosomal dominant mutations in rhodopsin that cause a progressive retinal degeneration that is similar to retinitis pigmentosa in humans. These lines of rats were obtained for the purpose of conducting gene therapy studies with rAAV-XIAP.

3.7.1 P23H Transgenic Rats

The NR plots show a steady decline in R_{max} in both eyes over time (Fig. 22). There were no observed differences between the injected eyes that received rAAV-XIAP and the GFP injected or uninjected eyes. The reasons for this will be addressed in the discussion.

3.7.2 P23H-1 and S334ter-4 Transgenic Rats

The rapid degeneration of lines P23H-1 and S334ter-4 is shown by the R_{max} values which at 48 days are already significantly lower than the P23H-3 line was at 177 days ($(F(1,20)=30.18$; $p<0.00002$, F crit=4.35) for P23H-1 and ($F(1,20)=37.79$; $p<0.000005$, F crit=4.35) for S334ter-4, respectively). Moreover, the NR plots are reduced in the injected eyes of both transgenic models (Fig. 23, 24) in comparison to the non-injected left eye. This reduction in the injected eyes was not observed in the

FIGURE 22. NR plots over time in untreated (**A**) and XIAP treated (**B**) eyes in the P23H-3 transgenic rat line. Each plot is an average of a minimum of 8 rats. The left eye served as an uninjected control. The trend shows a steady decline in retinal responsiveness over time. However, there are not any significant differences between the XIAP treated and uninjected eyes.

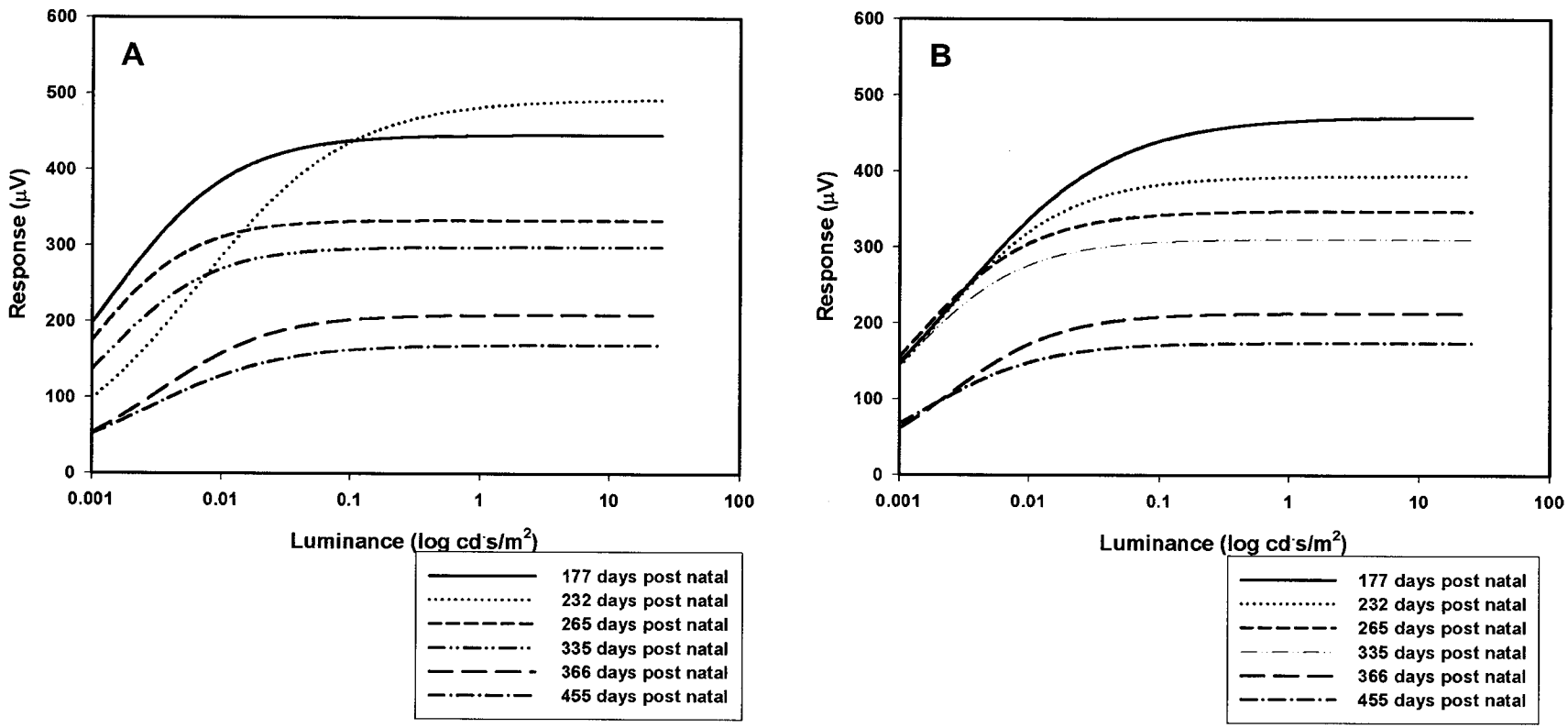
A
B
600
500
400
300
200
100
0
Response (μV)
0.001
0.01
0.1
1
10
100
Luminance (log cd·s/m²)
177 days post natal
232 days post natal
265 days post natal
335 days post natal
366 days post natal
455 days post natal

FIGURE 23. NR plots over time of the left (**A**) and XIAP treated right (**B**) eyes in the P23H-1 line of transgenic rats. Each plot is an average of a minimum of 8 rats.

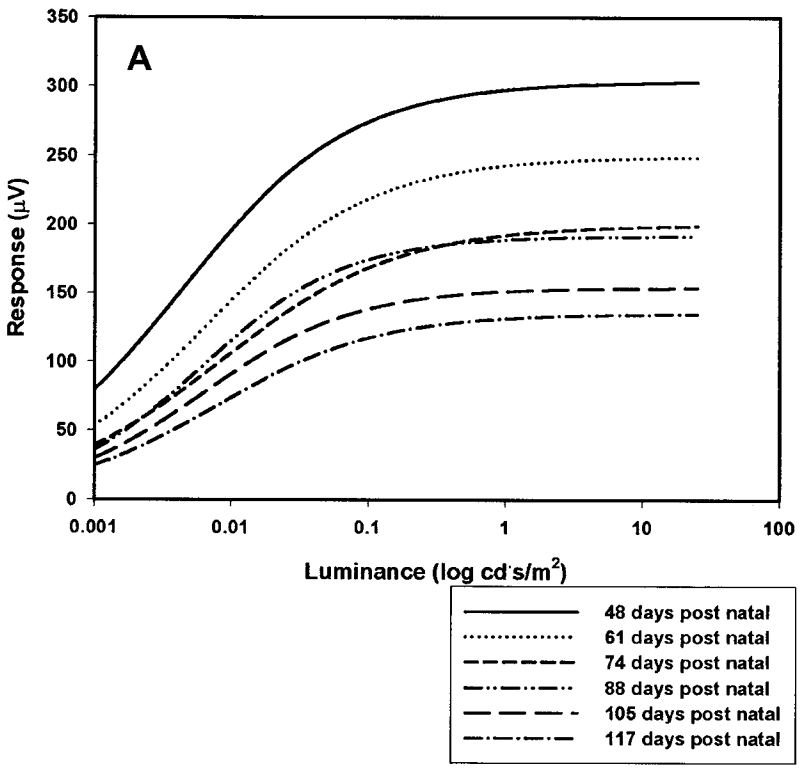
A
Response (μV)
350
300
250
200
150
100
50
0
0.001
0.01
0.1
1
10
100
Luminance (log cd·s/m²)
48 days post natal
61 days post natal
74 days post natal
88 days post natal
105 days post natal
117 days post natal

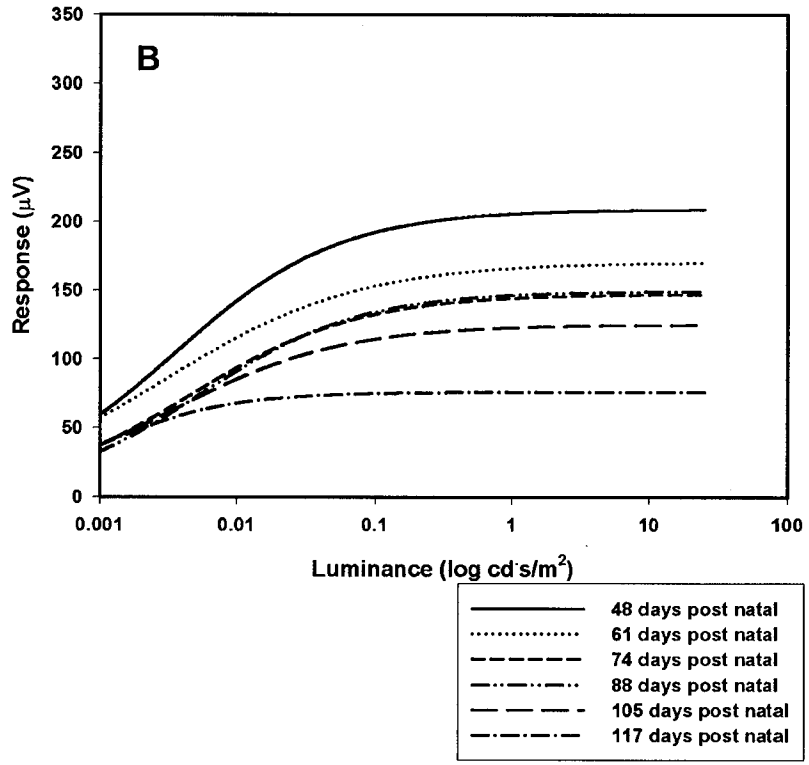
B
Response (μV)
350
300
250
200
150
100
50
0
0.001
0.01
0.1
1
10
100
Luminance (log cd·s/m²)
48 days post natal
61 days post natal
74 days post natal
88 days post natal
105 days post natal
117 days post natal

FIGURE 24. NR plots of the left (**A**) and XIAP treated right (**B**) eyes in the S334ter-4 line of transgenic rats over time. Each plot is an average of a minimum of 12 rats.

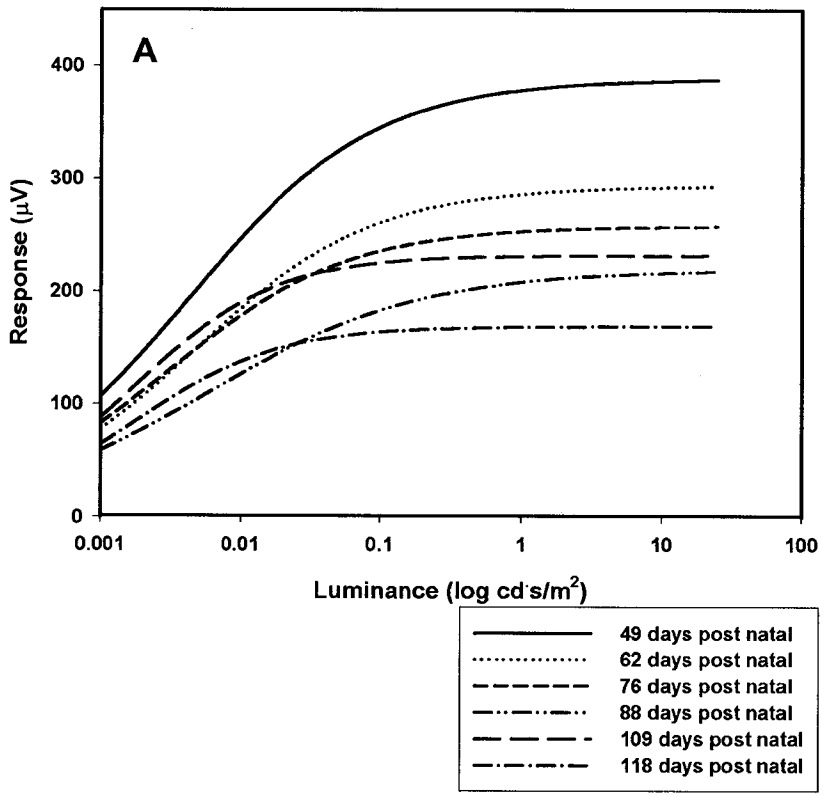
A
400
300
200
100
0
Response (μV)
0.001
0.01
0.1
1
10
100
Luminance (log cd·s/m²)
49 days post natal
62 days post natal
76 days post natal
88 days post natal
109 days post natal
118 days post natal

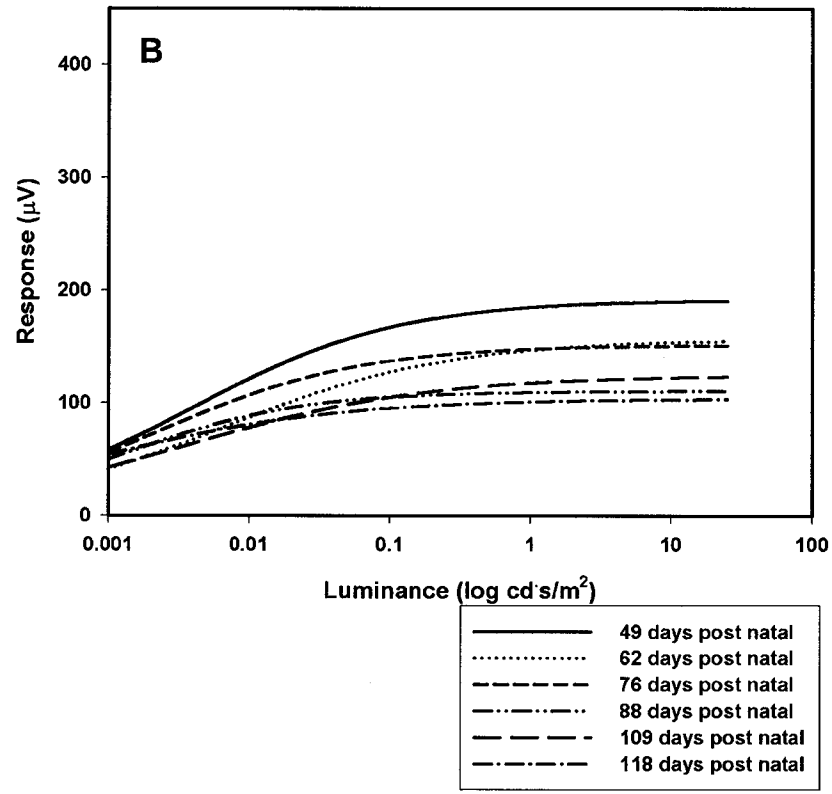
B
400
300
200
100
0
Response (μV)
0.001
0.01
0.1
1
10
100
Luminance (log cd·s/m²)
49 days post natal
62 days post natal
76 days post natal
88 days post natal
109 days post natal
118 days post natal

P23H-3 model (Fig. 22). However it should be noted that the injection procedure often causes damage which resolves with time. Since the P23H-1 and S334ter-4 rats were examined at earlier time points than the P23H-3 rats, this difference between eyes may not be significant and might possibly resolve in time if these animals continued to be monitored.

Figures 25 and 26 are the NR plots of the GFP animals in the P23H-1 and S334ter-4 transgenic rats, respectively. There were fewer animals in these treatment groups than in the XIAP treated groups and the rate of loss in ERG response is more variable than in the XIAP treated animals.

In looking at R_{max} reduction over time, in the P23H-1 line (Fig. 27A) there is a 30% greater loss in R_{max} in the left eye than in the treated eye over the course of the disease. In the S334ter-4 line (Fig. 27B) a similar trend is observed, with a greater reduction in R_{max} in the left eye (42%) over the course of time than in the injected eye. The significance of this will be addressed in the discussion.

3.8 The Generation of Transgenics Over-expressing XIAP in the Retina

A study that was run concurrently with the gene therapy experiments was the generation of mice that had a photoreceptor specific promoter driving the expression of XIAP. The reason for generating these mice was to cross them with mice that have existing retinal degeneration (rd) phenotypes. It was hoped that the resulting offspring would have a reduced rate of photoreceptor cell loss and retain a functional ERG for an extended duration over affected littermates without the transgene. There were two attempts made to generate transgenic mice that over-expressed XIAP in the retina. The

FIGURE 25. P23H-1 NR plots of GFP treated animals over time. Panel **A**, untreated (OS) panel **B,** GFP treated (OD). ERG recordings were taken from a minimum of four animals at each time point.

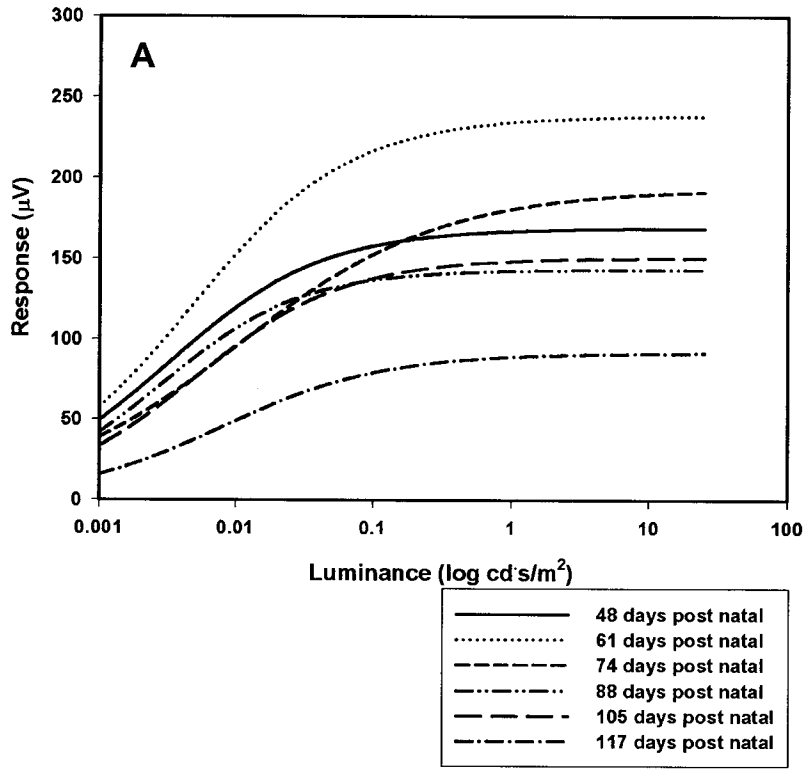
A
300
250
200
150
100
50
0
Response (μV)
0.001
0.01
0.1
1
10
100
Luminance (log cd·s/m²)
48 days post natal
61 days post natal
74 days post natal
88 days post natal
105 days post natal
117 days post natal

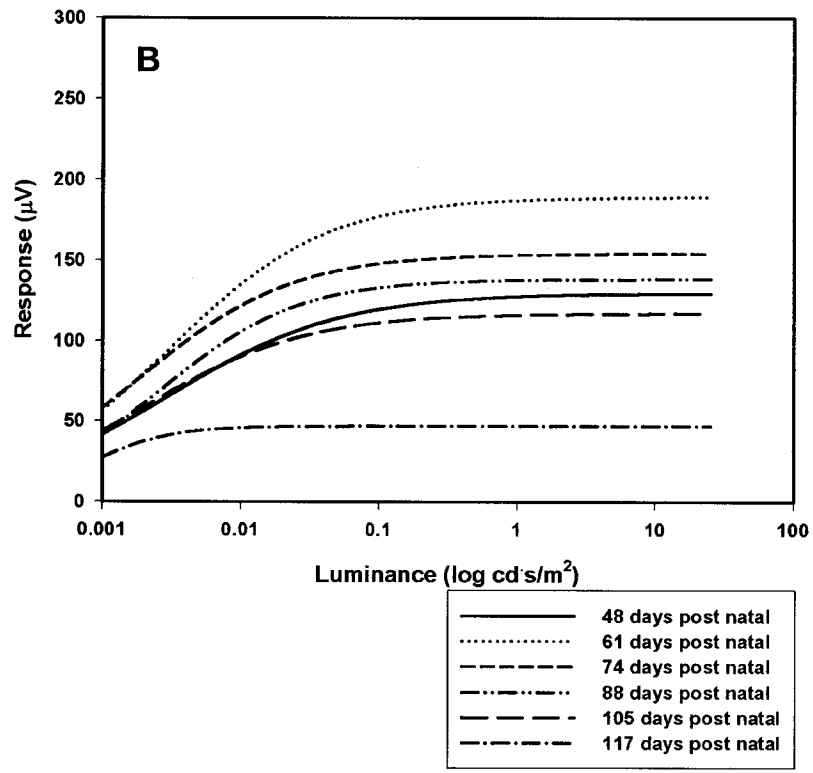
B
300
250
200
150
100
50
0
Response (μV)
0.001
0.01
0.1
1
10
100
Luminance (log cd·s/m²)
48 days post natal
61 days post natal
74 days post natal
88 days post natal
105 days post natal
117 days post natal

FIGURE 26. S334ter-4 NR plots of GFP treated animals over time. Panel **A**, untreated (OS) panel **B**, GFP treated (OD). ERG recordings were taken from a minimum of four animals at each time point.

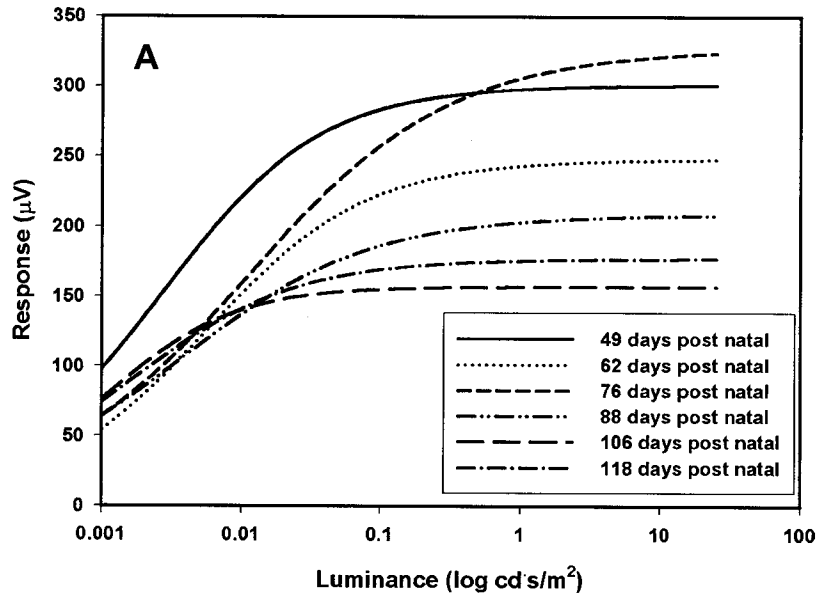
A
Response (μV)
350
300
250
200
150
100
50
0
0.001
0.01
0.1
1
10
100
Luminance (log cd·s/m²)
49 days post natal
62 days post natal
76 days post natal
88 days post natal
106 days post natal
118 days post natal

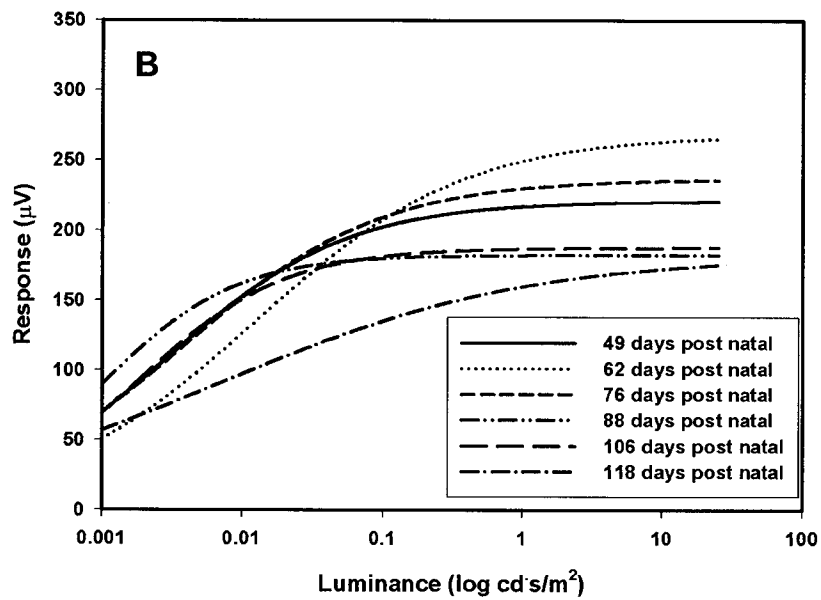
B
Response (μV)
350
300
250
200
150
100
50
0
0.001
0.01
0.1
1
10
100
Luminance (log cd·s/m²)
49 days post natal
62 days post natal
76 days post natal
88 days post natal
106 days post natal
118 days post natal

FIGURE 27. Regression analysis of R_{max} values for P23H-1 (**A**) and S334ter-4 (**B**) rats over time. Note the more rapid decrease of R_{max} values in the uninjected eye over time in both transgenic lines.

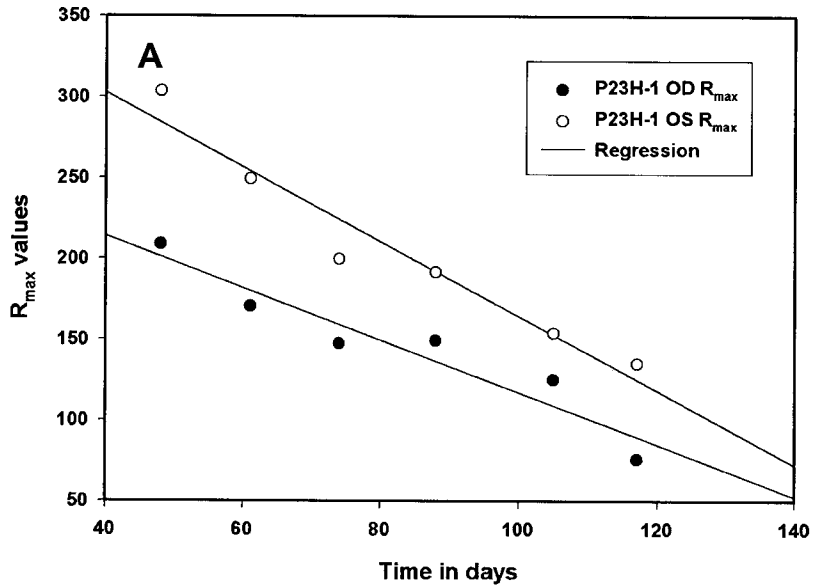
A
P23H-1 OD R_{max}
P23H-1 OS R_{max}
Regression
R_{max} values
Time in days
350
300
250
200
150
100
50
40
60
80
100
120
140

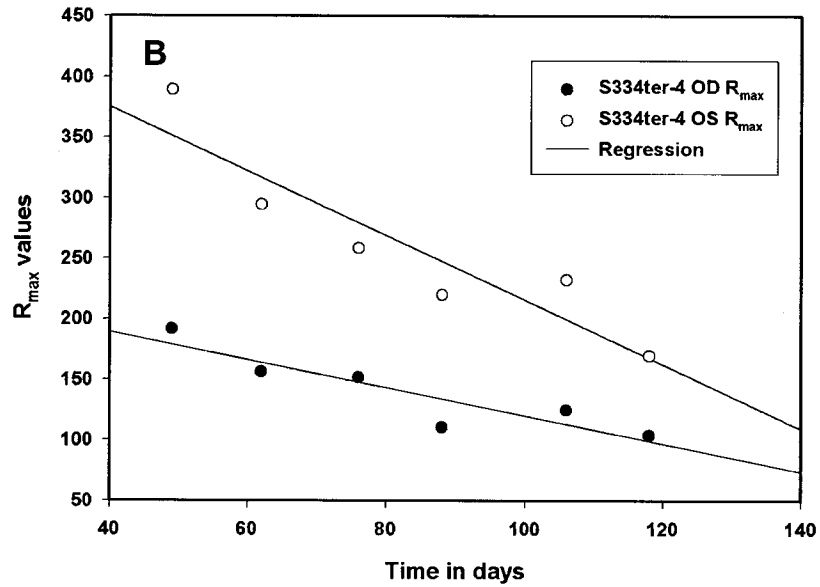
B
S334ter-4 OD R_{max}
S334ter-4 OS R_{max}
Regression
R_{max} values
Time in days
450
400
350
300
250
200
150
100
50
40
60
80
100
120
140

first attempt used the MOP500-IRES-HA-XIAP construct. This construct contained the HA-tagged XIAP driven by the mouse opsin minimal promoter. The endogenous IRES element of XIAP was included in the construct since in cell culture experiments the IRES element allowed XIAP translation under cellular stress, when cap dependent translation was shut down (Holcik and Korneluk, 2000; Holcik et al., 2000). A number of lines of transgenic mice were found to carry the transgene as demonstrated by PCR (Fig. 28A). In addition, real time quantitative PCR revealed that the mRNA of XIAP was expressed at varying levels in the different lines (Fig. 28B). Care was taken to ensure that the RNA quantity was equal in each sample as measured by spectrophotometry and that they were free of genomic contamination by pretreating the RNA with DNAse. Standard deviation was calculated based on triplicate samples. However, Western analysis failed to detect XIAP protein derived from the transgene (Fig. 28C).

Since, in the chemotoxic model there was protection from the XIAP construct that did not contain the IRES element but no protection from the construct that contained IRES, another transgene was engineered that had the IRES element excised. In addition, the HA-tag was replaced by the 6myc-tag, which often works better in immunohistochemistry applications. The resulting construct MOP500-6myc-XIAP was used to generate transgenic mice. Three lines of mice were found to harbour the transgene as demonstrated by PCR (Fig. 29A). Though there was XIAP mRNA expression, (Fig. 29B) these mice still failed to express XIAP protein (Fig. 29C) in the retina.

At the same time as the MOP500-6myc-XIAP mouse lines were being characterized, Peter Liston had generated a transgenic mouse that had the ubiquitin

FIGURE 28. Expression of XIAP mRNA and protein in MOP500-IRES-HA-XIAP mice. Panel **A.** PCR amplification of a 600bp fragment of the MOP500-IRES-HA-XIAP transgene from mouse-tail DNA. This is an F_2 generation litter. Lanes 1 and 11, 1kb ladder. Lane 10 is the water control. Panel **B** shows the mRNA expression levels from the 4 founder lines. Panel **C** is the Western blot analysis of transgenic and wild type litter mates retinae using the RIAP3 antibody. Lanes 3-5 and 7-8 are transgenic mice.

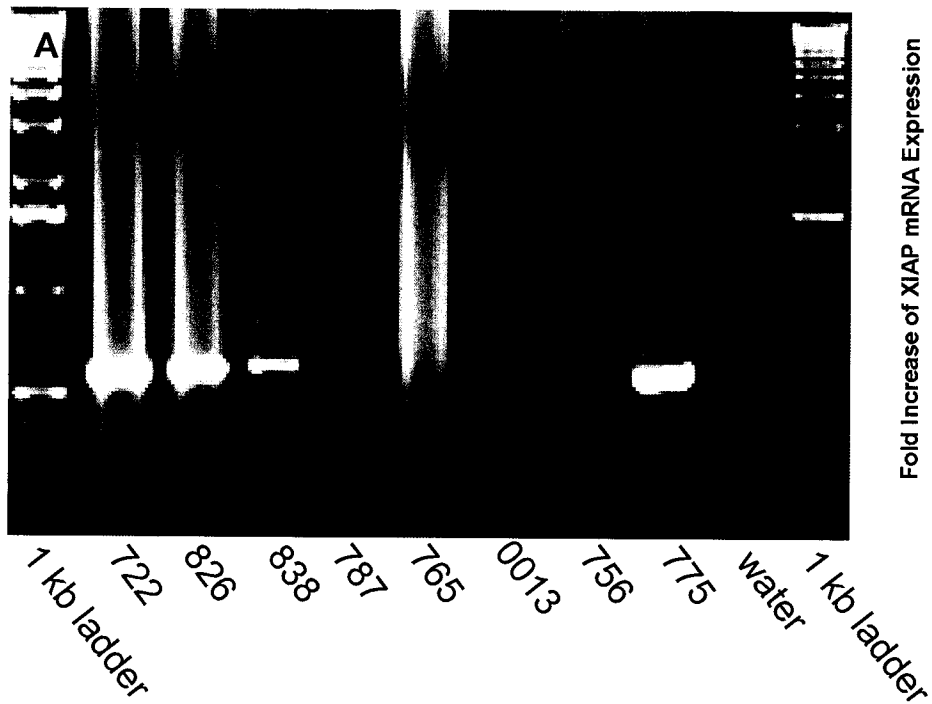
A
1 kb ladder
722
826
838
787
765
0013
756
775
water
1 kb ladder

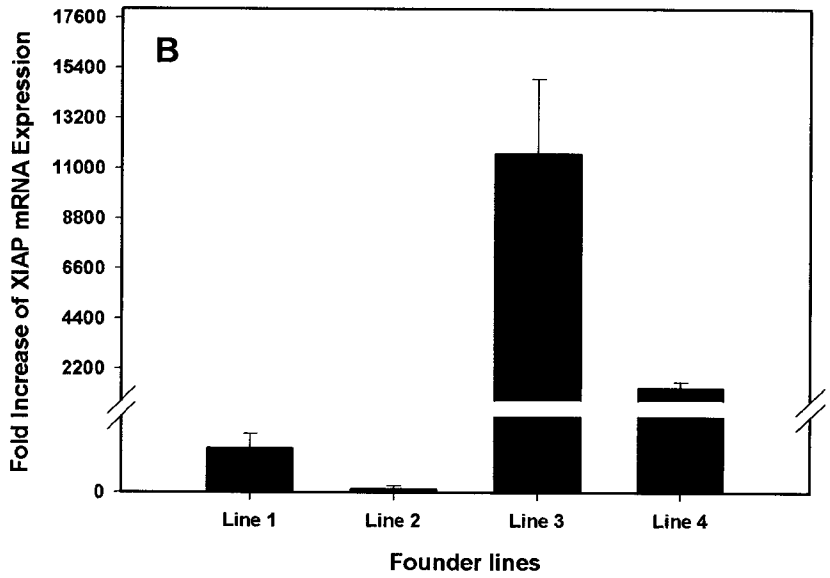
B
Fold Increase of XIAP mRNA Expression
17600
15400
13200
11000
8800
6600
4400
2200
0
Line 1
Line 2
Line 3
Line 4
Founder lines

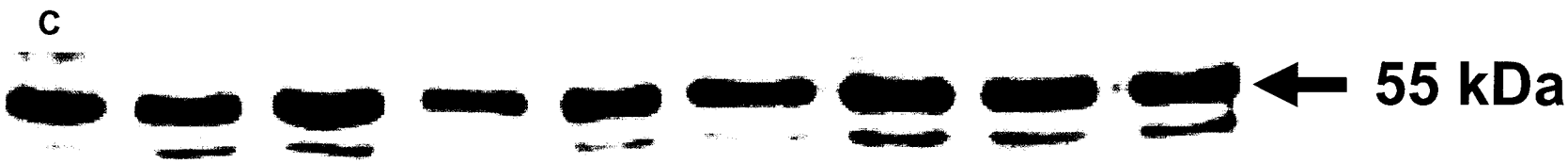
C
55 kDa

FIGURE 29. Expression of XIAP mRNA and protein in MOP500-6myc-XIAP mice. Panel **A.** PCR amplification of a 283bp fragment of the BIR3 domain of human XIAP in MOP500-6myc-XIAP transgenic mice. Rodent GAPDH was in all reactions as a DNA control. Panel **B** illustrates the various levels of over-expression in three lines of transgenic mice. Panel **C** is a Western blot of wild type and transgenic littermate retinae using the RIAP3 antibody. Lane 1 is the positive control sample of Ub-6myc-XIAP brain demonstrating a 10kDa shift due to the myc tag added to the transgene. Note that the MOP500-6myc-XIAP transgenic mice do not express the protein.

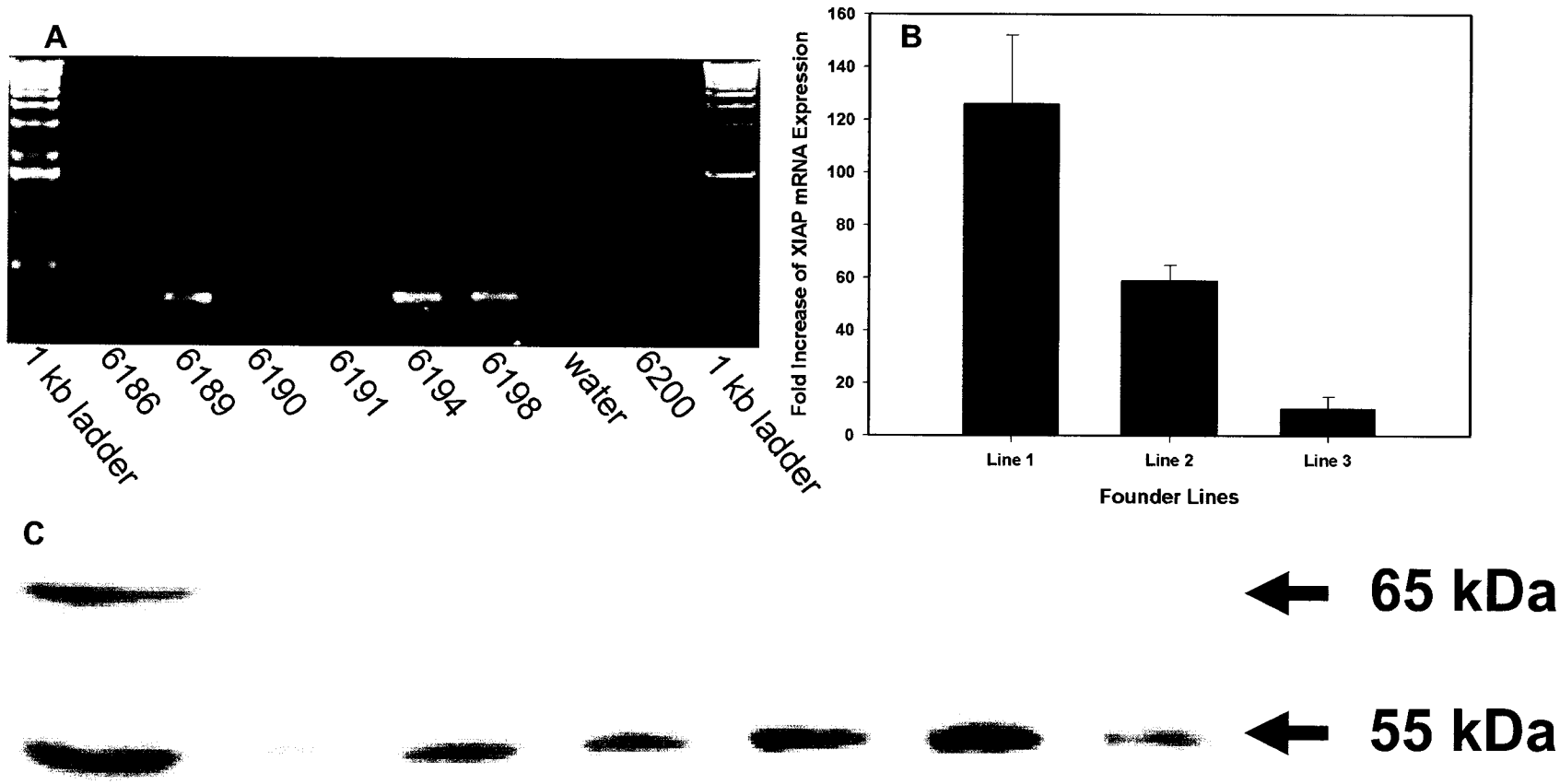
A
1 kb ladder
6186
6189
6190
6191
6194
6198
water
6200
1 kb ladder
B
Fold Increase of XIAP mRNA Expression
160
140
120
100
80
60
40
20
0
Line 1
Line 2
Line 3
Founder Lines
C
65 kDa
55 kDa

promoter driving XIAP (Ub-6myc-XIAP). These mice were analyzed to determine whether they were appropriate for studying retinal degenerations. A random selection of heterozygous and homozygous mice showed a normal ERG and NR plots comparable to wild type littermates (Fig.30).

The Ub-6myc-XIAP mice expressed XIAP throughout the neural retina as shown by antibody staining of the 6-myc tag (Fig. 31). Histological sections revealed that the mice have normal retinal morphology (Fig. 32 A-C). A number of antibodies were used on retinal sections in wild type, and in XIAP hetero- and homozygous mice to determine if retinal morphology was altered due to XIAP over-expression. Anti rhodopsin localizes to the outer segments of the photoreceptors and is not altered in either the heterozygote or homozygote XIAP mice (Fig. 32 D-F). GFAP is a marker that stains astrocytes. In damaged retinae, or aging retinae, GFAP is expressed in Müller cells. The astrocytic staining pattern in the transgenic retinae is indistinguishable from wild type (Fig. 32 G-I). This shows that the Müller cells are unaffected in the transgenic animals.

FIGURE 30. Ub-6myc-XIAP mice have a normally functioning retina. NR plots from a wild type mouse (**A**), an Ub-6myc-XIAP heterozygote (**B**) and a Ub-6myc-XIAP homozygote (**C**) are similar. (**D**) A bar graph of the ERG amplitudes of wild type and transgenic mice shows no statistical difference between animals (n=8). Student's t-test $p<0.05$

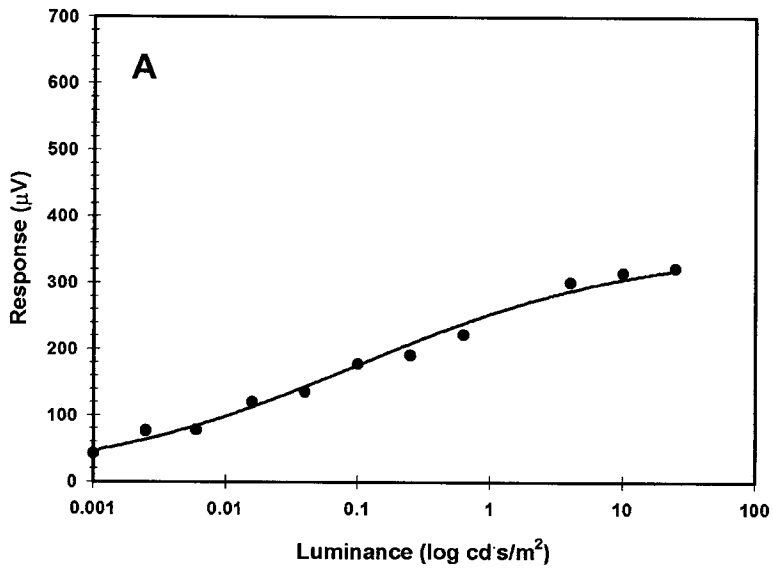
A
Response (μV)
700
600
500
400
300
200
100
0
0.001
0.01
0.1
1
10
100
Luminance (log cd·s/m²)

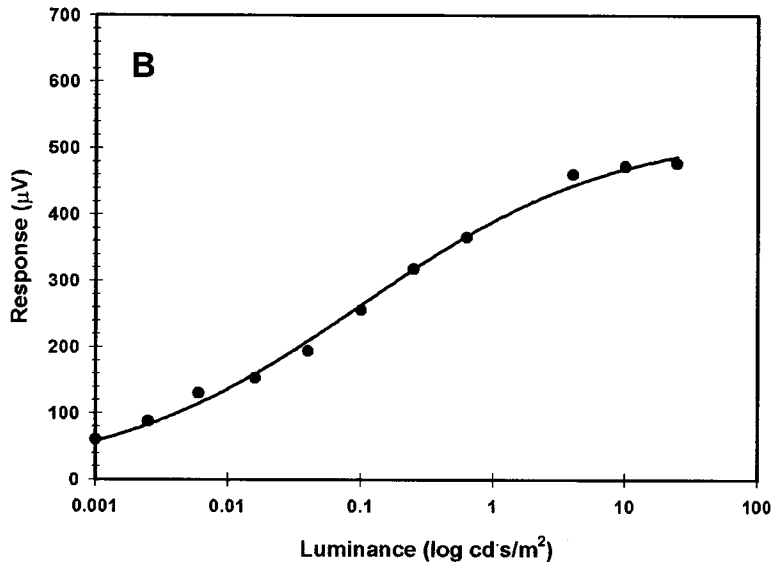
B
Response (μV)
700
600
500
400
300
200
100
0
0.001
0.01
0.1
1
10
100
Luminance (log cd·s/m²)

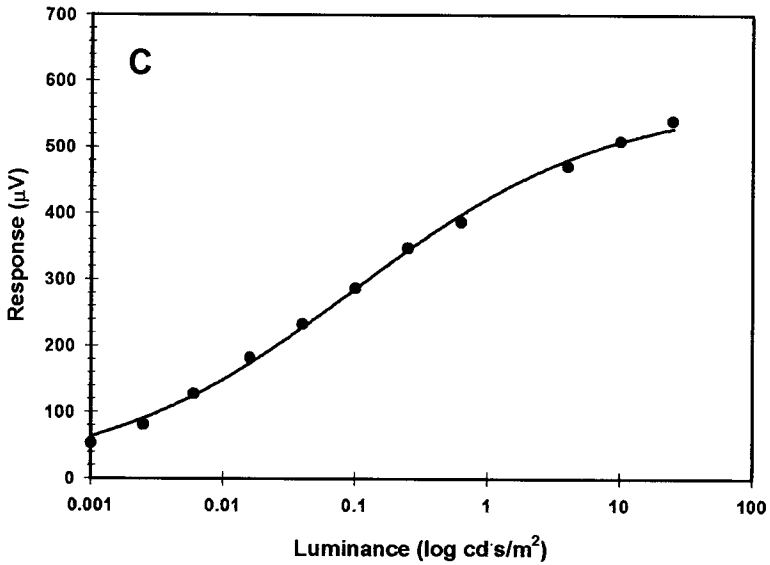
C
Response (μV)
700
600
500
400
300
200
100
0
0.001
0.01
0.1
1
10
100
Luminance (log cd·s/m²)

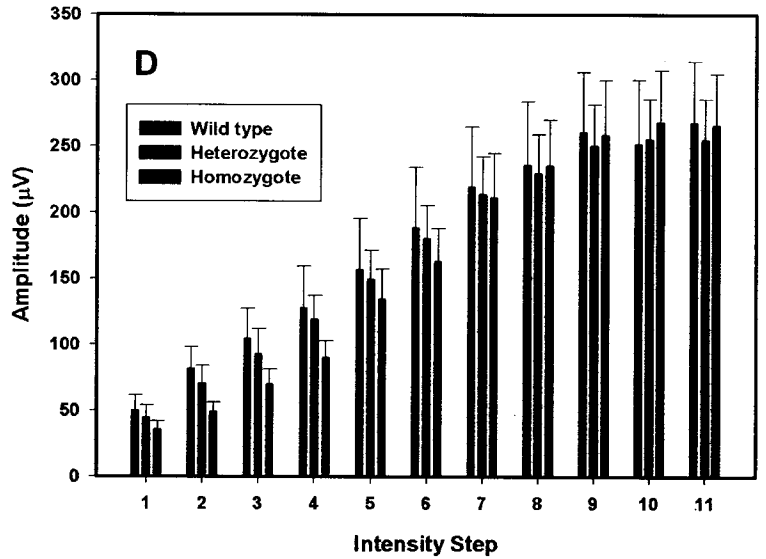
D
Wild type
Heterozygote
Homozygote
Amplitude (μV)
350
300
250
200
150
100
50
0
1
2
3
4
5
6
7
8
9
10
11
Intensity Step

FIGURE 31. XIAP is over-expressed in the retina in Ub-6myc-XIAP transgenic mice. The top panel is a Western blot showing over-expression of XIAP in the retinae. The bottom panel shows myc expression is found throughout the neural retina. In the heterozygote (**C**) there is less intense staining than in the homozygote (**D**). The wild type littermate (**B**) does not show over-expression of myc. Panel **A** is the control using secondary antibody (ALEXA 488) alone. 400x magnification

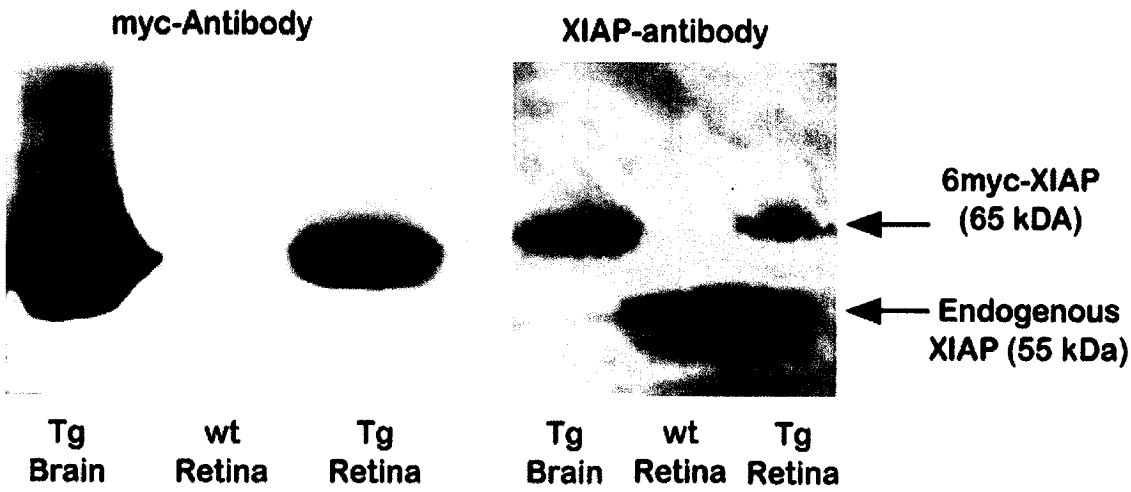
myc-Antibody
XIAP-antibody
6myc-XIAP
(65 kDA)
Endogenous
XIAP (55 kDa)
Tg
Brain
wt
Retina
Tg
Retina
Tg
Brain
wt
Retina
Tg
Retina

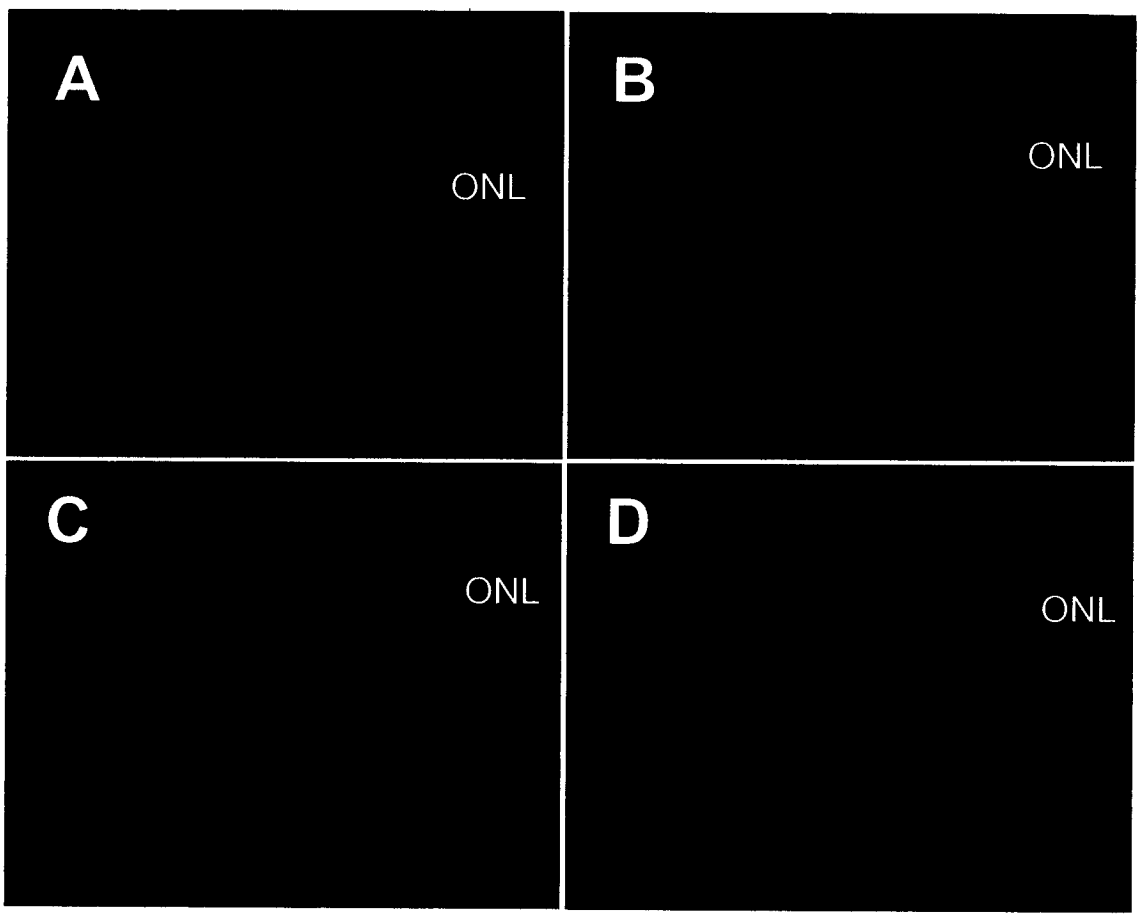
A
ONL
B
ONL
C
ONL
D
ONL

FIGURE 32. Retinal morphology of Ub-6myc-XIAP mice is normal. The top plate shows histological retinal sections of heterozygous (**B**) and homozygous (**C**) Ub-6myc-XIAP mice. Panel **A** is a wild type littermate. The second plate shows staining of rhodopsin in wild type (**E**) and a homozygous Ub-6myc-XIAP mouse (**F**). Panel **D** is the control using the secondary antibody alone. The third plate shows staining of astrocytic cells using the GFAP antibody in a wild type (**H**) and homozygous (**I**) mouse. Panel **G** is the control using secondary antibody alone. The second and third plates have been counterstained with DAPI. 400x magnification

Haematoxylin and Eosin Stained Sections

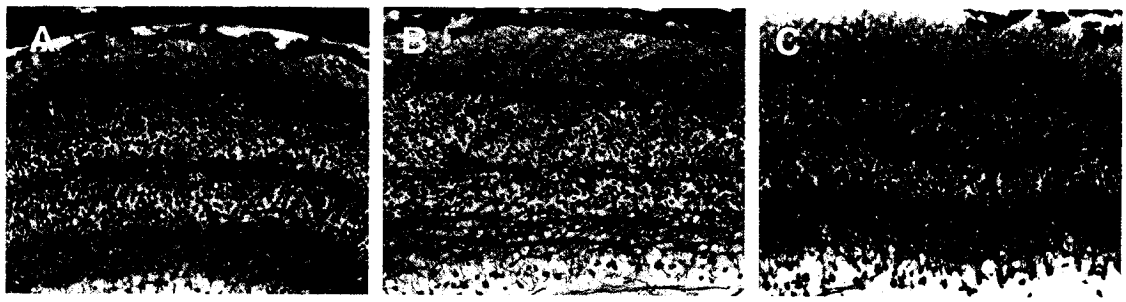

Wild type | Heterozygote | Homozygote

Anti-rhodopsin Staining

Secondary alone | Wild type | Homozygote

Anti-GFAP Staining

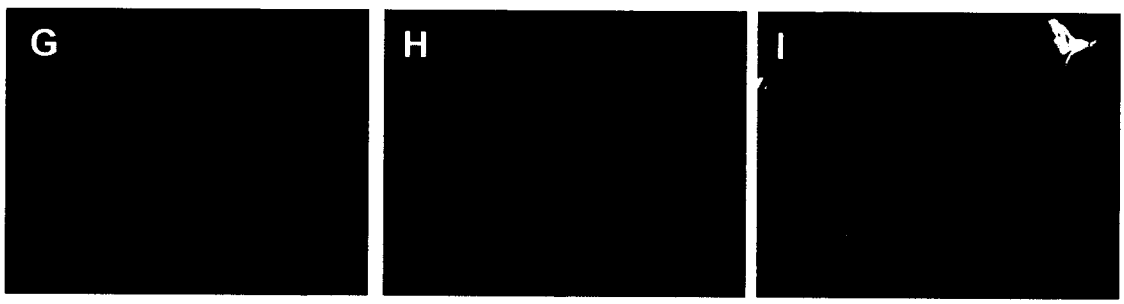

Secondary alone | Wild type | Homozygote

4 DISCUSSION

The purpose of the research conducted in this thesis was to examine the therapeutic potential of XIAP in various models of retinal degeneration. The retina is an ideal tissue for studying the effects of therapeutic agents because retinal function can be assessed repeatedly using non-invasive electroretinography. Recently, an Espion™ system was purchased for the purpose of studying the effects of XIAP in rats and mice. Normative ERG recordings were obtained for both wild type and transgenic animals. It is estimated that the Ganzfeld has flashed greater than 150 000 times since it was first used thus accruing a large amount of baseline and experimental data. The standardization of the Espion™ has given future researchers important normative data to compare to their experimental results.

Researchers have used MNU to study photoreceptor apoptosis in acute models of retinal degeneration. Published reports have used MNU at 60 mg/kg and higher. This dose extinguishes the ERG waveform and since these reports focused on cell death it is not surprising that investigators would choose a dose sufficient enough to cause complete loss of photoreceptors. Very few studies have investigated therapeutic agents using this chemotoxic trigger. Consequently, a dose titration experiment was carried out to determine a dose that would cause a significant drop in ERG response but not sufficient enough to extinguish the ERG. This dose could then be used to quickly screen therapeutic agents in the treatment of retinal degenerations.

XIAP is known to inhibit apoptosis in various animal models of neurodegeneration and MNU is known to cause rapid photoreceptor cell death. Thus, XIAP was used as a gene therapy payload using rAAV in an MNU model of retinal

degeneration to assess whether it could prevent photoreceptor cell loss. XIAP was also tested in genetic models of retinal disease using transgenic rats that have autosomal dominant mutations in rhodopsin. Due to the nature of the subretinal injection, the rAAV-XIAP vector infects a small percentage of photoreceptors. Thus, various transgenic mice were engineered to express XIAP in photoreceptors (MOP500-IRES-HA-XIAP and MOP500-6myc-XIAP) and in all tissues (Ub-6myc-XIAP) in the hope that crossing these mice with mice that have retinal degeneration phenotypes would slow down, if not stop disease progression in their offspring.

4.1 Controls for Using the Espion™ System

The Espion™ ERG system is a light emitting diode (LED) based system that is more compact than its predecessors, has less variability than a gas discharge system, and is compatible with today's technology. Thus, it was important to set-up ERG protocols and test the Espion™ system on normal subjects prior to doing any experimental trials.

4.1.1 The Electroretinogram Intensity Series

The intensity protocol that is outlined in the methods was chosen because it encompasses a scotopic-photopic stimulus range. Thus in a single intensity series, one can see the rod and cone mediated responses. In clinical electroretinography, the stimulus strength of a standard flash ranges from 1.5 to 3.0 cd·s/m^2. The intensity series that was used in all the studies presented here was from 0.001 to 25 cd·s/m^2. The reason for choosing such a broad range of intensities is that the rodent retina is quite different than the primate retina. The retinae of rats and mice are comprised mainly of rod photoreceptors (~97%) with cones that are dispersed throughout the retina (Carter-

Dawson and LaVail, 1979; Soucy et al., 1998). In primates, the retina is organized such that the cones are concentrated in the central retina, an area known as the macula, and the rods are located peripheral to this region (Hee et al., 1995). By using eleven stimulus intensities, trends can be seen, and true intraocular differences can be observed which may be missed if fewer intensities were used. The highest stimulus intensity is around eight-fold greater than that which is typically used in the clinic (Marmor et al., 2003). This was done to ensure the maximal response of the retina. After 40 animals were tested, the maximal b-wave amplitude that was observed in this intensity series became apparent on average between the eighth intensity (0.63 cd·s/m^2) and tenth intensity (10 cd·s/m^2) in both rats and mice indicating that the intensity series was ideal in stimulating the retina to its fullest potential.

The intensity series in both rats and mice reveal oscillatory potentials (OPs). These OPs are wavelets that are observed typically on the ascending limb of the b-wave and are likely to originate from amacrine cells within the inner retina interacting with bipolar and retinal ganglion cells (Heynen et al., 1985; Wachtmeister, 1998). In the rats that have had their ERGs recorded throughout these experiments, the 3rd or 4th OP gave the highest b-wave amplitude. However, in mice, this is not the case. In fact the OP that gives the highest b-wave amplitude at the lower intensities, is not the one that gives the maximal amplitude at the higher intensities. Because of this effect observed in the ERG response, scoring of the raw data is needed for comparison between eyes and between groups of mice. Thus, the third OP was chosen in all the mouse trials since at the lower intensities, the fourth is the maximal b-wave amplitude and at the higher intensities, the second becomes the maximal b-wave amplitude. Choosing one OP at the outset of all the

experiments eliminates investigator bias and maintains consistency throughout the experiment.

Pigmented Long Evans rats were also tested using the same scotopic-photopic protocol and the ERG traces obtained from this strain of rat do not differ from the albino Sprague Dawley strain. These rats will be bred to the degeneration lines to produce pigmented offspring with the autosomal dominant retinal degeneration phenotype. This is of critical importance since in the Sprague Dawley albino strain, multifocal ERG (mERG) is much more difficult to perform. This is due to the strain having a non-pigmented retinal epithelium, which makes imaging the fundus with an infrared light source impossible. In the Long Evans strain, the fundus can be imaged much more easily and the optic disc can be located and also serves as a reference point in future recordings. This technique will allow investigators to map out how the degeneration progresses and in addition, find localized areas of functional protection from therapeutic agents such as XIAP.

In the rodent models presented here, the NR plot was utilized to show the difference between eyes in the same animal and between different groups of animals. Utilizing scored data from the scotopic-photopic intensity series, the NR plot allows for a quick objective observation of the "strength" of the retinal b-wave response. This eliminates the need to identify at which intensity the maximal amplitude occurs in every animal. This equation is useful in comparing interocular retinal function between groups of animals at different time points. To measure if there are intraocular differences in retinal function ANOVA can be applied to the b-wave amplitude of every stimulus

intensity. This determines if there is a significant difference between the eyes within an animal.

Over the course of these experiments, there were no significant differences at baseline between left and right eyes in most of the animals tested. If differences were noted, these animals were removed from the data set prior to the experimental procedure as to not bias the results. A major cause for intraocular differences was the formation of a cataract in one eye. This causes a decrease in ERG response due to poor light transmission.

4.2 Dilation Effects and Test/Re-test Reproducibility

It has become standard practice with albino rats to use dilation drops prior to performing an ERG test (Aleman et al., 2001b; Machida et al., 2001). An experiment was set up to see if there was a significant intraocular difference in R_{max} in individual animals over the course of four consecutive days due to dilation. This study illustrated that there is no clear difference in ERG response due to dilation and in some cases the eye that did not receive the dilation drops had a stronger R_{max} than the eye that did.

Since no clear difference was observed between the two eyes in each animal on any given day, this experiment was used to examine the re-testability of the Espion™ system. In the clinic, depending on the electrode that is used, day-to-day ERG responses can vary as much as 20% (Grover et al., 2003). This re-testability study showed differences in ERG amplitudes from one day to the next in some animals. There are a number of factors that can account for the differences that are observed, the first of which is temperature. It has been reported in mice that a one degree Celsius drop in core body temperature can result in a 100 μV drop in b-wave amplitude (Kong and Gouras, 2003).

Other factors that can contribute to a decrease in ERG response are electrode placement, distance from the stimulus source and plane of anesthesia of the animal during the procedure (Nusinowitz et al., 2002). Since electrode placement and distance from the stimulus were relatively constant throughout the experiment, the most likely cause of the different responses one day to the next is temperature. Prior to the ERG procedure, the rats were kept at ambient temperature and then placed on a microwave-heated beanbag to prevent heat loss. Thus, the rats did not have their body heat tightly regulated on a day-to-day basis. On occasion, some rats require a topping up dose of anesthetic to ensure that they remain immobile during the test. This would also add another variable to the test since the "waiting time" for an animal to be anesthetized would increase and the rat can lose a substantial amount of heat in the process.

As a result of these experiments, all the factors that can influence ERG b-wave amplitudes (primarily temperature) are now much more tightly controlled to minimize variability from day-to-day.

4.3 MNU Dose Titration in Rats

MNU has been used extensively to study photoreceptor apoptosis in numerous rodent models using 60 mg/kg doses and greater (Ogino et al., 1993; Taomoto et al., 1998; Yuge et al., 1996). However, the 60 mg/kg dose may be disproportionately high to optimally evaluate neuroprotective effects of purported retinal therapies, since MNU typically produces total destruction of the photoreceptor layer within 36-48 hours. A lower MNU dose may provide less than total destruction of the photoreceptor layer or there may be a longer time course over which photoreceptor degeneration takes place.

Both of these conditions would allow a better determination of potential therapeutic effect.

In this study a range of MNU dosages (20 to 60 mg/kg) were used to determine the optimal dosage that would cause enough photoreceptor apoptosis to render a sufficient decrease in ERG amplitude, but not enough to completely extinguish the ERG. The results of this investigation clearly demonstrated that within 72 hours of MNU administration the ERGs were essentially extinguished with dosages of 50 or 60 mg/kg. It was equally apparent that dosages of 20 and 30 mg/kg of MNU produced no significant change in b-wave amplitude over a one-week period. At a MNU dosage of 40 mg/kg there was a clear reduction in b-wave amplitude noted within 24 hours following drug administration. This ERG reduction had certainly stabilized by 72 hours and remained unchanged at one week. Thus the 40 mg/kg dosage of MNU appears to be severe enough to cause apoptotic changes in the photoreceptor without completely extinguishing the ERG.

4.4 MNU Dose Response in Mice

The dose response curves that were obtained in the MNU titration experiment in rats revealed that a 40 mg/kg dose of MNU caused a significant drop in R_{max} but not severe enough to completely extinguish the ERG. However, the mice that were subjected to the 40 mg/kg dose had their ERGs extinguished, whereas a 35 mg/kg dose was sufficient to reduce the ERG response significantly, but not completely. A reason for the difference in the doses required to reduce the ERG may be species difference in MNU tolerance.

4.5 XIAP Protects Photoreceptors from Chemotoxic Insult

The first study that was conducted to examine the therapeutic potential of XIAP in the retina involved rAAV-XIAP therapy in the MNU model of retinal degeneration. In this study, AAV was used to deliver XIAP to the photoreceptors of the retina. AAV was chosen over adenovirus or lentivirus for several reasons. Adenoviral vectors have immune response and persistence problems (see reviews in (Dejneka and Bennett, 2001; Hauswirth and Beaufrere, 2000; Sakamoto et al., 2001)). The new-generation of "gutted" adenoviruses have fewer of these problems, but tissue tropism is a concern. Müller cells are the primary cell transduced on intravitreal delivery, (Hauswirth and Beaufrere, 2000; Sakamoto et al., 2001) and RPE cells are efficiently transduced by subretinal injection. This is problematic if ganglion cells or photoreceptors are the desired target. Lentiviral vectors show tremendous promise, because they can infect a variety of cell types and they can integrate in post-mitotic cells (Dejneka and Bennett, 2001; Sakamoto et al., 2001). However, the possibility of low-level infectious wild-type human immunodeficiency virus (HIV) contaminants remains a safety concern. AAV vectors, at present, appear to be the most promising for ocular gene therapy. Although rAAV has a limited packaging capacity (~4 kb), it is minimally toxic to photoreceptors, even at high dosages and initiates only a minimal immune response (Anand et al., 2000; Hauswirth and Beaufrere, 2000). Expression is long lived, persisting for at least 1 to 2 years after delivery (Bennett et al., 1999).

Photoreceptors of the retina are of neuronal lineage and in RP these cells die via apoptosis. It is possible that by inhibiting the apoptotic cascade via over-expression of XIAP, these cells can be induced to survive and function, as shown in other models of

neurodegeneration. Results presented here show that rAAV-XIAP conferred significant protection to the photoreceptor layer of the retina even at the highest MNU dose. No such protection was seen in rAAV-GFP injected eyes and the uninjected control. This experiment used MNU to induce rapid retinal degeneration in wild-type Sprague-Dawley rats. MNU is a DNA alkylating agent that causes DNA methylation at the O^6 position of guanine leading to the formation of the O^6-methylguanine adduct (O^6-meGua). This methylated nucleotide pairs with thymine instead of cytosine leading to GC $\rightarrow$ AT transition mutations. These mutations in the DNA of photoreceptor cells render them susceptible to death via the apoptotic cascade. XIAP protection was first apparent at 24 hours after MNU, where a much larger number of cells were undergoing apoptosis in the uninjected eye (and in the GFP injected eye) in relation to the rAAV-XIAP injected right eye. Morphological protection was seen in four of six animals up to 1 week after MNU, when the experiment was terminated. Most significantly, a good proportion (two of four) of the eyes that showed morphological protection also showed functional protection, as evidenced by ERG. It is important to note that there are three reports in the literature (Moriguchi et al., 2004; Moriguchi et al., 2003; Yoshizawa et al., 2000) showing only structural protection after MNU treatment. Two of the reports used docosahexaenoic acid dietary supplementation; the third used a caspase-3 inhibitor injected intravitreally at 0 and 10 hours after MNU treatment. . There is only one other study that showed functional protection from MNU treatment (Kiuchi et al., 2003). Immediately after the investigators injected 60 mg/kg MNU IP into Sprague-Dawley rats, 1 g/kg of nicotinamide was injected. This dose was sufficient to protect the rats by MNU-induced retinal degeneration. The study presented in this thesis using XIAP represents the first

and only evidence of functional protection of photoreceptors after treatment with MNU using a gene therapy approach.

The degree of functional protection was somewhat limited, and there are three possible explanations for this. First, the 2-μL injection of the virus covered, at best 20% of the rat retina (Flannery et al., 1997); consequently, only a fraction of the photoreceptors were efficiently transduced with the rAAV vector. This was confirmed by histological data that show regions of morphological protection adjacent to unprotected areas that lie outside the reach of the virus. The full-field ERG records the response of the whole retina (Birch and Anderson, 1992). Thus, the responses of fully protected regions were considerably diluted by most of the retina, which was not covered by the injection and underwent cell death. Clearly, full-field ERG significantly underestimates the degree of localized functional protection provided by rAAV-XIAP. Since this study showed that XIAP-injected eyes retained 5% to 15% of pre-MNU b-wave amplitudes and we estimate that at best only 20% of the retina was covered by the subretinal injection, this emphasizes the strong protective effect of XIAP in transfected photoreceptors.

Second, because XIAP over-expression cannot easily be tested in a retina that is severely stressed by MNU, we cannot be sure that all the subretinal injections were equally effective in over-expressing XIAP. Subtle differences in the injection procedure from one animal to the next could potentially result in differences in level of XIAP expression and in significant differences in morphologic and functional protection.

Third, and perhaps most important, MNU is a powerful alkylating agent in that it destroys the photoreceptor cells in such a short time (Yoshizawa et al., 1999; Yuge et al.,

1996) and is expected to cause severe damage to the DNA, even before the cell initiates apoptotic signals. It is thus remarkable that any functional protection was observed at all.

4.6 Age Related Study of rAAV-XIAP Treated Rats

Over the course of time photoreceptors degenerate in humans (Curcio et al., 1993) as well as in other animals including rats (Lin et al., 1997; Townes-Anderson et al., 1998). Although the sample size in this age related study is small (n=4), the trend showed that the XIAP treated eyes had significantly stronger ERG amplitudes across the first eight flash intensities. At lower flash intensities one sees a response being generated exclusively from rod photoreceptors. Thus the trend that was observed is expected since XIAP was expressed under the control of a rod specific promoter. This finding is impressive since the subretinal injection procedure using a balanced salt solution causes a decrease in ERG amplitude. This augmented ERG response in the treated eye indicates that XIAP may have prevented age related rod photoreceptor cell loss in these animals. Though this effect was transient and the difference in ERG response between the two eyes diminished by the ninth month, this nevertheless illustrates the potential of XIAP in treating age related photoreceptor cell loss.

4.7 XIAP Gene Therapy in Three Transgenic Rat Models of Retinal Degeneration

4.7.1 P23H-3 Transgenic Rats

XIAP was found to protect photoreceptors in an acute model of retinal degeneration using MNU. However, could XIAP protect the photoreceptors at a functional level in a genetic model of RP? The P23H and the S334ter lines of transgenic rats have been used extensively in gene therapy approaches with many growth factors.

Several lines of these transgenic rats were used in the studies described in this thesis. The first experiments involved the P23H-3 rats which have a slow progressive RP. These rats, according to the literature, go blind within the first year of life. Two sets of experiments were conducted with this line. In the first trial, rAAV-XIAP was subretinally injected and the progression of disease was monitored for approximately nine and a half months. Since the viral constructs had been tested and verified in the MNU experiment, they were not re-tested prior to this experiment. Unfortunately, after nine months of monitoring disease progression with no apparent differences between the treated and untreated eyes, it was learned from our collaborator, William Hauswirth, that the wrong virus had been sent to the lab. In the second experiment, XIAP cDNA in the virus stock was confirmed by PCR. ERGs commenced at 117 days and were carried out beyond one year of age. The reason for starting ERGs at this time point was the hope that degeneration in the left eye would be near completion, and that a small retention of an ERG response would be evident in the treated right eye.

However, again there were no significant differences between the injected and uninjected eyes. The ONL thickness in the P23H-3 rats has been documented to decrease quite rapidly in the first few weeks and then continue at a slower rate from about 120 days until about 1 year (LaVail, 2002). By 117 days when the first ERG was conducted, there is over 80% loss in photoreceptors. It was expected that a similar trend would be observed in the ERG response. However, the ERG response did not deteriorate in a similar fashion. In fact, the ERG results that were obtained in this line and fitted to the NR equation at the 117-day time point were comparable to wild type animals. This retention in ERG response is perplexing when compared to the documented data on ONL

thinning. By 455 days, when the final ERGs were taken, the ONL thins to approximately 2 μm (LaVail, 2002). The ERG should consequently have been almost extinguished, and this clearly did not occur. Nevertheless, when the initial NR plot at 117 days PN is compared to the final time point, 455 days PN, the result clearly shows a marked decrease in responsiveness in the retina of these animals. It is possible that even though a vast number of photoreceptors have been lost, the remaining photoreceptors can still elicit an ERG response, indicating redundancy within the retina. The retina is organized such that every photoreceptor interacts with numerous second order neurons called bipolar cells (Kolb et al., 2003). With retinal degeneration, there is considerable synaptic remodeling, such that the remaining neurons establish new neuronal connections (Jones et al., 2003; Marc et al., 2003). This may help to retain the ERG waveform (Kolb et al., 2003). The waveform may only deteriorate when there is a sufficient loss of photoreceptor-second order neuron interactions.

4.7.2 P23H-1 and S334ter-4 Transgenic Rats

In light of the slow disease progression in the P23H-3 rats, it was decided to examine XIAP gene therapy in more rapid lines in which the results would be more quickly available. The P23H-1 and the S334ter-4 lines of transgenic rats have similar rates of retinal degeneration, both faster than the P23H-3. The disease course is completed by six months of age whereas in the P23H-3 line, the disease takes approximately one year. In theses lines, as in the P23H-3, rAAV-XIAP (serotype 2) was injected subretinally in the right eye and the left eye served as the contralateral control. Disease progression was followed by recording ERGs for a period of four months. Unfortunately, again there were no significant functional differences between XIAP-

treated and untreated eyes. The reasons for this may be explained by the following. First AAV serotype 2 optimally expresses the gene of interest at around six weeks of age. In looking at published reports of ONL thickness in these degenerating models, by this point in time, there is anywhere from a 25%-50% reduction in ONL thickness (LaVail, 2002). This lag in expression of XIAP may mean that photoreceptor cell death is extensive before gene therapy is initiated. Another possibility is the promoter construct that was used to specifically target photoreceptors. There has been speculation that the minimal rhodopsin promoter (MOP500) does not drive expression of each construct equally well (Hauswirth, personal comm.). This may have been the case with XIAP. These two issues have recently been addressed in an ongoing experiment. First, a serotype that expresses viral products more rapidly has been engineered (serotype 5) to express XIAP and secondly, a less tissue specific promoter, chicken beta actin (CBA) has replaced MOP500.

Even though the above experiments did not show functional protection by XIAP, the ERG data on the uninjected eye helped to fully characterize disease progression in the three genetic models of RP. Many of the previous studies have documented the thinning of the ONL over the course of the disease (Liang et al., 2001; McGee Sanftner et al., 2001). Few studies to date have studied ERG amplitudes over an extended course of the disease in these rats (Machida et al., 2000) and none have investigated the NR plots in these degeneration models.

In the P23H-3 and S334ter-4 rapid degeneration lines, the NR plots in the treated eyes were much reduced compared to the untreated eye. This may be attributed to injury to the retina from the subretinal injection. The surgical procedure used to deliver XIAP to

the subretinal space compromises the photoreceptor cells around the area of injection. In addition to this, the retinal detachment caused by injecting the virus may not resolve, also compromising electrophysiological function. This is observed in a lower ERG response in the injected eye compared to the contralateral control. The cells that are infected with the virus may survive quite well and function optimally. However, the function of these photoreceptors maybe overshadowed by the initial surgical insult which the retina cannot recover from. By looking at the NR curve fits alone, it is noted that the left eye does perform better at all time points. However, the different rate of change in R_{max} in the treated eye compared to the untreated eye suggests that the XIAP can slow disease progression.

In both of these lines of transgenic rats, the rate of change in R_{max} is slower in the right eye than in the untreated left eye. A t-test analysis of the slopes of the lines of best fit in the P23H-1 line revealed that the loss of R_{max} from the untreated eye to the treated eye was not significantly different ($t=-1.8$, $P=0.102$). However, in the S334ter-4 line, the difference in the loss of R_{max} was significantly different between the two eyes ($t=1.504$, $P=0.034$). The lower rate of loss of ERG response in the treated eye may be indicative of a protective effect of XIAP in this group of rats. Alternatively, since the injected eyes have lower ERGs than non-injected eyes, they may have less ERG response to lose and this would account for the reduced slope in XIAP treated eyes.

4.8 Normal and XIAP Transgenic Mice

Since the bcl-2 mice that have been generated in the past undergo retinal degeneration over time (Chen et al., 1996; Quiambao et al., 2001), once the Ub-XIAP transgenic mice were generated, it was important to ensure that the mice did in fact

express XIAP in the photoreceptors and furthermore, that the expression of the transgene did not have any adverse effect on retinal structure or function over time. Standard histology, immunohistochemistry with retinal specific antibodies and ERGs were used to assess retinal structure and function.

Using the anti-myc antibody on mouse retinal sections revealed that XIAP is expressed in the Ub-XIAP mouse retina. The expression was ubiquitously seen in all retinal layers, and copy number of the transgene plays an important role in expression levels. Wild type littermates do not express the transgene. Thus this transgenic mouse can be used to study the protective effects of XIAP in various models of retinal degeneration, ischemia and glaucoma.

With respect to function, both the hetero- and homozygous animals at two months of age retain retinal function comparable to the wild type animals. Both the NR plots and b-wave amplitudes are comparable to wild type mice. This is a promising trend since the bcl-2 transgenic mice had signs of functional retinal impairment by this time (Quiambao et al., 2001). Of course mice will have ERGs recorded on a continuing basis to assess retinal function later in life.

Apoptosis of neuronal cells is a normal event in the development of the central nervous system (CNS) (Marin-Teva et al., 2004; Urase et al., 2003; Wielgus et al., 2004). Since the photoreceptors cells are of neuronal lineage (Milam et al., 2000), there was a concern that the retina, in addition to other parts of the CNS, would be adversely affected by the ectopic expression of XIAP in all tissues. This is particularly true in the ganglion cell layer of the retina where developmental apoptosis has been shown (Mayordomo et al., 2003). The ERG results imply that the retina functions normally in this transgenic

mouse. However, to ensure that retinal structure was not adversely affected by over-expression of XIAP in the Ub-XIAP transgenic, H&E staining was performed. These results show that at two months of age, the transgenics have the same ONL thickness when compared to wild type controls. This is in contrast to the bcl-2 transgenic mouse which has thinning of the ONL layer, indicating retinal degeneration due to ectopic expression of bcl-2 (Quiambao et al., 2001).

Immunohistochemistry with retina-specific antibodies shows further proof that the XIAP transgene does not affect morphology. Anti-rhodopsin localizes to the outer segments of the photoreceptors (McNally et al., 1999) and is not altered in the hetero- or homozygous mice when compared to the wild type littermate. Glial fibrillary acidic protein (GFAP) is a glial cell marker and stains Müller cells in the retina (Grosche et al., 1995). Müller cells are important for structural integrity and span the entire height of the retina (Kolb et al., 2003). The staining pattern again is unaltered in the hetero- and homozygotic Ub-XIAP transgenic mice compared to the wild type littermate.

Thus, the Ub-XIAP mouse has been shown to express XIAP in the photoreceptors and this ectopic expression does not alter function or morphology. This bodes well for the use of XIAP as a gene therapy payload in retinal degenerations. The advantage of the transgenic approach is that the Ub-XIAP mice over-express XIAP in every photoreceptor, whereas in the viral approach, only a small percentage of the photoreceptors can be infected with the desired gene of interest without causing extensive damage to the retina. In crossing the Ub-XIAP mouse with rd mice, the effect of the transgene will be pan retinal rather than localized to a small portion of the retina. If XIAP can slow down

retinal degeneration, this effect can be measured by ERG and by routine histology during the normal disease course in the various rd offspring.

5 Summary

Work presented in this thesis has shown that XIAP can protect photoreceptors in an acute model of retinal degeneration. Though the gene therapy attempts with earlier viral vectors have not succeeded, a number of issues have been resolved which include addressing the problems of the onset of viral expression and the use of different promoters to drive expression of XIAP in the photoreceptors. A large amount of ERG normative data has been collected which will aid future researchers in charting the disease course in the P23H-1, 3 and S334ter-4 transgenic rats. The Ub-XIAP transgenic mouse has been generated that has a structurally sound retina that functions as well as its wild type counterparts. This mouse will become an invaluable tool when crossed with mice that have retinal degeneration phenotypes in the hope of slowing down disease progression caused by genetic mutations.

Given that XIAP is able to confer functional protection of the photoreceptors in an acute chemotoxic model of retinal degeneration, it holds promise as a therapeutic agent in slower genetic models of retinal degeneration. More than 150 genes, a large number of which are expressed in the photoreceptors, are implicated in causing retinal dystrophies when mutated (Daiger S, Rossiter B, Greengerg J, Christoffels A, Hide W, ARVO Abstract 1352, 1998). Mutations impede the cell's ability to function optimally and cause an inability to repair damage induced by extrinsic (Sakamoto et al., 2001) (intense light) (Reme et al., 1998; Wenzel et al., 2000) or intrinsic (genetic) factors (Jones et al., 2000a; Jones et al., 2000b; Portera-Cailliau et al., 1994) For RP alone, at least 32

different genetic loci have been identified, and 25 genes have been cloned (summarized in the Retinal Information Network [RetNet]; http://www.sph.uth.tmc.edu/retnet/home.htm, provided by the University of Texas Houston Health Science Centre). Every chromosome has a least one locus that can give rise to retinal degeneration. The end point, regardless of the mutation involved, is the death of the photoreceptors by apoptosis.

Given all the different genes that can cause RP, targeting individual mutations for gene therapy strategies may not be a practical approach. The results from the MNU model suggest that XIAP may allow the broad protection of photoreceptors in many forms of RP, regardless of the initial disease-causing mutation. Moreover, the long time course and the progressive nature of many retinal degenerations implies that even if intervention is implemented after diagnosis, there is still hope that antiapoptotic strategies can effect a significant delay, if not a full halt, in disease progression. In RP, all the photoreceptors in an affected individual have the mutation, yet they function normally for many years before they begin to die. Photoreceptor cell death continues to occur slowly over a long period. It is possible that if the apoptotic threshold in the diseased photoreceptor cells could be raised, the cells could survive and function for longer periods.

REFERENCES

ADA protocol 1990. The ADA human gene therapy clinical protocol. Hum Gene Ther 1:327-62.

Acharya, U., S. Patel, E. Koundakjian, K. Nagashima, X. Han, and J. K. Acharya. 2003. Modulating sphingolipid biosynthetic pathway rescues photoreceptor degeneration. Science 299:1740-3.

Acland, G. M., G. D. Aguirre, J. Ray, Q. Zhang, T. S. Aleman, A. V. Cideciyan, S. E. Pearce-Kelling, V. Anand, Y. Zeng, A. M. Maguire, S. G. Jacobson, W. W. Hauswirth, and J. Bennett. 2001. Gene therapy restores vision in a canine model of childhood blindness. Nat Genet 28:92-5.

Adler, R. 1996. Mechanisms of photoreceptor death in retinal degenerations. From the cell biology of the 1990s to the ophthalmology of the 21st century? Arch Ophthalmol 114:79-83.

Afanasieva, T. A., V. Pekarik, M. Grazia D'Angelo, M. A. Klein, T. Voigtlander, C. Stocking, and A. Aguzzi. 2001. Insertional mutagenesis of preneoplastic astrocytes by Moloney murine leukemia virus. J Neurovirol 7:169-81.

Ahuja, P., A. R. Caffe, I. Holmqvist, A. K. Soderpalm, D. P. Singh, T. Shinohara, and T. van Veen. 2001. Lens epithelium-derived growth factor (LEDGF) delays photoreceptor degeneration in explants of rd/rd mouse retina. Neuroreport 12:2951-5.

Aleman, T. S., J. L. Duncan, M. L. Bieber, E. de Castro, D. A. Marks, L. M. Gardner, J. D. Steinberg, A. V. Cideciyan, M. G. Maguire, and S. G. Jacobson. 2001a. Macular pigment and lutein supplementation in retinitis pigmentosa and Usher syndrome. Invest Ophthalmol Vis Sci 42:1873-81.

Aleman, T. S., M. M. LaVail, R. Montemayor, G. Ying, M. M. Maguire, A. M. Laties, S. G. Jacobson, and A. V. Cideciyan. 2001b. Augmented rod bipolar cell function in partial receptor loss: an ERG study in P23H rhodopsin transgenic and aging normal rats. Vision Res 41:2779-97.

Ali, R. R., M. B. Reichel, A. J. Thrasher, R. J. Levinsky, C. Kinnon, N. Kanuga, D. M. Hunt, and S. S. Bhattacharya. 1996. Gene transfer into the mouse retina mediated by an adeno-associated viral vector. Hum Mol Genet 5:591-4.

Ali, R. R., G. M. Sarra, C. Stephens, M. D. Alwis, J. W. Bainbridge, P. M. Munro, S. Fauser, M. B. Reichel, C. Kinnon, D. M. Hunt, S. S. Bhattacharya, and A. J. Thrasher. 2000. Restoration of photoreceptor ultrastructure and function in retinal degeneration slow mice by gene therapy. Nat Genet 25:306-10.

Allard, R. E. 1983. Retinitis pigmentosa--an overview. J Am Optom Assoc 54:793-800.

Alloway, P. G., L. Howard, and P. J. Dolph. 2000. The formation of stable rhodopsin-arrestin complexes induces apoptosis and photoreceptor cell degeneration. Neuron 28:129-38.

Anand, V., N. Chirmule, M. Fersh, A. M. Maguire, and J. Bennett. 2000. Additional transduction events after subretinal readministration of recombinant adeno-associated virus. Hum Gene Ther 11:449-57.

Anand, V., B. Duffy, Z. Yang, N. S. Dejneka, A. M. Maguire, and J. Bennett. 2002. A deviant immune response to viral proteins and transgene product is generated on subretinal administration of adenovirus and adeno-associated virus. Mol Ther 5:125-32.

Aonuma, H., K. Koide, K. Masuda, and I. Watanabe. 1997. Retinal light damage: protective effect of alpha-tocopherol. Jpn J Ophthalmol 41:160-7.

Auricchio, A., G. Kobinger, V. Anand, M. Hildinger, E. O'Connor, A. M. Maguire, J. M. Wilson, and J. Bennett. 2001. Exchange of surface proteins impacts on viral vector cellular specificity and transduction characteristics: the retina as a model. Hum Mol Genet 10:3075-81.

Balacco Gabrieli, C., F. Regine, E. M. Vingolo, E. Rispoli, and A. Isidori. 2003. Acute electroretinographic changes during sildenafil (Viagra) treatment for erectile dysfunction. Doc Ophthalmol 107:111-4.

Bartlett, E. J., J. C. Lenzo, S. Sivamoorthy, J. P. Mansfield, V. S. Cull, and C. M. James. 2004. Type I IFN-beta gene therapy suppresses cardiac CD8 T-cell infiltration during autoimmune myocarditis.

Bartz-Schmidt, K. U., R. Brunner, P. Esser, C. Luke, P. Walter, and W. Sickel. 1996. The triple flash electroretinogram and its significance in macular diseases. B-wave recovery as a diagnostic tool. Graefes Arch Clin Exp Ophthalmol 234:604-11.

Baumgartner, W. A. 2000. Etiology, pathogenesis, and experimental treatment of retinitis pigmentosa. Med Hypotheses 54:814-24.

Bennett, J., A. M. Maguire, A. V. Cideciyan, M. Schnell, E. Glover, V. Anand, T. S. Aleman, N. Chirmule, A. R. Gupta, Y. Huang, G. P. Gao, W. C. Nyberg, J. Tazelaar, J. Hughes, J. M. Wilson, and S. G. Jacobson. 1999. Stable transgene expression in rod photoreceptors after recombinant adeno-associated virus-mediated gene transfer to monkey retina. Proc Natl Acad Sci U S A 96:9920-5.

Bennett, J., T. Tanabe, D. Sun, Y. Zeng, H. Kjeldbye, P. Gouras, and A. M. Maguire. 1996. Photoreceptor cell rescue in retinal degeneration (rd) mice by in vivo gene therapy. Nat Med 2:649-54.

Bennett, J., Y. Zeng, R. Bajwa, L. Klatt, Y. Li, and A. M. Maguire. 1998. Adenovirus-mediated delivery of rhodopsin-promoted bcl-2 results in a delay in photoreceptor cell death in the rd/rd mouse. Gene Ther 5:1156-64.

Bergsma, D. R., and M. L. Wolf. 1977. A therapeutic trial of vitamin A in patients with pigmentary retinal degenerations: a negative study. Adv Exp Med Biol 77:197-209.

Berson, E. L. 1973. Retinitis pigmentosa, the electroretinogram, and Mendel's laws. Trans Pa Acad Ophthalmol Otolaryngol 26:109-13.

Berson, E. L., B. Rosner, M. A. Sandberg, K. C. Hayes, B. W. Nicholson, C. Weigel-DiFranco, and W. Willett. 1993a. A randomized trial of vitamin A and vitamin E supplementation for retinitis pigmentosa. Arch Ophthalmol 111:761-72.

Berson, E. L., B. Rosner, M. A. Sandberg, K. C. Hayes, B. W. Nicholson, C. Weigel-DiFrano, and W. Willett. 1993b. Vitamin A supplementation for retinitis pigmentosa. Arch Ophthalmol 111:1456-9.

Birch, D. G., and J. L. Anderson. 1992. Standardized full-field electroretinography. Normal values and their variation with age. Arch Ophthalmol 110:1571-6.

Birnbaum, M. J., R. J. Clem, and L. K. Miller. 1994. An apoptosis-inhibiting gene from a nuclear polyhedrosis virus encoding a polypeptide with Cys/His sequence motifs. J Virol 68:2521-8.

Bode, C., and U. Wolfrum. 2003. Caspase-3 inhibitor reduces apototic photoreceptor cell death during inherited retinal degeneration in tubby mice. Mol Vis 9:144-50.

Boughman, J. A., P. M. Conneally, and W. E. Nance. 1980. Population genetic studies of retinitis pigmentosa. Am J Hum Genet 32:223-35.

Bramson, J. L., N. Grinshtein, R. A. Meulenbroek, J. Lunde, D. Kottachchi, I. A. Lorimer, B. J. Jasmin, and R. J. Parks. 2004. Helper-dependent adenoviral vectors containing modified fiber for improved transduction of developing and mature muscle cells. Hum Gene Ther 15:179-88.

Brown, B. D., C. X. Shi, S. Powell, D. Hurlbut, F. L. Graham, and D. Lillicrap. 2004. Helper-dependent adenoviral vectors mediate therapeutic factor VIII expression for several months with minimal accompanying toxicity in a canine model of severe hemophilia A. Blood 103:804-10.

Browning, M. T., R. D. Schmidt, K. A. Lew, and T. A. Rizvi. 2001. Primate and feline lentivirus vector RNA packaging and propagation by heterologous lentivirus virions. J Virol 75:5129-40.

Brunetti-Pierri, N., D. J. Palmer, A. L. Beaudet, K. D. Carey, M. Finegold, and P. Ng. 2004. Acute toxicity after high-dose systemic injection of helper-dependent adenoviral vectors into nonhuman primates. Hum Gene Ther 15:35-46.

Caffe, A. R., A. K. Soderpalm, I. Holmqvist, and T. van Veen. 2001. A combination of CNTF and BDNF rescues rd photoreceptors but changes rod differentiation in the presence of RPE in retinal explants. Invest Ophthalmol Vis Sci 42:275-82.

Cao, W., J. Tombran-Tink, R. Elias, S. Sezate, D. Mrazek, and J. F. McGinnis. 2001. In vivo protection of photoreceptors from light damage by pigment epithelium-derived factor. Invest Ophthalmol Vis Sci 42:1646-52.

Carmody, R. J., and T. G. Cotter. 2000. Oxidative stress induces caspase-independent retinal apoptosis in vitro. Cell Death Differ 7:282-91.

Carr, R. E. 1969. The night-blinding disorders. Int Ophthalmol Clin 9:971-1003.

Carter-Dawson, L. D., and M. M. LaVail. 1979. Rods and cones in the mouse retina. I. Structural analysis using light and electron microscopy. J Comp Neurol 188:245-62.

Cayouette, M., D. Behn, M. Sendtner, P. Lachapelle, and C. Gravel. 1998. Intraocular gene transfer of ciliary neurotrophic factor prevents death and increases responsiveness of rod photoreceptors in the retinal degeneration slow mouse. J Neurosci 18:9282-93.

Cayouette, M., and C. Gravel. 1997. Adenovirus-mediated gene transfer of ciliary neurotrophic factor can prevent photoreceptor degeneration in the retinal degeneration (rd) mouse. Hum Gene Ther 8:423-30.

Cayouette, M., S. B. Smith, S. P. Becerra, and C. Gravel. 1999. Pigment epithelium-derived factor delays the death of photoreceptors in mouse models of inherited retinal degenerations. Neurobiol Dis 6:523-32.

Chai, J., E. Shiozaki, S. M. Srinivasula, Q. Wu, P. Datta, E. S. Alnemri, Y. Shi, and P. Dataa. 2001. Structural basis of caspase-7 inhibition by XIAP. Cell 104:769-80.

Chatzinoff, A., E. Nelson, N. Stahl, and A. Clahane. 1968. Eleven-CIS vitamin A in the treatment of retinitis pigmentosa. A negative study. Arch Ophthalmol 80:417-9.

Chen, J., J. G. Flannery, M. M. LaVail, R. H. Steinberg, J. Xu, and M. I. Simon. 1996. bcl-2 overexpression reduces apoptotic photoreceptor cell death in three different retinal degenerations. Proc Natl Acad Sci U S A 93:7042-7.

Chen, T. A., F. Yang, G. M. Cole, and S. O. Chan. 2001. Inhibition of caspase-3-like activity reduces glutamate induced cell death in adult rat retina. Brain Res 904:177-88.

Chierzi, S., M. C. Cenni, L. Maffei, T. Pizzorusso, V. Porciatti, G. M. Ratto, and E. Strettoi. 1998. Protection of retinal ganglion cells and preservation of function after optic nerve lesion in bcl-2 transgenic mice. Vision Res 38:1537-43.

Chong, N. H., R. A. Alexander, L. Waters, K. C. Barnett, A. C. Bird, and P. J. Luthert. 1999. Repeated injections of a ciliary neurotrophic factor analogue leading to long-term photoreceptor survival in hereditary retinal degeneration. Invest Ophthalmol Vis Sci 40:1298-305.

Cory, S., D. C. Huang, and J. M. Adams. 2003. The Bcl-2 family: roles in cell survival and oncogenesis. Oncogene 22:8590-607.

Coultas, L., and A. Strasser. 2003. The role of the Bcl-2 protein family in cancer. Semin Cancer Biol 13:115-23.

Crocker, S. J., P. Liston, H. Anisman, C. J. Lee, P. D. Smith, N. Earl, C. S. Thompson, D. S. Park, R. G. Korneluk, and G. S. Robertson. 2003. Attenuation of MPTP-induced neurotoxicity and behavioural impairment in NSE-XIAP transgenic mice. Neurobiol Dis 12:150-61.

Crook, N. E., R. J. Clem, and L. K. Miller. 1993. An apoptosis-inhibiting baculovirus gene with a zinc finger-like motif. J Virol 67:2168-74.

Curcio, C. A., C. L. Millican, K. A. Allen, and R. E. Kalina. 1993. Aging of the human photoreceptor mosaic: evidence for selective vulnerability of rods in central retina. Invest Ophthalmol Vis Sci 34:3278-96.

Dagnelie, G., I. S. Zorge, and T. M. McDonald. 2000. Lutein improves visual function in some patients with retinal degeneration: a pilot study via the Internet. Optometry 71:147-64.

Daiger, S. P., L. S. Sullivan, and B. J. F. Rossiter. 2002. RetNet: Retinal Information NetworkDaiger, S. P.

Davidson, F. F., and H. Steller. 1998. Blocking apoptosis prevents blindness in Drosophila retinal degeneration mutants. Nature 391:587-91.

De Vivo, D. C. 1993. The expanding clinical spectrum of mitochondrial diseases. Brain Dev 15:1-22.

Dejneka, N. S., and J. Bennett. 2001. Gene therapy and retinitis pigmentosa: advances and future challenges. Bioessays 23:662-8.

Deveraux, Q. L., and J. C. Reed. 1999. IAP family proteins--suppressors of apoptosis. Genes Dev 13:239-52.

Dong, J. Y., P. D. Fan, and R. A. Frizzell. 1996. Quantitative analysis of the packaging capacity of recombinant adeno-associated virus. Hum Gene Ther 7:2101-12.

Duisit, G., H. Conrath, S. Saleun, S. Folliot, N. Provost, F. L. Cosset, V. Sandrin, P. Moullier, and F. Rolling. 2002. Five recombinant simian immunodeficiency virus pseudotypes lead to exclusive transduction of retinal pigmented epithelium in rat. Mol Ther 6:446-54.

Eberhardt, O., R. V. Coelln, S. Kugler, J. Lindenau, S. Rathke-Hartlieb, E. Gerhardt, S. Haid, S. Isenmann, C. Gravel, A. Srinivasan, M. Bahr, M. Weller, J. Dichgans, and J. B. Schulz. 2000. Protection by synergistic effects of adenovirus-mediated X-chromosome- linked inhibitor of apoptosis and glial cell line-derived neurotrophic factor gene transfer in the 1-methyl-4-phenyl-1,2,3,6-tetrahydropyridine model of Parkinson's disease. J Neurosci 20:9126-34.

Ehrhardt, A., H. Xu, A. M. Dillow, D. A. Bellinger, T. C. Nichols, and M. A. Kay. 2003. A gene-deleted adenoviral vector results in phenotypic correction of canine hemophilia B without liver toxicity or thrombocytopenia. Blood 102:2403-11.

Einthoven, W., and W. A. Jolly. 1908. The form and magnitude of the electrical response of the eye to stimulation by light at various intensities. Quaterly Journal of Experimental Physiology 1:373-416.

el-Hifnawi el, S., D. T. Lincoln, and H. Dashti. 1995. Effects of vitamin E on the retina and retinal pigment epithelium of IRCS rats. Nutrition 11:576-81.

Eversole-Cire, P., F. A. Concepcion, M. I. Simon, S. Takayama, J. C. Reed, and J. Chen. 2000. Synergistic effect of Bcl-2 and BAG-1 on the prevention of photoreceptor cell death. Invest Ophthalmol Vis Sci 41:1953-61.

Faktorovich, E. G., R. H. Steinberg, D. Yasumura, M. T. Matthes, and M. M. LaVail. 1990. Photoreceptor degeneration in inherited retinal dystrophy delayed by basic fibroblast growth factor. Nature 347:83-6.

Faktorovich, E. G., R. H. Steinberg, D. Yasumura, M. T. Matthes, and M. M. LaVail. 1992. Basic fibroblast growth factor and local injury protect photoreceptors from light damage in the rat. J Neurosci 12:3554-67.

Fink, D. J., J. Glorioso, and M. Mata. 2003. Therapeutic gene transfer with herpes-based vectors: studies in Parkinson's disease and motor nerve regeneration. Exp Neurol 184 Suppl 1:S19-24.

Fisher, K. J., H. Choi, J. Burda, S. J. Chen, and J. M. Wilson. 1996. Recombinant adenovirus deleted of all viral genes for gene therapy of cystic fibrosis. Virology 217:11-22.

Flannery, J. G., S. Zolotukhin, M. I. Vaquero, M. M. LaVail, N. Muzyczka, and W. W. Hauswirth. 1997. Efficient photoreceptor-targeted gene expression in vivo by recombinant adeno-associated virus. Proc Natl Acad Sci U S A 94:6916-21.

Fox, D. A., A. T. Poblenz, L. He, J. B. Harris, and C. J. Medrano. 2003. Pharmacological strategies to block rod photoreceptor apoptosis caused by calcium overload: a mechanistic target-site approach to neuroprotection. Eur J Ophthalmol 13 Suppl 3:S44-56.

Frasson, M., S. Picaud, T. Leveillard, M. Simonutti, S. Mohand-Said, H. Dreyfus, D. Hicks, and J. Sabel. 1999. Glial cell line-derived neurotrophic factor induces histologic and functional protection of rod photoreceptors in the rd/rd mouse. Invest Ophthalmol Vis Sci 40:2724-34.

Freund, C. L., C. Y. Gregory-Evans, T. Furukawa, M. Papaioannou, J. Looser, L. Ploder, J. Bellingham, D. Ng, J. A. Herbrick, A. Duncan, S. W. Scherer, L. C. Tsui, A. Loutradis-Anagnostou, S. G. Jacobson, C. L. Cepko, S. S. Bhattacharya, and R. R. McInnes. 1997. Cone-rod dystrophy due to mutations in a novel photoreceptor-specific homeobox gene (CRX) essential for maintenance of the photoreceptor. Cell 91:543-53.

Garcia-Valenzuela, E., W. Gorczyca, Z. Darzynkiewicz, and S. C. Sharma. 1994. Apoptosis in adult retinal ganglion cells after axotomy. J Neurobiol 25:431-8.

Gervais, F. G., D. Xu, G. S. Robertson, J. P. Vaillancourt, Y. Zhu, J. Huang, A. LeBlanc, D. Smith, M. Rigby, M. S. Shearman, E. E. Clarke, H. Zheng, L. H. Van Der Ploeg, S. C. Ruffolo, N. A. Thornberry, S. Xanthoudakis, R. J. Zamboni, S. Roy, and D. W. Nicholson. 1999. Involvement of caspases in proteolytic cleavage of Alzheimer's amyloid-beta precursor protein and amyloidogenic A beta peptide formation. Cell 97:395-406.

Gilbert, R., R. W. Dudley, A. B. Liu, B. J. Petrof, J. Nalbantoglu, and G. Karpati. 2003. Prolonged dystrophin expression and functional correction of mdx mouse muscle following gene transfer with a helper-dependent (gutted) adenovirus-encoding murine dystrophin. Hum Mol Genet 12:1287-99.

Gottvall, E., and O. Textorius. 1997. Changes in the direct-current electroretinogram of albino rabbits during prolonged intermittent recording. Eur J Ophthalmol 7:73-81.

Granit, R. 1933. The components of the retinal action potential in mammals and their relation to the discharge in the optic nerve. J Physiol 77:207-239.

Green, D. G., and N. V. Kapousta-Bruneau. 1999. Electrophysiological properties of a new isolated rat retina preparation. Vision Res 39:2165-77.

Green, E. S., K. G. Rendahl, S. Zhou, M. Ladner, M. Coyne, R. Srivastava, W. C. Manning, and J. G. Flannery. 2001. Two animal models of retinal degeneration are rescued by recombinant adeno-associated virus-mediated production of FGF-5 and FGF-18. Mol Ther 3:507-15.

Grimm, C., A. Wenzel, F. Hafezi, S. Yu, T. M. Redmond, and C. E. Reme. 2000. Protection of Rpe65-deficient mice identifies rhodopsin as a mediator of light-induced retinal degeneration. Nat Genet 25:63-6.

Grimm, D., A. Kern, K. Rittner, and J. A. Kleinschmidt. 1998. Novel tools for production and purification of recombinant adenoassociated virus vectors. Hum Gene Ther 9:2745-60.

Grosche, J., W. Hartig, and A. Reichenbach. 1995. Expression of glial fibrillary acidic protein (GFAP), glutamine synthetase (GS), and Bcl-2 protooncogene protein by Muller (glial) cells in retinal light damage of rats. Neurosci Lett 185:119-22.

Grover, S., G. A. Fishman, D. G. Birch, K. G. Locke, and B. Rosner. 2003. Variability of full-field electroretinogram responses in subjects without diffuse photoreceptor cell disease. Ophthalmology 110:1159-63.

Grumet, A. E., J. L. Wyatt, Jr., and J. F. Rizzo, 3rd. 2000. Multi-electrode stimulation and recording in the isolated retina. J Neurosci Methods 101:31-42.

Gu, S. M., D. A. Thompson, C. R. Srikumari, B. Lorenz, U. Finckh, A. Nicoletti, K. R. Murthy, M. Rathmann, G. Kumaramanickavel, M. J. Denton, and A. Gal. 1997. Mutations in RPE65 cause autosomal recessive childhood-onset severe retinal dystrophy. Nat Genet 17:194-7.

Guy, J., X. Qi, N. Muzyczka, and W. W. Hauswirth. 1999. Reporter expression persists 1 year after adeno-associated virus-mediated gene transfer to the optic nerve. Arch Ophthalmol 117:929-37.

Hacein-Bey-Abina, S., C. Von Kalle, M. Schmidt, M. P. McCormack, N. Wulffraat, P. Leboulch, A. Lim, C. S. Osborne, R. Pawliuk, E. Morillon, R. Sorensen, A. Forster, P. Fraser, J. I. Cohen, G. de Saint Basile, I. Alexander, U. Wintergerst, T. Frebourg, A. Aurias, D. Stoppa-Lyonnet, S. Romana, I. Radford-Weiss, F. Gross, F. Valensi, E. Delabesse, E. Macintyre, F. Sigaux, J. Soulier, L. E. Leiva, M. Wissler, C. Prinz, T. H. Rabbitts, F. Le Deist, A. Fischer, and M. Cavazzana-Calvo. 2003. LMO2-associated clonal T cell proliferation in two patients after gene therapy for SCID-X1. Science 302:415-9.

Hafezi, F., J. P. Steinbach, A. Marti, K. Munz, Z. Q. Wang, E. F. Wagner, A. Aguzzi, and C. E. Reme. 1997. The absence of c-fos prevents light-induced apoptotic cell death of photoreceptors in retinal degeneration in vivo. Nat Med 3:346-9.

Hahn, W., S. H. Ho, J. G. Jeong, E. Y. Hahn, S. Kim, S. S. Yu, and J. M. Kim. 2004. Viral vector-mediated transduction of a modified thrombospondin-2 cDNA inhibits tumor growth and angiogenesis. Gene Ther 11:739-45.

Haijema, B. J., H. Volders, and P. J. Rottier. 2004. Live, attenuated coronavirus vaccines through the directed deletion of group-specific genes provide protection against feline infectious peritonitis. J Virol 78:3863-71.

Hanna, M. B. 1965. Management of night-blindness with vitamins A and E. Bull Ophthalmol Soc Egypt 58:219-24.

Hao, W., A. Wenzel, M. S. Obin, C. K. Chen, E. Brill, N. V. Krasnoperova, P. Eversole-Cire, Y. Kleyner, A. Taylor, M. I. Simon, C. Grimm, C. E. Reme, and J. Lem. 2002. Evidence for two apoptotic pathways in light-induced retinal degeneration. Nat Genet 32:254-60.

Hauswirth, W. W., and L. Beaufrere. 2000. Ocular gene therapy: quo vadis? Invest Ophthalmol Vis Sci 41:2821-6.

Hauswirth, W. W., M. M. LaVail, J. G. Flannery, and A. S. Lewin. 2000. Ribozyme gene therapy for autosomal dominant retinal disease. Clin Chem Lab Med 38:147-53.

Hauswirth, W. W., and R. R. McInnes. 1998. Retinal gene therapy 1998: summary of a workshop. Mol Vis 4:11.

Hee, M. R., J. A. Izatt, E. A. Swanson, D. Huang, J. S. Schuman, C. P. Lin, C. A. Puliafito, and J. G. Fujimoto. 1995. Optical coherence tomography of the human retina. Arch Ophthalmol 113:325-32.

Heynen, H., L. Wachtmeister, and D. van Norren. 1985. Origin of the oscillatory potentials in the primate retina. Vision Res 25:1365-73.

Hofer-Warbinek, R., J. A. Schmid, C. Stehlik, B. R. Binder, J. Lipp, and R. de Martin. 2000. Activation of NF-kappa B by XIAP, the X chromosome-linked inhibitor of apoptosis, in endothelial cells involves TAK1. J Biol Chem 275:22064-8.

Holcik, M., H. Gibson, and R. G. Korneluk. 2001. XIAP: Apoptotic brake and promising therapeutic target. Apoptosis 6:253-61.

Holcik, M., and R. G. Korneluk. 2000. Functional characterization of the X-linked inhibitor of apoptosis (XIAP) internal ribosome entry site element: role of La autoantigen in XIAP translation. Mol Cell Biol 20:4648-57.

Holcik, M., C. Yeh, R. G. Korneluk, and T. Chow. 2000. Translational upregulation of X-linked inhibitor of apoptosis (XIAP) increases resistance to radiation induced cell death. Oncogene 19:4174-7.

Holopigian, K., V. C. Greenstein, W. Seiple, D. C. Hood, and R. E. Carr. 2004. Rod and cone photoreceptor function in patients with cone dystrophy. Invest Ophthalmol Vis Sci 45:275-81.

Hood, D. C., and D. G. Birch. 1990. The A-wave of the human electroretinogram and rod receptor function. Invest Ophthalmol Vis Sci 31:2070-81.

Hood, D. C., and D. G. Birch. 1996. Beta wave of the scotopic (rod) electroretinogram as a measure of the activity of human on-bipolar cells. J Opt Soc Am A 13:623-33.

Inglehearn, C. F. 1998. Molecular genetics of human retinal dystrophies. Eye 12:571-9.

Iwata, A., V. M. Stevenson, A. Minard, M. Tasch, J. Tupper, E. Lagasse, I. Weissman, J. M. Harlan, and R. K. Winn. 2003. Over-expression of Bcl-2 provides protection in septic mice by a trans effect. J Immunol 171:3136-41.

Jolicoeur, P., C. Hu, T. W. Mak, J. C. Martinou, and D. G. Kay. 2003. Protection against murine leukemia virus-induced spongiform myeloencephalopathy in mice overexpressing Bcl-2 but not in mice deficient for interleukin-6, inducible nitric oxide synthetase, ICE, Fas, Fas ligand, or TNF-R1 genes. J Virol 77:13161-70.

Jones, B. W., C. B. Watt, J. M. Frederick, W. Baehr, C. K. Chen, E. M. Levine, A. H. Milam, M. M. Lavail, and R. E. Marc. 2003. Retinal remodeling triggered by photoreceptor degenerations. J Comp Neurol 464:1-16.

Jones, S. E., C. Jomary, J. Grist, H. J. Stewart, and M. J. Neal. 2000a. Altered expression of secreted frizzled-related protein-2 in retinitis pigmentosa retinas. Invest Ophthalmol Vis Sci 41:1297-301.

Jones, S. E., C. Jomary, J. Grist, H. J. Stewart, and M. J. Neal. 2000b. Modulated expression of secreted frizzled-related proteins in human retinal degeneration. Neuroreport 11:3963-7.

Jones, S. E., J. D. McHugh, C. Jomary, A. Shallal, and M. J. Neal. 1994. Assessment of liposomal transfection of ocular tissues in vivo. Gene Ther 1:S61.

Joseph, R. M., and T. Li. 1996. Overexpression of Bcl-2 or Bcl-XL transgenes and photoreceptor degeneration. Invest Ophthalmol Vis Sci 37:2434-46.

Kamili, S., J. Spelbring, D. Carson, and K. Krawczynski. 2004. Protective efficacy of hepatitis E virus DNA vaccine administered by gene gun in the cynomolgus macaque model of infection. J Infect Dis 189:258-64.

Kearns, W. G., S. A. Afione, S. B. Fulmer, M. C. Pang, D. Erikson, M. Egan, M. J. Landrum, T. R. Flotte, and G. R. Cutting. 1996. Recombinant adeno-associated virus (AAV-CFTR) vectors do not integrate in a site-specific fashion in an immortalized epithelial cell line. Gene Ther 3:748-55.

Keegan, D. J., P. Kenna, M. M. Humphries, P. Humphries, D. I. Flitcroft, P. J. Coffey, R. D. Lund, and J. M. Lawrence. 2003. Transplantation of syngeneic Schwann cells to the retina of the rhodopsin knockout (rho(-/-)) mouse. Invest Ophthalmol Vis Sci 44:3526-32.

Khan, N. W., J. A. Jamison, J. A. Kemp, and P. A. Sieving. 2001. Analysis of photoreceptor function and inner retinal activity in juvenile X-linked retinoschisis. Vision Res 41:3931-42.

Kido, M., K. A. Rich, G. Yang, E. Barron, D. B. Kohn, M. R. al-Ubaidi, J. C. Blanks, and G. Lang. 1996. Use of a retroviral vector with an internal opsin promoter to direct gene expression to retinal photoreceptor cells. Curr Eye Res 15:833-44.

Kiselev, A., M. Socolich, J. Vinos, R. W. Hardy, C. S. Zuker, and R. Ranganathan. 2000. A molecular pathway for light-dependent photoreceptor apoptosis in Drosophila. Neuron 28:139-52.

Kiuchi, K., M. Kondo, S. Ueno, K. Moriguchi, K. Yoshizawa, Y. Miyake, M. Matsumura, and A. Tsubura. 2003. Functional rescue of N-methyl-N-nitrosourea-induced retinopathy by nicotinamide in Sprague-Dawley rats. Curr Eye Res 26:355-62.

Kiuchi, K., K. Yoshizawa, N. Shikata, M. Matsumura, and A. Tsubura. 2002. Nicotinamide prevents N-methyl-N-nitrosourea-induced photoreceptor cell apoptosis in Sprague-Dawley rats and C57BL mice. Exp Eye Res 74:383-92.

Kolb, H., E. Fernandez, and R. Nelson. 2003. Webvision: The organization of the retina and visual system.

Kong, J., and P. Gouras. 2003. The effect of body temperature on the murine electroretinogram. Doc Ophthalmol 106:239-42.

Kotin, R. M., R. M. Linden, and K. I. Berns. 1992. Characterization of a preferred site on human chromosome 19q for integration of adeno-associated virus DNA by non-homologous recombination. Embo J 11:5071-8.

Kotin, R. M., J. C. Menninger, D. C. Ward, and K. I. Berns. 1991. Mapping and direct visualization of a region-specific viral DNA integration site on chromosome 19q13-qter. Genomics 10:831-4.

Kreppel, F., T. T. Luther, I. Semkova, U. Schraermeyer, and S. Kochanek. 2002. Long-term transgene expression in the RPE after gene transfer with a high-capacity adenoviral vector. Invest Ophthalmol Vis Sci 43:1965-70.

Krill, A. E. 1972. Retinitis pigmentosa: a review. Sight Sav Rev 42:21-8.

Kucharczak, J., M. J. Simmons, Y. Fan, and C. Gelinas. 2003. To be, or not to be: NF-kappaB is the answer--role of Rel/NF-kappaB in the regulation of apoptosis. Oncogene 22:8961-82.

Kugler, S., G. Straten, F. Kreppel, S. Isenmann, P. Liston, and M. Bahr. 2000. The X-linked inhibitor of apoptosis (XIAP) prevents cell death in axotomized CNS neurons in vivo. Cell Death Differ 7:815-24.

Kumar-Singh, R., and D. B. Farber. 1998. Encapsidated adenovirus mini-chromosome-mediated delivery of genes to the retina: application to the rescue of photoreceptor degeneration. Hum Mol Genet 7:1893-900.

LaCasse, E. C., S. Baird, R. G. Korneluk, and A. E. MacKenzie. 1998. The inhibitors of apoptosis (IAPs) and their emerging role in cancer. Oncogene 17:3247-59.

Lambiase, A., and L. Aloe. 1996. Nerve growth factor delays retinal degeneration in C3H mice. Graefes Arch Clin Exp Ophthalmol 234 Suppl 1:S96-100.

Lau, D., L. H. McGee, S. Zhou, K. G. Rendahl, W. C. Manning, J. A. Escobedo, and J. G. Flannery. 2000. Retinal degeneration is slowed in transgenic rats by AAV-mediated delivery of FGF-2. Invest Ophthalmol Vis Sci 41:3622-33.

Laughlin, C. A., N. Jones, and B. J. Carter. 1982. Effect of deletions in adenovirus early region 1 genes upon replication of adeno-associated virus. J Virol 41:868-76.

LaVail, M. M. 2002. Outer nuclear layer thickness over time in P23H and S334ter transgenic rats (unpublished results).

LaVail, M. M., E. G. Faktorovich, J. M. Hepler, K. L. Pearson, D. Yasumura, M. T. Matthes, and R. H. Steinberg. 1991. Basic fibroblast growth factor protects photoreceptors from light-induced degeneration in albino rats. Ann N Y Acad Sci 638:341-7.

LaVail, M. M., K. Unoki, D. Yasumura, M. T. Matthes, G. D. Yancopoulos, and R. H. Steinberg. 1992. Multiple growth factors, cytokines, and neurotrophins rescue photoreceptors from the damaging effects of constant light. Proc Natl Acad Sci U S A 89:11249-53.

LaVail, M. M., D. Yasumura, M. T. Matthes, C. Lau-Villacorta, K. Unoki, C. H. Sung, and R. H. Steinberg. 1998. Protection of mouse photoreceptors by survival factors in retinal degenerations. Invest Ophthalmol Vis Sci 39:592-602.

Lawrence, J. M., D. J. Keegan, E. M. Muir, P. J. Coffey, J. H. Rogers, M. J. Wilby, J. W. Fawcett, and R. D. Lund. 2004. Transplantation of Schwann cell line clones secreting GDNF or BDNF into the retinas of dystrophic Royal College of Surgeons rats. Invest Ophthalmol Vis Sci 45:267-74.

Levy, Y. S., D. Merims, H. Panet, Y. Barhum, E. Melamed, and D. Offen. 2003. Induction of neuron-specific enolase promoter and neuronal markers in differentiated mouse bone marrow stromal cells. J Mol Neurosci 21:121-32.

Lewis, G. P., P. A. Erickson, C. J. Guerin, D. H. Anderson, and S. K. Fisher. 1992. Basic fibroblast growth factor: a potential regulator of proliferation and intermediate filament expression in the retina. J Neurosci 12:3968-78.

Lewis, J., E. Burstein, S. B. Reffey, S. B. Bratton, A. B. Roberts, and C. S. Duckett. 2004. Uncoupling of the Signaling and Caspase-inhibitory Properties of X-linked Inhibitor of Apoptosis. J Biol Chem 279:9023-9.

Li, F., J. K. Craigo, L. Howe, J. D. Steckbeck, S. Cook, C. Issel, and R. C. Montelaro. 2003a. A live attenuated equine infectious anemia virus proviral vaccine with a modified S2 gene provides protection from detectable infection by intravenous virulent virus challenge of experimentally inoculated horses. J Virol 77:7244-53.

Li, J. Z., G. R. Hankins, C. Kao, H. Li, J. Kammauff, and G. A. Helm. 2003b. Osteogenesis in rats induced by a novel recombinant helper-dependent bone morphogenetic protein-9 (BMP-9) adenovirus. J Gene Med 5:748-56.

Li, T., M. A. Sandberg, B. S. Pawlyk, B. Rosner, K. C. Hayes, T. P. Dryja, and E. L. Berson. 1998. Effect of vitamin A supplementation on rhodopsin mutants threonine-17 --> methionine and proline-347 --> serine in transgenic mice and in cell cultures. Proc Natl Acad Sci U S A 95:11933-8.

Liang, F. Q., T. S. Aleman, N. S. Dejneka, L. Dudus, K. J. Fisher, A. M. Maguire, S. G. Jacobson, and J. Bennett. 2001. Long-term protection of retinal structure but not function using RAAV.CNTF in animal models of retinitis pigmentosa. Mol Ther 4:461-72.

Liang, Q., K. Nguyen, N. Satyamurthy, J. R. Barrio, M. E. Phelps, S. S. Gambhir, and H. R. Herschman. 2002. Monitoring adenoviral DNA delivery, using a mutant herpes simplex virus type 1 thymidine kinase gene as a PET reporter gene. Gene Ther 9:1659-66.

Lin, N., W. Fan, H. J. Sheedlo, and J. E. Turner. 1997. Basic fibroblast growth factor treatment delays age-related photoreceptor degeneration in Fischer 344 rats. Exp Eye Res 64:239-48.

Liston, P., N. Roy, K. Tamai, C. Lefebvre, S. Baird, G. Cherton-Horvat, R. Farahani, M. McLean, J. E. Ikeda, A. MacKenzie, and R. G. Korneluk. 1996. Suppression of apoptosis in mammalian cells by NAIP and a related family of IAP genes. Nature 379:349-53.

Liu, C., Y. Li, M. Peng, A. M. Laties, and R. Wen. 1999. Activation of caspase-3 in the retina of transgenic rats with the rhodopsin mutation s334ter during photoreceptor degeneration. J Neurosci 19:4778-85.

Luthert, P. J., and N. H. Chong. 1998. Photoreceptor rescue. Eye 12:591-6.

MacFarlane, M., W. Merrison, S. B. Bratton, and G. M. Cohen. 2002. Proteasome-mediated degradation of Smac during apoptosis: XIAP promotes Smac ubiquitination in vitro. J Biol Chem.

Machida, S., P. Chaudhry, T. Shinohara, D. P. Singh, V. N. Reddy, L. T. Chylack, Jr., P. A. Sieving, and R. A. Bush. 2001. Lens epithelium-derived growth factor promotes photoreceptor survival in light-damaged and RCS rats. Invest Ophthalmol Vis Sci 42:1087-95.

Machida, S., M. Kondo, J. A. Jamison, N. W. Khan, L. T. Kononen, T. Sugawara, R. A. Bush, and P. A. Sieving. 2000. P23H rhodopsin transgenic rat: correlation of retinal function with histopathology. Invest Ophthalmol Vis Sci 41:3200-9.

Marc, R. E., B. W. Jones, C. B. Watt, and E. Strettoi. 2003. Neural remodeling in retinal degeneration. Prog Retin Eye Res 22:607-55.

Marin-Teva, J. L., I. Dusart, C. Colin, A. Gervais, N. van Rooijen, and M. Mallat. 2004. Microglia promote the death of developing Purkinje cells. Neuron 41:535-47.

Marmor, M. F. 1979. The electroretinogram in retinitis pigmentosa. Arch Ophthalmol 97:1300-4.

Marmor, M. F., and G. A. Fishman. 1989. At last. A standard electroretinography protocol. Arch Ophthalmol 107:813-4.

Marmor, M. F., G. E. Holder, M. W. Seeliger, and Y. Shuichi. 2003. Standard for clinical electroretinography. International Society for Clinical Electrophysiology of Vision (2003 Update). ISCEV website:1-19.

Marmor, M. F., and E. Zrenner. 1998. Standard for clinical electroretinography (1999 update). International Society for Clinical Electrophysiology of Vision. Doc Ophthalmol 97:143-56.

Marshall, E. 2001. Gene therapy. Viral vectors still pack surprises. Science 294:1640.

Martin-Martinez, M. D., M. Stoenoiu, C. Verkaeren, O. Devuyst, and C. Delporte. 2004. Recombinant adenovirus administration in rat peritoneum: endothelial expression and safety concerns. Nephrol Dial Transplant 19:1293-7.

Massof, R. W., and D. Finkelstein. 1993. Supplemental vitamin A retards loss of ERG amplitude in retinitis pigmentosa. Arch Ophthalmol 111:751-4.

Mayordomo, R., A. I. Valenciano, E. J. de la Rosa, and F. Hallbook. 2003. Generation of retinal ganglion cells is modulated by caspase-dependent programmed cell death. Eur J Neurosci 18:1744-50.

McGee Sanftner, L. H., H. Abel, W. W. Hauswirth, and J. G. Flannery. 2001. Glial cell line derived neurotrophic factor delays photoreceptor degeneration in a transgenic rat model of retinitis pigmentosa. Mol Ther 4:622-9.

McKinnon, S. J., N. L. Ransom, N. G. Tahzib, D. M. Lehman, and W. W. Hauswirth. 2001. Intravitreal gene therapy using adeno-associated virus (AAV) delivery of X-linked inhibitor of apoptosis protein (XIAP) protects optic nerve axons in a hypertensive rat model of glaucoma (abstract). IOVS 42(4):2209.

McNally, N., P. Kenna, M. M. Humphries, A. H. Hobson, N. W. Khan, R. A. Bush, P. A. Sieving, P. Humphries, and G. J. Farrar. 1999. Structural and functional rescue of

murine rod photoreceptors by human rhodopsin transgene. Hum Mol Genet 8:1309-12.

Merin, S., and E. Auerbach. 1976. Retinitis pigmentosa. Surv Ophthalmol 20:303-46.

Milam, A. H., A. E. Hendrickson, M. Xiao, J. E. Smith, D. E. Possin, S. K. John, and P. M. Nishina. 2000. Localization of tubby-like protein 1 in developing and adult human retinas. Invest Ophthalmol Vis Sci 41:2352-6.

Miller, R. F., and J. E. Dowling. 1970. Intracellular responses of the Muller (glial) cells of mudpuppy retina: their relation to b-wave of the electroretinogram. J Neurophysiol 33:323-41.

Mitani, K., F. L. Graham, C. T. Caskey, and S. Kochanek. 1995. Rescue, propagation, and partial purification of a helper virus-dependent adenovirus vector. Proc Natl Acad Sci U S A 92:3854-8.

Miyazaki, M., Y. Ikeda, Y. Yonemitsu, Y. Goto, T. Sakamoto, T. Tabata, Y. Ueda, M. Hasegawa, S. Tobimatsu, T. Ishibashi, and K. Sueishi. 2003. Simian lentiviral vector-mediated retinal gene transfer of pigment epithelium-derived factor protects retinal degeneration and electrical defect in Royal College of Surgeons rats. Gene Ther 10:1503-11.

Moriguchi, K., K. Yoshizawa, N. Shikata, T. Yuri, H. Takada, T. Hada, and A. Tsubura. 2004. Suppression of N-methyl-N-nitrosourea-induced photoreceptor apoptosis in rats by docosahexaenoic acid. Ophthalmic Res 36:98-105.

Moriguchi, K., T. Yuri, K. Yoshizawa, K. Kiuchi, H. Takada, Y. Inoue, T. Hada, M. Matsumura, and A. Tsubura. 2003. Dietary docosahexaenoic acid protects against N-methyl-N-nitrosourea-induced retinal degeneration in rats. Exp Eye Res 77:167-73.

Murata, T., H. Kimura, T. Sakamoto, R. Osusky, C. Spee, T. J. Stout, D. R. Hinton, and S. J. Ryan. 1997. Ocular gene therapy: experimental studies and clinical possibilities. Ophthalmic Res 29:242-51.

Naka, K. I., and W. A. Rushton. 1966. S-potentials from luminosity units in the retina of fish (Cyprinidae). J Physiol 185:587-99.

Nambu, H., K. Yuge, M. Nakajima, N. Shikata, K. Takahashi, H. Miki, M. Uyama, and A. Tsubura. 1997. Morphologic characteristics of N-methyl-N-nitrosourea-induced retinal degeneration in C57BL mice. Pathol Int 47:377-83.

Nathwani, A. C., A. M. Davidoff, H. Hanawa, Y. Hu, F. A. Hoffer, A. Nikanorov, C. Slaughter, C. Y. Ng, J. Zhou, J. N. Lozier, T. D. Mandrell, E. F. Vanin, and A. W. Nienhuis. 2002. Sustained high-level expression of human factor IX (hFIX) after liver-targeted delivery of recombinant adeno-associated virus encoding the hFIX gene in rhesus macaques. Blood 100:1662-9.

Nguyen, T. H., J. Oberholzer, J. Birraux, P. Majno, P. Morel, and D. Trono. 2002. Highly efficient lentiviral vector-mediated transduction of nondividing, fully reimplantable primary hepatocytes. Mol Ther 6:199-209.

Noell, W. K. 1954. The origin of the electroretinogram. American Journal of Ophthalmology 38:78-90.

Noell, W. K., and R. Albrecht. 1971. Irreversible effects on visible light on the retina: role of vitamin A. Science 172:76-9.

Nozaki, S., M. Wakakura, and S. Ishikawa. 1983. Circadian rhythm of human electroretinogram. Jpn J Ophthalmol 27:346-52.

Nusinowitz, S., W. H. Ridder III, and J. R. Heckenlively. 2002. Electrophysiological Testing of the Mouse Visual System. Pages 320-344 *in* Systemic Evaluation of the Mouse Eye: Anatomy, Pathology, and Biomethods (R. S. Smith, ed.) CRS Press, Boca Raton.

Ogata, N., M. Wada, T. Otsuji, N. Jo, J. Tombran-Tink, and M. Matsumura. 2002. Expression of pigment epithelium-derived factor in normal adult rat eye and experimental choroidal neovascularization. Invest Ophthalmol Vis Sci 43:1168-75.

Ogilvie, J. M., and J. D. Speck. 2002. Dopamine has a critical role in photoreceptor degeneration in the rd mouse. Neurobiol Dis 10:33-40.

Ogino, H., M. Ito, K. Matsumoto, S. Yagyu, H. Tsuda, I. Hirono, C. P. Wild, and R. Montesano. 1993. Retinal degeneration induced by N-methyl-N-nitrosourea and detection of 7-methyldeoxyguanosine in the rat retina. Toxicol Pathol 21:21-5.

Ohyama, T., D. H. Hackos, S. Frings, V. Hagen, U. B. Kaupp, and J. I. Korenbrot. 2000. Fraction of the dark current carried by Ca(2+) through cGMP-gated ion channels of intact rod and cone photoreceptors. J Gen Physiol 116:735-54.

Okoye, G., J. Zimmer, J. Sung, P. Gehlbach, T. Deering, H. Nambu, S. Hackett, M. Melia, N. Esumi, D. J. Zack, and P. A. Campochiaro. 2003. Increased expression of brain-derived neurotrophic factor preserves retinal function and slows cell death from rhodopsin mutation or oxidative damage. J Neurosci 23:4164-72.

Olshevskaya, E. V., A. N. Ennilov, and A. M. Dizhoor. 2002. Factors that affect regulation of cGMP synthesis in vertebrate photoreceptors and their genetic link to human retinal degeneration. Mol Cell Biochem 230:139-47.

Onodera, M., T. Ariga, N. Kawamura, I. Kobayashi, M. Ohtsu, M. Yamada, A. Tame, H. Furuta, M. Okano, S. Matsumoto, H. Kotani, G. J. McGarrity, R. M. Blaese, and Y. Sakiyama. 1998. Successful peripheral T-lymphocyte-directed gene transfer for a patient with severe combined immune deficiency caused by adenosine deaminase deficiency. Blood 91:30-6.

Pagon, R. A. 1988. Retinitis pigmentosa. Surv Ophthalmol 33:137-77.

Palczewski, K., T. Kumasaka, T. Hori, C. A. Behnke, H. Motoshima, B. A. Fox, I. Le Trong, D. C. Teller, T. Okada, R. E. Stenkamp, M. Yamamoto, and M. Miyano. 2000. Crystal structure of rhodopsin: A G protein-coupled receptor. Science 289:739-45.

Parks, R. J., L. Chen, M. Anton, U. Sankar, M. A. Rudnicki, and F. L. Graham. 1996. A helper-dependent adenovirus vector system: removal of helper virus by Cre-mediated excision of the viral packaging signal. Proc Natl Acad Sci U S A 93:13565-70.

Pasantes-Morales, H., H. Quiroz, and O. Quesada. 2002. Treatment with taurine, diltiazem, and vitamin E retards the progressive visual field reduction in retinitis pigmentosa: a 3-year follow-up study. Metab Brain Dis 17:183-97.

Peachey, N. S., and S. L. Ball. 2003. Electrophysiological analysis of visual function in mutant mice. Doc Ophthalmol 107:13-36.

Pepe, I. M. 1999. Rhodopsin and phototransduction. J Photochem Photobiol B 48:1-10.

Pepe, I. M., C. Cugnoli, M. Peluso, L. Vergani, and A. Boero. 1987. Structure of a protein catalyzing the formation of 11 cis-retinal in the visual cycle of invertebrate eyes. Cell Biophys 10:15-22.

Perrelet, D., A. Ferri, P. Liston, P. Muzzin, R. G. Korneluk, and A. C. Kato. 2002. IAPs are essential for GDNF-mediated neuroprotective effects in injured motor neurons in vivo. Nat Cell Biol 4:175-9.

Perry, J., J. Du, H. Kjeldbye, and P. Gouras. 1995. The effects of bFGF on RCS rat eyes. Curr Eye Res 14:585-92.

Petrin, D., A. Baker, S. G. Coupland, P. Liston, M. Narang, K. Damji, B. Leonard, V. A. Chiodo, A. Timmers, W. Hauswirth, R. G. Korneluk, and C. Tsilfidis. 2003. Structural and functional protection of photoreceptors from MNU-induced retinal degeneration by the X-linked inhibitor of apoptosis. Invest Ophthalmol Vis Sci 44:2757-63.

Ponnazhagan, S., D. Erikson, W. G. Kearns, S. Z. Zhou, P. Nahreini, X. S. Wang, and A. Srivastava. 1997. Lack of site-specific integration of the recombinant adeno-associated virus 2 genomes in human cells. Hum Gene Ther 8:275-84.

Portera-Cailliau, C., C. H. Sung, J. Nathans, and R. Adler. 1994. Apoptotic photoreceptor cell death in mouse models of retinitis pigmentosa. Proc Natl Acad Sci U S A 91:974-8.

Pulsinelli, W. A., and A. M. Buchan. 1988. The four-vessel occlusion rat model: method for complete occlusion of vertebral arteries and control of collateral circulation. Stroke 19:913-4.

Quiambao, A. B., E. Tan, S. Chang, N. Komori, M. I. Naash, N. S. Peachey, H. Matsumoto, D. S. Ucker, and M. R. Al-Ubaidi. 2001. Transgenic Bcl-2 expressed in photoreceptor cells confers both death-sparing and death-inducing effects. Exp Eye Res 73:711-21.

Ranchon, I., J. M. Gorrand, J. Cluzel, M. T. Droy-Lefaix, and M. Doly. 1999. Functional protection of photoreceptors from light-induced damage by dimethylthiourea and Ginkgo biloba extract. Invest Ophthalmol Vis Sci 40:1191-9.

Rangaswamy, N. V., D. C. Hood, and L. J. Frishman. 2003. Regional variations in local contributions to the primate photopic flash ERG: revealed using the slow-sequence mfERG. Invest Ophthalmol Vis Sci 44:3233-47.

Raper, S. E., N. Chirmule, F. S. Lee, N. A. Wivel, A. Bagg, G. P. Gao, J. M. Wilson, and M. L. Batshaw. 2003. Fatal systemic inflammatory response syndrome in a ornithine transcarbamylase deficient patient following adenoviral gene transfer. Mol Genet Metab 80:148-58.

Reme, C. E., C. Grimm, F. Hafezi, A. Marti, and A. Wenzel. 1998. Apoptotic cell death in retinal degenerations. Prog Retin Eye Res 17:443-64.

Riedl, S. J., M. Renatus, R. Schwarzenbacher, Q. Zhou, C. Sun, S. W. Fesik, R. C. Liddington, and G. S. Salvesen. 2001. Structural basis for the inhibition of caspase-3 by XIAP. Cell 104:791-800.

Robson, J. G., and L. J. Frishman. 1998. Dissecting the dark-adapted electroretinogram. Doc Ophthalmol 95:187-215.

Roecker, E. B., E. Pulos, G. H. Bresnick, and M. Severns. 1992. Characterization of the electroretinographic scotopic B-wave amplitude in diabetic and normal subjects. Invest Ophthalmol Vis Sci 33:1575-83.

Ross, M. H., L. G. Romrell, and G. I. Kaye. 1995. Histology: A text and atlas, 3rd edition. Williams and Wilkins, Baltimore.

Rotstein, N. P., L. E. Politi, O. L. German, and R. Girotti. 2003. Protective effect of docosahexaenoic acid on oxidative stress-induced apoptosis of retina photoreceptors. Invest Ophthalmol Vis Sci 44:2252-9.

Roy, N., Q. L. Deveraux, R. Takahashi, G. S. Salvesen, and J. C. Reed. 1997. The c-IAP-1 and c-IAP-2 proteins are direct inhibitors of specific caspases. Embo J 16:6914-25.

Safars, M., J. C. Jeanny, M. Mosnier, and Y. Courtois. 1997. Protection against light-induced retinal degeneration with naftidrofuryl (Praxilene) in the rat. J Ocul Pharmacol Ther 13:89-94.

Sakamoto, T., Y. Ikeda, and Y. Yonemitsu. 2001. Gene targeting to the retina. Adv Drug Deliv Rev 52:93-102.

Sanna, M. G., J. da Silva Correia, O. Ducrey, J. Lee, K. Nomoto, N. Schrantz, Q. L. Deveraux, and R. J. Ulevitch. 2002a. IAP suppression of apoptosis involves distinct mechanisms: the TAK1/JNK1 signaling cascade and caspase inhibition. Mol Cell Biol 22:1754-66.

Sanna, M. G., J. Da Silva Correia, Y. Luo, B. Chuang, L. M. Paulson, B. Nguyen, Q. L. Deveraux, and R. J. Ulevitch. 2002b. ILPIP, a novel anti-apoptotic protein that enhances XIAP-mediated activation of JNK1 and protection against apoptosis. J Biol Chem.

Sargan, D. R., P. J. Clements, A. Sohal, C. Y. Gregory, S. S. Bhattacharya, and S. M. Petersen-Jones. 1994. Progressive retinal atrophy: a model for retinitis pigmentosa in companion animals. Gene Ther 1:S89.

Sargent, K. L., P. Ng, C. Evelegh, F. L. Graham, and R. J. Parks. 2004. Development of a size-restricted pIX-deleted helper virus for amplification of helper-dependent adenovirus vectors. Gene Ther 11:504-11.

Sarra, G. M., C. Stephens, M. de Alwis, J. W. Bainbridge, A. J. Smith, A. J. Thrasher, and R. R. Ali. 2001. Gene replacement therapy in the retinal degeneration slow (rds) mouse: the effect on retinal degeneration following partial transduction of the retina. Hum Mol Genet 10:2353-61.

Schertler, G. F., C. Villa, and R. Henderson. 1993. Projection structure of rhodopsin. Nature 362:770-2.

Schnell, T., P. Foley, M. Wirth, J. Munch, and K. Uberla. 2000. Development of a self-inactivating, minimal lentivirus vector based on simian immunodeficiency virus. Hum Gene Ther 11:439-47.

Schwarzer, A., H. Schauf, and P. J. Bauer. 2000. Binding of the cGMP-gated channel to the Na/Ca-K exchanger in rod photoreceptors. J Biol Chem 275:13448-54.

Shinoda, K., Y. Nakamura, K. Matsushita, K. Shimoda, H. Okita, M. Fukuma, T. Yamada, H. Ohde, Y. Oguchi, J. Hata, and A. Umezawa. 2001. Light induced apoptosis is accelerated in transgenic retina overexpressing human EAT/mcl-1, an anti-apoptotic bcl-2 related gene. Br J Ophthalmol 85:1237-43.

Sieving, P. A., and C. Nino. 1988. Scotopic threshold response (STR) of the human electroretinogram. Invest Ophthalmol Vis Sci 29:1608-14.

Simonovic, M., P. G. Gettins, and K. Volz. 2001. Crystal structure of human PEDF, a potent anti-angiogenic and neurite growth-promoting factor. Proc Natl Acad Sci U S A 98:11131-5.

Simons, M., S. Beinroth, M. Gleichmann, P. Liston, R. G. Korneluk, A. E. MacKenzie, M. Bahr, T. Klockgether, G. S. Robertson, M. Weller, and J. B. Schulz. 1999. Adenovirus-mediated gene transfer of inhibitors of apoptosis protein delays apoptosis in cerebellar granule neurons. J Neurochem 72:292-301.

Smith, S. B., C. B. Cooke, and K. L. Yielding. 1988. Effects of the antioxidant butylated hydroxytoluene (BHT) on retinal degeneration induced transplacentally by a single low dosage of N-methyl-N-nitrosourea (MNU). Teratog Carcinog Mutagen 8:175-89.

Sohocki, M. M., L. S. Sullivan, H. A. Mintz-Hittner, D. Birch, J. R. Heckenlively, C. L. Freund, R. R. McInnes, and S. P. Daiger. 1998. A range of clinical phenotypes associated with mutations in CRX, a photoreceptor transcription-factor gene. Am J Hum Genet 63:1307-15.

Soucy, E., Y. Wang, S. Nirenberg, J. Nathans, and M. Meister. 1998. A novel signaling pathway from rod photoreceptors to ganglion cells in mammalian retina. Neuron 21:481-93.

Srinivasula, S. M., R. Hegde, A. Saleh, P. Datta, E. Shiozaki, J. Chai, R. A. Lee, P. D. Robbins, T. Fernandes-Alnemri, Y. Shi, and E. S. Alnemri. 2001. A conserved XIAP-interaction motif in caspase-9 and Smac/DIABLO regulates caspase activity and apoptosis. Nature 410:112-6.

Stanziale, S. F., H. Petrowsky, P. S. Adusumilli, L. Ben-Porat, M. Gonen, and Y. Fong. 2004. Infection with oncolytic herpes simplex virus-1 induces apoptosis in neighboring human cancer cells: a potential target to increase anticancer activity. Clin Cancer Res 10:3225-32.

Steinberg, R. H., S. K. Fisher, and D. H. Anderson. 1980. Disc morphogenesis in vertebrate photoreceptors. J Comp Neurol 190:501-8.

Steinberg, R. H., R. Schmidt, and K. T. Brown. 1970. Intracellular responses to light from cat pigment epithelium: origin of the electroretinogram c-wave. Nature 227:728-30.

Straten, G., C. Schmeer, A. Kretz, E. Gerhardt, S. Kugler, J. B. Schulz, C. Gravel, M. Bahr, and S. Isenmann. 2002. Potential synergistic protection of retinal ganglion cells from axotomy-induced apoptosis by adenoviral administration of glial cell line-derived neurotrophic factor and X-chromosome-linked inhibitor of apoptosis. Neurobiol Dis 11:123-33.

Strettoi, E., and M. Volpini. 2002. Retinal organization in the bcl-2-overexpressing transgenic mouse. J Comp Neurol 446:1-10.

Sugawara, T., P. A. Sieving, P. M. Iuvone, and R. A. Bush. 1998. The melatonin antagonist luzindole protects retinal photoreceptors from light damage in the rat. Invest Ophthalmol Vis Sci 39:2458-65.

Sukumar, S., V. Notario, D. Martin-Zanca, and M. Barbacid. 1983. Induction of mammary carcinomas in rats by nitroso-methylurea involves malignant activation of H-ras-1 locus by single point mutations. Nature 306:658-61.

Sun, C., M. Cai, A. H. Gunasekera, R. P. Meadows, H. Wang, J. Chen, H. Zhang, W. Wu, N. Xu, S. C. Ng, and S. W. Fesik. 1999. NMR structure and mutagenesis of the inhibitor-of-apoptosis protein XIAP. Nature 401:818-22.

Susin, S. A., N. Zamzami, M. Castedo, T. Hirsch, P. Marchetti, A. Macho, E. Daugas, M. Geuskens, and G. Kroemer. 1996. Bcl-2 inhibits the mitochondrial release of an apoptogenic protease. J Exp Med 184:1331-41.

Suzuki, Y., Y. Nakabayashi, and R. Takahashi. 2001. Ubiquitin-protein ligase activity of X-linked inhibitor of apoptosis protein promotes proteasomal degradation of caspase-3 and enhances its anti-apoptotic effect in Fas-induced cell death. Proc Natl Acad Sci U S A 98:8662-7.

Swaroop, A., Q. L. Wang, W. Wu, J. Cook, C. Coats, S. Xu, S. Chen, D. J. Zack, and P. A. Sieving. 1999. Leber congenital amaurosis caused by a homozygous mutation (R90W) in the homeodomain of the retinal transcription factor CRX: direct evidence for the involvement of CRX in the development of photoreceptor function. Hum Mol Genet 8:299-305.

Takahashi, M., H. Miyoshi, I. M. Verma, and F. H. Gage. 1999. Rescue from photoreceptor degeneration in the rd mouse by human immunodeficiency virus vector-mediated gene transfer. J Virol 73:7812-6.

Takahashi, R., Q. Deveraux, I. Tamm, K. Welsh, N. Assa-Munt, G. S. Salvesen, and J. C. Reed. 1998. A single BIR domain of XIAP sufficient for inhibiting caspases. J Biol Chem 273:7787-90.

Taomoto, M., H. Nambu, H. Senzaki, N. Shikata, Y. Oishi, T. Fujii, H. Miki, M. Uyama, and A. Tsubura. 1998. Retinal degeneration induced by N-methyl-N-nitrosourea in Syrian golden hamsters. Graefes Arch Clin Exp Ophthalmol 236:688-95.

Thomson, L. R., Y. Toyoda, F. C. Delori, K. M. Garnett, Z. Y. Wong, C. R. Nichols, K. M. Cheng, N. E. Craft, and C. Kathleen Dorey. 2002a. Long term dietary supplementation with zeaxanthin reduces photoreceptor death in light-damaged Japanese quail. Exp Eye Res 75:529-42.

Thomson, L. R., Y. Toyoda, A. Langner, F. C. Delori, K. M. Garnett, N. Craft, C. R. Nichols, K. M. Cheng, and C. K. Dorey. 2002b. Elevated retinal zeaxanthin and prevention of light-induced photoreceptor cell death in quail. Invest Ophthalmol Vis Sci 43:3538-49.

Thorne, P. S., P. B. McCray, T. S. Howe, and M. A. O'Neill. 1999. Early-onset inflammatory responses in vivo to adenoviral vectors in the presence or absence of lipopolysaccharide-induced inflammation. Am J Respir Cell Mol Biol 20:1155-64.

Timmers, A. M., H. Zhang, A. Squitieri, and C. Gonzalez-Pola. 2001. Subretinal injections in rodent eyes: effects on electrophysiology and histology of rat retina. Mol Vis 7:131-7.

Toietta, G., D. R. Koehler, M. J. Finegold, B. Lee, J. Hu, and A. L. Beaudet. 2003. Reduced inflammation and improved airway expression using helper-dependent adenoviral vectors with a K18 promoter. Mol Ther 7:649-58.

Tomita, T. 1963. Electrical activity in the vertebrate retina. J Opt Soc Am 53:49-57.

Townes-Anderson, E., A. Colantonio, and R. S. St Jules. 1998. Age-related changes in the tiger salamander retina. Exp Eye Res 66:653-67.

Travis, G. H. 1998. Mechanisms of cell death in the inherited retinal degenerations. Am J Hum Genet 62:503-8.

Tsang, S. H., J. Chen, H. Kjeldbye, W. S. Li, M. I. Simon, P. Gouras, and S. P. Goff. 1997. Retarding photoreceptor degeneration in Pdegtm1/Pdegtml mice by an apoptosis suppressor gene. Invest Ophthalmol Vis Sci 38:943-50.

Tsujimoto, Y., M. M. Bashir, I. Givol, J. Cossman, E. Jaffe, C. M. Croce, N. Ikegaki, M. L. Cleary, S. D. Smith, J. Sklar, L. R. Finger, J. Yunis, and P. C. Nowell. 1987. DNA rearrangements in human follicular lymphoma can involve the 5' or the 3' region of the bcl-2 gene. Proc Natl Acad Sci U S A 84:1329-31.

Tsujimoto, Y., and C. M. Croce. 1986. Analysis of the structure, transcripts, and protein products of bcl-2, the gene involved in human follicular lymphoma. Proc Natl Acad Sci U S A 83:5214-8.

Tsujimoto, Y., L. R. Finger, J. Yunis, P. C. Nowell, and C. M. Croce. 1984. Cloning of the chromosome breakpoint of neoplastic B cells with the t(14;18) chromosome translocation. Science 226:1097-9.

Tuohy, G., S. Millington-Ward, P. F. Kenna, P. Humphries, and G. J. Farrar. 2002. Sensitivity of photoreceptor-derived cell line (661W) to baculoviral p35, Z-VAD.FMK, and Fas-associated death domain. Invest Ophthalmol Vis Sci 43:3583-9.

Ueno, S., M. Kondo, Y. Niwa, H. Terasaki, and Y. Miyake. 2004. Luminance dependence of neural components that underlies the primate photopic electroretinogram. Invest Ophthalmol Vis Sci 45:1033-40.

Urase, K., Y. Kouroku, E. Fujita, and T. Momoi. 2003. Region of caspase-3 activation and programmed cell death in the early development of the mouse forebrain. Brain Res Dev Brain Res 145:241-8.

Uteza, Y., J. S. Rouillot, A. Kobetz, D. Marchant, S. Pecqueur, E. Arnaud, H. Prats, J. Honiger, J. L. Dufier, M. Abitbol, and M. Neuner-Jehle. 1999. Intravitreous transplantation of encapsulated fibroblasts secreting the human fibroblast growth factor 2 delays photoreceptor cell degeneration in Royal College of Surgeons rats. Proc Natl Acad Sci U S A 96:3126-31.

Vaegan, and T. J. Millar. 1994. Effect of kainic acid and NMDA on the pattern electroretinogram, the scotopic threshold response, the oscillatory potentials and the electroretinogram in the urethane anaesthetized cat. Vision Res 34:1111-25.

van der Bliek, A. M., and E. M. Meyerowitz. 1991. Dynamin-like protein encoded by the Drosophila shibire gene associated with vesicular traffic. Nature 351:411-4.

van Soest, S., A. Westerveld, P. T. de Jong, E. M. Bleeker-Wagemakers, and A. A. Bergen. 1999. Retinitis pigmentosa: defined from a molecular point of view. Surv Ophthalmol 43:321-34.

Verhagen, A. M., E. J. Coulson, and D. L. Vaux. 2001. Inhibitor of apoptosis proteins and their relatives: IAPs and other BIRPs. Genome Biol 2:REVIEWS3009.

von Coelln, R., S. Kugler, M. Bahr, M. Weller, J. Dichgans, and J. B. Schulz. 2001. Rescue from death but not from functional impairment: caspase inhibition protects dopaminergic cells against 6-hydroxydopamine-induced apoptosis but not against the loss of their terminals. J Neurochem 77:263-73.

Von Seggern, D. J., E. Aguilar, K. Kinder, S. K. Fleck, J. C. Gonzalez Armas, S. C. Stevenson, P. Ghazal, G. R. Nemerow, and M. Friedlander. 2003. In vivo transduction of photoreceptors or ciliary body by intravitreal injection of pseudotyped adenoviral vectors. Mol Ther 7:27-34.

Wachtmeister, L. 1998. Oscillatory potentials in the retina: what do they reveal. Prog Retin Eye Res 17:485-521.

Waldmeier, P. C., and W. G. Tatton. 2004. Interrupting apoptosis in neurodegenerative disease: potential for effective therapy? Drug Discov Today 9:210-8.

Wali, N., and L. E. Leguire. 1992. Fundus pigmentation and the dark-adapted electroretinogram. Doc Ophthalmol 80:1-11.

Wang, L., R. Hernandez-Alcoceba, V. Shankar, M. Zabala, S. Kochanek, B. Sangro, M. G. Kramer, J. Prieto, and C. Qian. 2004. Prolonged and inducible transgene expression in the liver using gutless adenovirus: a potential therapy for liver cancer. Gastroenterology 126:278-89.

Wenzel, A., C. Grimm, A. Marti, N. Kueng-Hitz, F. Hafezi, G. Niemeyer, and C. E. Reme. 2000. c-fos controls the "private pathway" of light-induced apoptosis of retinal photoreceptors. J Neurosci 20:81-8.

Wenzel, A., C. Grimm, M. W. Seeliger, G. Jaissle, F. Hafezi, R. Kretschmer, E. Zrenner, and C. E. Reme. 2001. Prevention of photoreceptor apoptosis by activation of the glucocorticoid receptor. Invest Ophthalmol Vis Sci 42:1653-9.

Whiteley, S. J., H. Klassen, P. J. Coffey, and M. J. Young. 2001. Photoreceptor rescue after low-dose intravitreal IL-1beta injection in the RCS rat. Exp Eye Res 73:557-68.

Wibrand, F., K. Ravn, M. Schwartz, T. Rosenberg, N. Horn, and J. Vissing. 2001. Multisystem disorder associated with a missense mutation in the mitochondrial cytochrome b gene. Ann Neurol 50:540-3.

Wielgus, J. J., L. Corbin Downey, K. W. Ewald, M. E. Hatley, K. C. Wilson, and R. H. Yeilding. 2004. Exposure to low concentrations of nicotine during cranial nerve development inhibits apoptosis and causes cellular hypertrophy in the ventral oculomotor nuclei of the chick embryo. Brain Res 1000:123-33.

Wong, F. 1995. Photoreceptor apoptosis in animal models. Implications for retinitis pigmentosa research. Arch Ophthalmol 113:1245-7.

Wu, G., J. Chai, T. L. Suber, J. W. Wu, C. Du, X. Wang, and Y. Shi. 2000. Structural basis of IAP recognition by Smac/DIABLO. Nature 408:1008-12.

Wu, P., Y. Ye, and C. N. Svendsen. 2002. Transduction of human neural progenitor cells using recombinant adeno-associated viral vectors. Gene Ther 9:245-55.

Wurziger, K., T. Lichtenberger, and R. Hanitzsch. 2001. On-bipolar cells and depolarising third-order neurons as the origin of the ERG-b-wave in the RCS rat. Vision Res 41:1091-101.

Xu, D., Y. Bureau, D. C. McIntyre, D. W. Nicholson, P. Liston, Y. Zhu, W. G. Fong, S. J. Crocker, R. G. Korneluk, and G. S. Robertson. 1999. Attenuation of ischemia-induced cellular and behavioral deficits by X chromosome-linked inhibitor of apoptosis protein overexpression in the rat hippocampus. J Neurosci 19:5026-33.

Xu, X. J., J. Xu, B. Huang, C. T. Livsey, and C. J. Karwoski. 1991. Comparison of pharmacological agents (aspartate vs. aminophosphonobutyric plus kynurenic acids) to block synaptic transmission from retinal photoreceptors in frog. Exp Eye Res 52:691-8.

Yang, Y., S. Fang, J. P. Jensen, A. M. Weissman, and J. D. Ashwell. 2000. Ubiquitin protein ligase activity of IAPs and their degradation in proteasomes in response to apoptotic stimuli. Science 288:874-7.

Yang, Y. L., and X. M. Li. 2000. The IAP family: endogenous caspase inhibitors with multiple biological activities. Cell Res 10:169-77.

Yin, K. J., J. M. Lee, S. D. Chen, J. Xu, and C. Y. Hsu. 2002. Amyloid-beta induces Smac release via AP-1/Bim activation in cerebral endothelial cells. J Neurosci 22:9764-70.

Yoshizawa, K., K. Kiuchi, H. Nambu, J. Yang, H. Senzaki, Y. Kiyozuka, N. Shikata, and A. Tsubura. 2002. Caspase-3 inhibitor transiently delays inherited retinal degeneration in C3H mice carrying the rd gene. Graefes Arch Clin Exp Ophthalmol 240:214-9.

Yoshizawa, K., H. Nambu, J. Yang, Y. Oishi, H. Senzaki, N. Shikata, H. Miki, and A. Tsubura. 1999. Mechanisms of photoreceptor cell apoptosis induced by N-methyl-N-nitrosourea in Sprague-Dawley rats. Lab Invest 79:1359-67.

Yoshizawa, K., J. Yang, H. Senzaki, Y. Uemura, Y. Kiyozuka, N. Shikata, Y. Oishi, H. Miki, and A. Tsubura. 2000. Caspase-3 inhibitor rescues N -methyl- N -nitrosourea-induced retinal degeneration in Sprague-Dawley rats. Exp Eye Res 71:629-35.

Yuge, K., H. Nambu, H. Senzaki, I. Nakao, H. Miki, M. Uyama, and A. Tsubura. 1996. N-methyl-N-nitrosourea-induced photoreceptor apoptosis in the mouse retina. In Vivo 10:483-8.

Zern, M. A., I. Ozaki, L. Duan, R. Pomerantz, S. L. Liu, and D. S. Strayer. 1999. A novel SV40-based vector successfully transduces and expresses an alpha 1-antitrypsin ribozyme in a human hepatoma-derived cell line. Gene Ther 6:114-20.

Ziegler, R. J., S. M. Lonning, D. Armentano, C. Li, D. W. Souza, M. Cherry, C. Ford, C. M. Barbon, R. J. Desnick, G. Gao, J. M. Wilson, R. Peluso, S. Godwin, B. J. Carter, R. J. Gregory, S. C. Wadsworth, and S. H. Cheng. 2004. AAV2 vector harboring a liver-restricted promoter facilitates sustained expression of therapeutic levels of alpha-galactosidase A and the induction of immune tolerance in Fabry mice. Mol Ther 9:231-40.

Zolotukhin, S., M. Potter, W. W. Hauswirth, J. Guy, and N. Muzyczka. 1996. A "humanized" green fluorescent protein cDNA adapted for high-level expression in mammalian cells. J Virol 70:4646-54.

Professional experience

Research Assistant at the University of Ottawa. I am familiar with PCR and different PCR strategies such as anchored, and RACE PCR. I have worked with radioactive isotopes (^{32}P, ^{33}P and ^{35}S). I am familiar with cDNA synthesis and subcloning, purification of DNA and cell culture. I have used numerous molecular techniques as well as basic microbiological techniques to a great extent in my Masters project. I have experience in recording electroretinograms from mice and rats using the Espion system and related software. I am experienced in performing intravitreal and sub-retinal injections in rats.

Publications and Presentations

Graeme C.M. Black, Chantal J. Mazerolle, Yaping Wang, Katrina D. Campsall, ***Dino Petrin****, Brian C. Leonard, Karim F. Damji, David McLeod, Valerie A. Wallace. Abnormalities of the vitreoretinal interface caused by dysregulated Hedgehog signaling during retinal development. Human Molecular Genetics, 12 (24) 3269-76, 2003.*

Dino Petrin, *Adam Baker, Jennifer Brousseau, Stuart Coupland, Petrin Liston, William W. Hauswirth, Robert G. Korneluk, Catherine Tsilfidis. XIAP Protects Photoreceptors From N-methyl-N-nitrosourea-Induced Retinal Degeneration. In Retinal Degenerations, Mechanisms and Experimenal Therapy. Advances in Experimental Medicine and Biology Vol 533 pp 385-393. Eds. M.M. LaVail, J.G. Hollyfield, R.E. Anderson.Kluwer Academic/Plenum Publishers New York.*

Petrin, D.*, Baker, A., Coupland, S.G., Narang, M., Liston, P., Timmers, A., Hauswirth, W.W., Korneluk, R.G., Tsilfidis, C. Structural and Functional Protection of Photoreceptors from MNU-Induced Retinal Degeneration by the X-Linked Inhibitor of Apoptosis (XIAP). Invest Ophthalmol Vis Sci, 44 (6) 2757-63, 2003.*

Petrin, D., *Petrin, V. Focus on the Family. Living with a relative with RP. Vision Quest 2002, November 9th, 2002, Toronto, Canada.*

Petrin, D.P.*, Baker, A., Coupland, S.G., Liston, P., Timmers, A., Hauswirth, W.W., Korneluk, R.G., Tsilfidis, C. Protection of Photoreceptors from N-methyl-N-nitrosourea Induced Retinal Degeneration by the X-Linked Inhibitor of Apoptosis (XIAP). ARVO, Ft. Lauderdale, FL, May 5th-10th, 2002.*

Coupland, S.G., ***Petrin, D.****, Baker, A., Liston, P., Timmers, A., Hauswirth, W.W. Electrophysiologic Evidence of Functional Neuroprotection of Photoreceptors by X-Linked Inhibitor of Apoptosis (XIAP) in a Chemotoxic Model of Retinal Degeneration. ARVO, Ft. Lauderdale, FL, May 5th-10th, 2002.*

***Petrin, D.**, Baker, A., Tsilfidis, C., Coupland, S., Timmers, A., Hauswirth, W., Hewitt, K., Narang, M., Liston, P., Korneluk, R.G. rAAV-XIAP Protects Photoreceptors in a Chemotoxic Model of Retinal Degeneration in Sprague-Dawley Rats. 8Th Annual Ottawa Life Sciences Internatinoal Conference, Ottawa, ON, November 5th-7th, 2001.*

*Tsilfidis, C., **Petrin, D.**, Baker, A., Coupland, S., Hauswirth, W.W., Timmers, A., Liston, P., Korneluk, R.G. Protection of Photoreceptors from N-methyl-N-nitrosourea Induced Retinal Degeneration by the X-Linked Inhibitor of Apoptosis (XIAP). Animal Models of Retinal Degeneration: New Approaches and Applications, the 5th Annual Vision Research Conference, Ft. Lauderbale, April 27th-28th, 2001.*

***Petrin, D.**, Baker, A., Tsilfidis, C., Liston, P., Korneluk, R.G. XIAP Protects Photoreceptors in Sprague-Dawley Rats from N-methyl-N-nitrosourea-Induced Retinal Degeneration. Cell Signaling in Normal and Cancer Cells, Banff, AB, March 2nd-6th, 2001.*

*Korneluk, R.G., **Petrin, D.** From the Bench to the Bedside: Inhibiting Apoptosis as a Gene Therapy Approach for Retinitis Pigmentosa. Vision Quest 2000 and the 11th World Congress of Retina International, Toronto, ON, July 14th-16th, 2000.*

***Petrin, D.**, Delgaty, K., Bhatt, R., Garber, G.E. Clinical and Microbiological Aspects of Trichomonas vaginalis. Clinical Microbiological Reviews. 11;2: 300-317; 1998.*

***Petrin, D.**, Garber, G.E. Butanol Production in Trichomonas vaginalis. Interscience Conference on Antimicrobial Agents and Chemotherapy 37th Annual Meeting, Toronto, 1997.*

***Petrin, D.**, Garber, G.E. Characterization of an NADPH-Dependent Butanol Dehydrogenase Gene in Trichomonas vaginails. Canadian Infectious Disease Society Meeting, Toronto, 1997.*

***Petrin, D.**, Bhatt, R., Garber, G.E. New Trends in the Pathogenesis of Trichomonas vaginalis. Infectious Disease Practice for the Clinician. 20;6 June; 1996*

*Bhatt, R., Abraham, M., **Petrin, D.**, Garber, G.E. New Concepts in the Diagnosis and Pathogenesis of Trichomonas vaginalis. Canadian Journal of Infectious Disease. 7;5:321-325; 1996*

***Petrin, D.**, Garber, G.E. The Characterization of Extracellular Protease Gene(s) of the Genital Pathogen Trichomonas vaginalis. Royal College Of Physicians and Surgeons 64Th Annual Meeting, Montreal, 1995.*

***Petrin, D**, Leduc, L. Curing of Plasmids in Three Isolates of Thiobacillus ferrooxidans Biology Day Trent University, Peterborough, Ontario, 1992.*

Grants and Awards

Ontario Graduate Scholarship in Science and Technology (OGSST) 2 year term (1999 and 2000)
Travel Awardee for the Xth International Symposium on Retinal Degeneration September 30th-October 5th 2002, Burgenstock Switzerland
Foundation Fighting Blindness-Canada Gradaute Studentship 3 year term (2001-2004)
University of Ottawa Excellence Award 3 year term (2001-2004)